

**PERTURBATIVE QUANTUM FIELD THEORY AND  
OTHER PHYSICAL PERTURBATIONS – GOING TO  
HIGHER ORDER WITH ANALYTICAL AND  
APPROXIMATIVE SCHEMES**

By

ERIC V. STEINFELDS

Bachelor of Arts  
Luther College  
Decorah, Iowa  
May, 1986

Master of Arts  
Kent State University  
Kent, Ohio  
May, 1990

Submitted to the Faculty of the  
Graduate College of the  
Oklahoma State University  
in partial fulfillment of  
the requirements for  
the Degree of  
**DOCTOR OF PHILOSOPHY**  
December, 1997

Name: Eric V. Steinfelds

Date of Degree: December 1997

Institution: Oklahoma State University

Location: Stillwater, Oklahoma

Title of Study: PERTURBATIVE QUANTUM FIELD THEORY AND OTHER  
PHYSICAL PERTURBATIONS - GOING TO HIGHER ORDER  
WITH ANALYTICAL AND APPROXIMATIVE SCHEMES

Pages in Study: 140

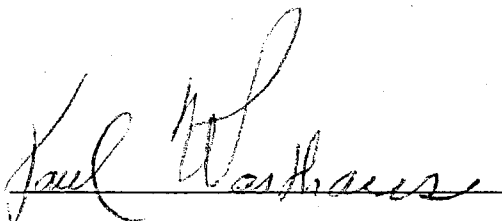
Candidate for the Degree of Doctor of Philosophy

Major Field: Physics

Scope and Method of Study: The main areas of research and summary include solving integral equations with application to diffusive scattering studies and calculating non-relativistic energy levels of particles subject to a tractable radially dependent potential plus a less manageable, large radially dependent potential term. The method developed in this thesis for calculating spectra of particles bound in a complicated radial potential can be applied to various spectrum calculations by using a good computer (with math co-processor) and the implementation of Mathematica style source code. Returning to the first mentioned area of rendition and application, diffusive scattering studies discussed and considered in this thesis center around the problem of analyzing and solving integral equations involving the diffusive scattering of radiation in biological material media. There are two things that are of common issue to both mentioned sub-topics of research. First of all, the expressions for the essential phenomena and observables can be and are often expressed as an infinite series. The failure of such an infinite series to get a convergent summation is the second item of common issue in this thesis. This problem occurs with integral equations and in the perturbative treatment given to the quantum mechanical spectra of atomic and nuclear systems. A formalism for partial fractions known as Padé approximants are introduced. These Padé approximants are used to make approximations of the sum that a given infinite series is formally representing.

Findings and Conclusions: Analytical as well as efficient methods for calculating the difficult higher order terms in many infinite series were successfully developed and demonstrated in chapters 2 through 5 of this thesis. Padé approximants, in turn have been applied successfully to all of the examples given (except for one in chapter 2) in order do find consistent convergent results of the various perturbative infinite series involved.

ADVISOR'S APPROVAL: \_\_\_\_\_



**PERTURBATIVE QUANTUM FIELD THEORY AND  
OTHER PHYSICAL PERTURBATIONS – GOING TO  
HIGHER ORDER WITH ANALYTICAL AND  
APPROXIMATIVE SCHEMES**

By

ERIC V. STEINFELDS

Bachelor of Arts  
Luther College  
Decorah, Iowa  
May, 1986

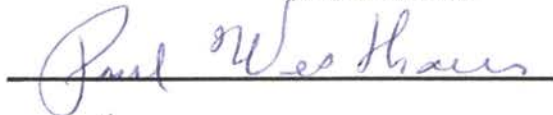
Master of Arts  
Kent State University  
Kent, Ohio  
May, 1990


Submitted to the Faculty of the  
Graduate College of the  
Oklahoma State University  
in partial fulfillment of  
the requirements for  
the Degree of  
**DOCTOR OF PHILOSOPHY**  
December, 1997

**PERTURBATIVE QUANTUM FIELD THEORY AND  
PHYSICAL PERTURBATIONS – GOING TO  
HIGHER ORDER ANALYTICAL  
AND APPROXIMATIVE SCHEMES**

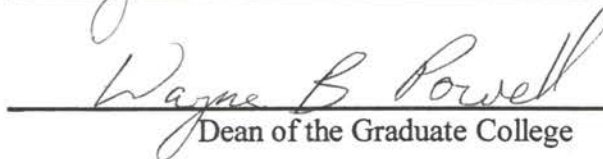
Thesis Approved:

  
\_\_\_\_\_  
Thesis Advisor

  
\_\_\_\_\_

  
\_\_\_\_\_

  
\_\_\_\_\_

  
\_\_\_\_\_  
Dean of the Graduate College

## Acknowledgments

I would like to express my gratitude to my research advisor, Dr. Mark A. Samuel, for his guidance and for his strong encouragement towards me to develop and use computationally oriented skills and insights for a wide array of physical and applied mathematical calculations. I also appreciate the example that Dr. Mark Samuel set for me with his excellent skills in the professional writing of scientific information in a manner fitting for current research journals.

I am especially thankful to Dr. Paul A. Westhaus for his role as a true mentor and deep instructor towards me in the earlier stages of my studies. I am also thankful to Dr. Westhaus for his state of always being available when help was needed in a scholastic as well as professional sense.

I would like to particularly thank Dr. Satya Nandi and Dr. Xincheng Xie for the education and broadening of knowledge which I received in courses taught by them. Dr. Nandi especially has exposed me to a broad and deep base of theoretical knowledge through his mentoring.

I would like to express my appreciation for very helpful student colleagues.

Last but not least, I would like to express my thanks to my parents for their constant support and my encouragement from my early years onward. I would like to especially thank one of my uncles for similar encouragement. I would like to thank my living grandmother other personal family members for their encouragement.

## Table Of Contents

Chapter	Page
I. INTRODUCTION.....	1
Overview.....	1
A Cause for Using Padé Approximants in QCD .....	13
Summary .....	13
II. LINEAR FREDHOLM INTEGRAL EQUATIONS.....	15
Mathematical Justification of Fredholm Series.....	15
Presentation of Results.....	25
III. THE RADIATIVE TRANSFER EQUATION AND THE H-FUNCTION.....	34
Mathematical Introduction, Showing Recursive Relation.....	34
Results of Series Iteration and Padé Approximants.....	42
IV. ANALYSIS OF NONLINEAR INTEGRAL EQUATION.....	48
V. NUMERICAL RESULTS OF ASYMPTOTIC PADÉ APPROXIMANT PREDICTIONS .....	53
VI. THE QUARTIC HARMONIC OSCILLATOR AND PERTURBATION THEORY.....	65
1. Overview .....	65
2. The Nature of Perturbation Theory.....	65
3. The Apparent Kinship of Some Perturbative Series to Stieljes Series .....	76
4. Introduction to Walker Green's Function Series Iteration.....	82
a. Orientation .....	82
b. A Scheme for Solving a Truncated Version of Equation (6.15), which is Catalogued in the Mathews and Walker Text .....	84
c. A Scheme for Solving a More Effective Version of a Truncated (Listed) Equation (6.15) when only 6 or Less Terms are Available.....	86
d. The Algorithm Required in Order to Realize the Concept From Subsection "4c" .....	86

5. Results of Calculations .....	88
6. Comparison of the Bender Perturbation Series to the Series Extracted From Optimized Padé Approximants .....	108
7. Comment on $V \cdot x^6$ Contributions and Closing Statement.....	112
<b>VII. ESTIMATING PERTURBATIVE COEFFICIENTS IN QUANTUM FIELD THEORY BY USING PADÉ APPROXIMANTS .....</b>	<b>113</b>
Padé Approximant Predictions .....	113
Predicting Higher Order Terms in QED .....	114
Padé Approximants Applied to QED.....	117
Applications of PAPs to Perturbative QCD .....	120
PAPs Applied to the Quantum Chromodynamic R Ratio .....	122
Concluding Statement of Chapter 7.....	127
<b>BIBLIOGRAPHY .....</b>	<b>129</b>
<b>APPENDIX A.....</b>	<b>132</b>
<b>APPENDIX B .....</b>	<b>136</b>
<b>APPENDIX C.....</b>	<b>138</b>
<b>APPENDIX D.....</b>	<b>140</b>

## List of Tables

Table	Page
2.1 Results of $G(x,y) = (x \cdot y)^2$ .....	26
2.2 Results of $G1(x,y) = (x \cdot y)^2$ .....	26
2.3 Results of $G1(x,y) = (x \cdot y)^2$ .....	27
2.4 Results $G(x,y) = (x \cdot y)^2 + (x \cdot y)^4$ .....	28
2.5 Results of $G(x,y) = (x \cdot y)^2 + (x \cdot y)^4$ .....	28
2.6 More results of $G(x,y) = (xy)^2 + (xy)^4$ .....	29
2.7 Results when this kernel is $G(x,y) = x \cdot y / (1 + (x+y)/2)$ .....	30
2.8 Results when the kernel is: $G4(x,y) = (x \cdot y) \cdot (1 + (x+y)/4)^{(1/6)}$ .....	31
2.9 Results when $G(x,y)$ is $Ei( x-y )$ .....	32
2.10 Results when $G(x,y) = Ei( x-y )$ .....	33
3.1 Example of the Values of $g_{\{n\}}(u)$ for Three Values of $u$ .....	41
3.2 Comparison of the Established Numerically Labored Values of the H-function to Padé Approximants .....	43
3.3 Table of percent error of the predictions from the book values .....	44
3.4 Comparison of Padé Approximants to the Respective Book Values .....	44
3.5 Table of percent error of the predictions from the book values .....	45
3.6 Example "3.6" .....	45
3.7 Table of percent error of the predictions from the book values .....	46
3.8 Example when $u = .9$ .....	46



3.9	List of $g_n(1.0)$ when $n = \{1,2,3 \dots 9\}$ .....	47
4.1	Comparison when $G(x,y) = (x \cdot y)^2$ .....	50
4.2	Comparison when $G_{xy} = (x \cdot y)^2$ , where $G(xy) = 1/(1 + (x + y)/2)$ .....	51
5.1	$H(.8,w)$ Functions obtained with ordinary Padé Approximants and with the Assistance of APAPs in PtSum[8] .....	56
5.2	Higher order Padé Approximants computed with the help of APAP's .....	57
5.3	The Coefficients $g_{(n)}(0.8)$ for the $H(.8,w)$ Function obtained from the Iteration Algorithm up to the seventh order and then the APAP for eighth Order and Beyond .....	57
5.4	$H(1.0,w)$ function obtained with Padé approximants and from partial sums with seventh order iterations. ....	58
5.5	Coefficients $g\{n\}(1)$ functions obtained from the iteration algorithm given Chapter 3 up to the seventh order .....	59
5.6	$H(1,w)$ functions computed Padé[3,4] and from the APAP and Asymptotic Padé assisted Partial Sum (PS) Methods .....	60
5.7a	Comparison of Predictions of $r[n]$ .....	61
5.7.b	Untitled but sequential .....	62
5.7.c	Untitled but sequential .....	62
5.8	Comparison of predictions of $r[n]$ in the Case when APAP[n,1] is used .....	63
6.1	When $n = 0$ , the Ground State Level. A Table in which $E(V)$ of the quartic oscillator is evaluated as a function of $V$ by NPT partial sums, Padé approximants, and by the numerical spectrum search explained with equations (6.4 and 6.5) .....	74
6.2	When $n = 1$ , the first excited level. A Table in which $E(V)$ of the quartic oscillator is evaluated as a function of $V$ .....	74
6.3	Table comparing ordinary Padé approximants to the respective optimal Padé approximants .....	90

6.4	A Table showing the Optimal Padé Approximants, in particular OpOptPadé[2,2], OpOptPadé[2,3], OpOptPadé[3,3], and OptPadé[3,4], of $E(V)$ when $n=0$ . (Note $E(V)$ grows positively with $V$ .).....	92
6.5	Table for the case $n = 1$ (The level of first excitation) .....	93
6.6	Table which lists coefficients of the Bender series for Ground State Energy.....	111
7.1	Comparison of the PAP for $a_u - a_e$ with known results .....	115
7.2	Padé Estimates for $a_e$ , which are compared to known results .....	116
7.3	PAPs for $a_u(\text{QED})$ , which are compared to known results.....	117
7.4	PAPs for the QCD beta function.....	121

## List of Figures

Figure	Page
1.1	Comparison of $\ln(1+x)$ , Padé[2,2], and the Partial Sum ..... 7
1.2	Comparison of the harmonic oscillator's ground state (spatial form of $1/(\pi^4)\cdot\exp(-x^2/2)$ ) to the fourth order series expression of the corrected ground state and the actually expected wave form of the corrected ground state..... 12
1.3	Comparison of $\text{amp} \cdot \exp(-x^2 \cdot .597)$ to the numerically predicted corrected ground state and to the Padé[2,2] prediction for the ground state which has the form $1/(\pi^4) \cdot \exp(-x^2/2)$ . ('amp' is an adjustable quantity.) ..... 12
6.1	The exact value for $1/2 + V/3 - V^2 \cdot (1 - 1! \cdot V + 2! \cdot V^2 - 3! \cdot V^3 + \dots)$ and Padé approximants such as Padé[2,2], Padé[3,2], and Padé[2,3]..... 80
6.2	The exact value for $1/2 + V/5 - V^2 \cdot (1 - 1! \cdot V + 2! \cdot V^2 - 3! \cdot V^3 + \dots)$ and Padé approximants such as Padé[2,2], Padé[3,2], and Padé[2,3]..... 80
6.3	The exact value for $1/2 - V/3 - V^2 \cdot (1 - 1! \cdot V + 2! \cdot V^2 - 3! \cdot V^3 + \dots)$ and Padé approximants such as Padé [2,2], Padé[3,2], and Padé[2,3]..... 81
6.4	Optimal Padé approximants for the four lowest levels of the 1-dimensional Quartic Harmonic Oscillator..... 95
6.5	Ordinary Padé approximants for the 4 lowest energy levels of the 1-dimensional Quartic Harmonic Oscillator..... 96
6.6	Naive Perturbation Theory series compared to the correct spectral energy levels ..... 97
6.7	Padé Spectrum for the two lowest energy levels ..... 98
6.8	NPT partial sums presented for the two lowest energy levels ..... 99
6.9	Padé Spectrum for level $s$ ( $n=2$ ) and ( $n=3$ ) ..... 100

6.10	NPT partial sums presented for 2 upper n's .....	101
6.11	Padé Spectrum (including Padé approximants) of the 3 lowest energies.....	102
6.12	Spectrum for the 3 lowest energies including NPT Series as well as Padé approximants.....	103
6.13	Energy curve for the lowest possible level when $l = 0$ , showing Padé[2,2], OpOptPadé[2,3], Padé[2,3], and the correct energy.....	104
6.14	Padé Spectrum for the ground orbit O energy (Padé[2,2] —, OpOptPadé[2,3] —, Padé[2,3], and exact —) and also the corresponding fourth order perturbation theory result —.....	105
6.15	Padé Spectrum for the lowest energy level when $l = 1$ , showing Padé[2,2] —, OpOptPadé[2,3] —, Padé[2,3] —, and the correct energy .....	106
6.16	Padé Spectrum for the lowest energy when when $l = 1$ , showing Padé[2,2] —, OpOptPadé[2,3] —, Padé[2,3] —, 2nd order NPT series — and the correct energy — .....	107
7.1	Comparison of PAP derived $r_3$ — and the analytically known $r_3$ — when $N_f = 1$ .....	124
7.2	Comparison of PAP derived $r_3$ — and the analytically known $r_3$ — when $N_f = 5$ .....	125
7.3	Comparison of the PAP[1,2] estimate of $r_4$ — with the PAP[2,1] estimate of $r_4$ and with the estimate using PAP[0,2] — when $N_f = 1$ .....	125
7.4	Comparison of the PAP[1,2] estimate of $r_4$ — with the PAP[2,1] estimate of $r_4$ — and with the estimate using PAP[0,2] — when $N_f = 5$ .....	126

## Nomenclature

cf. N	refer to the previous equation N
denom[N]	denominator manifested as N
eqn.	equation
LHS	left hand side of the equation
mini-defn	mini-definition
number[N]	numerator manifested as N
NT	Next Term
PAP	Padé Approximant Prediction
QCD	Quantum Chromodynamics
QED	Quantum Electrodynamics
RHS	right hand side of the equation
APAP	Asymptotic Padé Approximant Prediction
w.r.t.	with respect to

## Chapter 1

### Introduction

#### Overview.

The areas of discourse in this dissertation include a fairly broad range of issues. The three main areas include solving integral equations with application to diffusive scattering studies, calculating non-relativistic energy levels of particles subject to a tractable radially dependent potential plus a less manageable large radially dependent potential term, and finally calculating various relativistic field theory quantities which involve either perturbative QCD or perturbative QED. Calculations of the quantum chromodynamic beta function are discussed in chapter 7. This Quantum Chromodynamic quantity is expressed as a perturbative series expanded with respect to the strong coupling constant. Calculations of the quantum electrodynamic anomalous magnetic moments of the electron and muon are discussed in chapter 7. These two quantities are expressed as a perturbative series expanded with respect to the electrodynamic coupling constant.

The method developed in this thesis for calculating low energy spectra of particles bound in a complicated radial potential can be applied to various spectrum calculations by using an adequate work station (such as the DEC Alpha 3000 work station) and the implementation of appropriate source code in Maple or in a Mathematica operation platform. This method of finding energy levels should show much promise in a future endeavor in nuclear physics. In nuclear physics, this procedure could be applied to the modelling of the spectrum of the nucleus in a project such as the extension of the shell model or the collective model of nuclear physics with the addition of fine tuning potential

energy terms, which do include a mean field approximation of the effect of neighboring nucleons. This is of interest in nuclear spectroscopy described in terms of the individual nucleon [1].

Returning to the first mentioned area of thought and rendition, the diffusive scattering studies mentioned here give insight in the problem of analyzing and solving integral equations involving the diffusive scattering of radiation in biological material media. For example, it would be very useful to be able to analyze more precisely the data of tomographic scans from an improved theoretically based model of radiative scattering of X-rays. Likewise, improvements in the analysis of ultra-sound imaging based on improvements in phonon scattering theory are desirable.

There are two things that are of common issue to all three mentioned areas of discourse. First of all, the expressions for the essential phenomena and observables can be and are often expressed as an infinite series. Very often, the coefficients  $(\alpha_s/4\pi)^n$ <sup>(1)</sup> of a given series grow so quickly that only trivially small values for the expansion parameter will be able to maintain a convergent series. Indeed, the failure to get a convergent summation is a common problem. This is the second thing which is of common issue. This problem occurs with integral equations and in the perturbative treatment given to the quantum mechanical spectra of atomic and low/medium energy nuclear systems. This is especially true in Quantum Chromodynamics (QCD) and in Quantum Electrodynamics (QED). In QCD the majority of calculations for coupling constant, various system interaction strengths, scattering amplitudes, branch ratios for decays, etc. are carried out by

---

<sup>(1)</sup>  $\alpha_s/(4\pi)$  is the chosen expansion parameter here. Arbitrarily,  $z$  could be chosen as the main parameter.

carrying out perturbative quantum chromodynamics. Most relativistic perturbative quantum field theory calculations are infinite series, where  $\alpha_s$  (the strong coupling constant) and  $\alpha$  ( $1/137$ ) of QED serve as the expansion parameters. Any perturbative series in quantum chromodynamics is very difficult to work with in the sense that a large or medium numerical value for  $\alpha_s$  would result in a very (critically) divergent series. Furthermore, it is very difficult to calculate the individual higher order QCD terms. It is not known precisely what the practical size limit of  $\alpha_s$  is in order to generate a converging partial sum out to sixth, seventh, or eighth order of a typical perturbative QCD series. Asymptotic formulas are known for a number of series in QCD, including the strong beta function which determines the gradual energy dependence of  $\alpha_s$ . The terms of the QCD beta function grows at very high order in good approximation as  $1/(4\pi\beta_0)\cdot(-\beta_0)^n\cdot n!\cdot(\alpha_s)^n$  as  $n$  approaches infinity.  $\beta_0$  is from the 1st term of the beta function. (See ref. [2] for more detail.) However, these asymptotic expressions are not terribly helpful since they are not quantitatively reliable until very high orders exceeding 15 in the given perturbative series are reached. Very little is known in between order 7 and order 16. Nevertheless, it is especially desirable to find out what the true structure is of a given QCD or QED perturbative series in terms of  $\alpha$  and/or  $\alpha_s$ . Some examples of such functions of  $\alpha$  and  $\alpha_s$  are anomalous magnetic moments of leptons and the QCD beta function, which determines the energy dependence of  $\alpha_s$ . There is a *rather* reliable way to formally develop a sequence of approximate functions that sequentially approaches the correct form for many of the functions of  $\alpha$  and/or  $\alpha_s$ . This method for approximations involves developing a rational fraction in such a way that the rational fraction agrees term by term



with the original perturbative series all the way up to the  $(n+m)^{\text{th}}$  order, which includes the coefficient times  $(\alpha_s/4\pi)^{(n+m)}$ . Such rational fractions will be demonstrated as *being* effective in evaluating the analytical values and the experimentally agreeable values in a couple of examples of interesting QCD functions. In reference again to integral equations, it is possible to give a very strong argument for the validity and the virtually guaranteed success of the use of rational fractions as approximations to the solution of Fredholm integral equations of the second kind.

These specially adjusted rational fractions, developed as an ever improving sequence, are known as Padé approximants<sup>2</sup>. Padé approximants are expressed as

$$\text{Pade}[n,m], \text{ where } \text{Pade}[n,m] = \frac{(a_0 + a_1 \cdot x + a_2 \cdot x^2 + \dots + a_n \cdot x^n)}{(1 + b_1 \cdot x + \dots + b_m \cdot x^m)}. \quad (1.1)$$

This rational polynomial fraction is required as the approximation to describe optimally an infinite series through the technique of coefficient fitting. Alternately stated, these two expressions are to be matched:

$$\frac{(a_0 + a_1 \cdot x + a_2 \cdot x^2 + \dots + a_n \cdot x^n)}{(1 + b_1 \cdot x + \dots + b_m \cdot x^m)} \approx r_0 + r_1 x + r_2 x^2 + \dots + r_{[n+m]} x^{(n+m)}. \quad (1.2)$$

The right-hand side is the partial sum of the infinite series  $\sum_{i=0} r_i \cdot x^i$ , where  $x$  is the name given to the variable expansion parameter. It is necessary to match the coefficients of like powers of  $x$  on the left hand side (LHS) and right hand side (RHS) after multiplying with the denominator on both sides. Therefore, simultaneously for  $m$  equations:

$$\sum_{k=0}^m r_{(j-k)} b_k = 0, \text{ where } (j = n+1, n+2, \dots, n+m). \quad (1.3)$$

<sup>2</sup> Specifically, Padé type I approximants are used in this thesis.

By convention,  $b_0 = 1$ .

An additional consequence applies to the  $a_i$ 's of the numerator on LHS. A local definition for  $\text{diffs}(i-m)$  is given.

$$\text{diffs}(i-m) = (|i-m| + (i-m))/2. \text{ (Note that } \text{diffs}(i-m) \text{ equals 0 if } I \leq m.)$$

There are  $n+1$  simultaneous equations for  $a_i$  to evaluate after solving for  $b_k$ :

$$a_i = \sum_{l=\text{diffs}(i-m)}^i r_l b_{(i-l)}, \quad \text{where } (i = 0, 1, \dots, n). \quad (1.4)$$

After evaluating the  $a_i$ 's and  $b_i$ 's, we have the expression

$$\frac{(a_0 + a_1 \cdot x + a_2 \cdot x^2 + \dots + a_n \cdot x^n)}{(1 + b_1 \cdot x + \dots + b_m \cdot x^m)}$$

serving as the Pade[n,m] approximant to some function

$f(x)$ , expressible as  $f(x) = \sum_{i=0}^{\text{inFini}} r_j \cdot x^i$ . There is a successive array of Pade[N,M] ap-

proximants (e.g. Pade[2,3], Pade[3,3], Pade[3,4], Pade[4,4], etc.), where N and M are arbitrarily large non-negative integers. From the successful results of full Pade[N,M] predictions for hundreds of diverse series and from the guaranteed results of functions which generate a Stieltjes series [3], it is known that Pade[n,n+1] and Pade[n,n] give best approximation values to most of the interesting choices of  $f(x)$ . One deep implication of this is that this sequence {Pade[n,n], Pade[n,n+1]} gives approximations which approach the correct value and functional form of any member of the family of functions of  $x^{(3)}$  as  $n$  sequentially approaches infinity.  $\text{fun}(x)$  represents all of those family members which are continuous functions of  $x$  which are possible to approximate as these rational polynomials. There might exist some functions of  $x$  (or other parameter) which are not effectively expressed as Padé approximants. It is mathematically true however, that those

functions expressible as  $\sum_{i=0}^{\infty} r_j \cdot x^i$ , where the limit  $r_j$  approaches some  $K \cdot A^j$  ( $K \cdot A^j$  is a geometric series) or  $K \cdot j^n$  ( $n$  is an integer), have a special characteristic which identifies  $\text{fun}(x)$ . As  $n$  gets very large,  $\text{Pade}[n,n]$  and  $\text{Pade}[n,n+1]$  are guaranteed to converge to the same function with the same value as  $\text{fun}(x)$ .

In order to illustrate the effectiveness of the rational fraction, the example of  $\text{Pade}[2,2]$  of  $\ln(1+x)$  is considered. Let

$$f(x) = \ln(1+x) = x - x^2/2 + x^3/3 - x^4/4 + \dots \quad (1.5)$$

The partial sum is considered up to the fourth order. Exactly as done with equation (1.2), we end up with  $(a_0 + a_1 x + a_2 x^2) \approx (1 + b_1 x + b_2 x^2)(x - x^2/2 + x^3/3 - x^4/4)$ .

Matching powers of  $x$ , we obtain the following example of equations (1.3) and (1.4) :

$$1/3 - b_1/2 + b_2 = 0. \quad -1/4 + b_1/3 - b_2/2 = 0. \quad (1.6)$$

$$a_0 = 0. \quad a_1 = 1. \quad a_2 = b_1 - 1/2 \quad (1.7)$$

The  $a_i$ 's and  $b_i$ 's are determined. Then,  $\text{Pade}[2,2] = \frac{x + x^2}{1 + x + x^2/6}$ . Consider the fol-

lowing comparison to the partial sum  $(x - x^2/2 + x^3/3 - x^4/4)$ .<sup>3</sup>

Observe Figure 1.1).

---

<sup>3</sup>  $x$  is the name assigned to the one significant parameter used to generate the series.

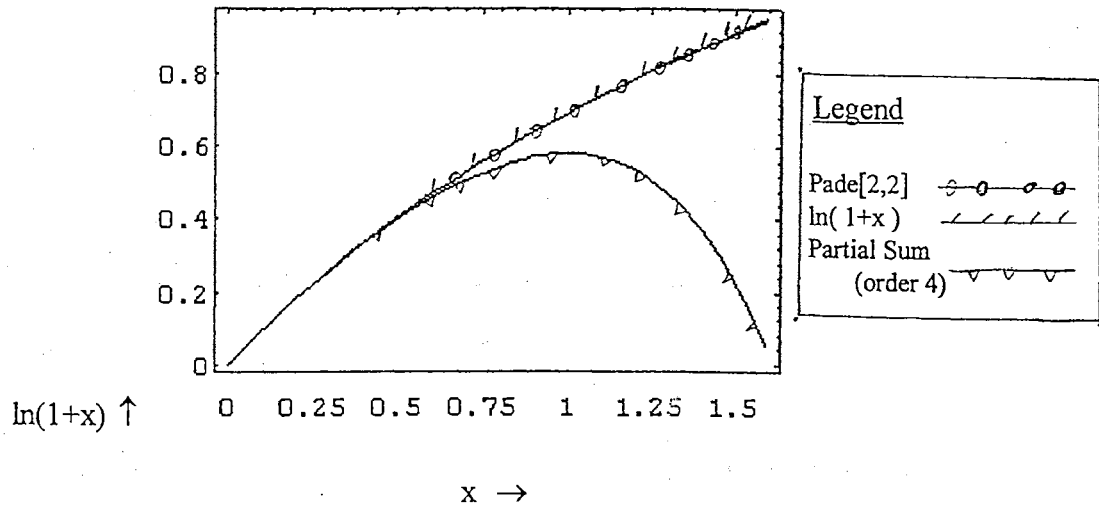


Figure 1.1) Comparison of  $\ln(1+x)$ , Pade[2,2], and the Partial Sum.

It is clear from figure 1, that the Padé approximant is much closer to the actual  $\ln(1+x)$  than  $(x - x^2/2 + x^3/3 - x^4/4)$  is. There are innumerable other examples of infinite series where the Padé approximants show this excellent improvement of the numerical values.

It would be illustrative to show the general formulas of Pade[1,1], Pade[1,2], and

Pade[2,2] for the series  $\sum_{i=0}^{\infty} r_i * x^i$ .

$$Pade_{[1,1]} = \frac{r_1 r_0 + (-r_0 r_2 + r_1^2) x}{r_1 - r_2 x} \quad (1.9)$$

$$Pade_{[1,2]} = \frac{r_0^2 r_2 - r_0 r_1^2 + (2 r_1 r_0 r_2 - r_1^3 - r_3 r_0^2) x}{(r_3 r_1 - r_2^2) x^2 + (-r_3 r_0 + r_2 r_1) x + r_0 r_2 - r_1^2} \quad (1.10)$$

$$Pade_{[2,2]} = \frac{\text{numerat}}{\text{denom}} \quad (1.11)$$

$$\begin{aligned}
\text{numerat} &= r_0 r_3 r_1 - r_0 r_2^2 + x r_3 r_1^2 - x r_1 r_2^2 - x r_0 r_1 r_4 + \\
&\quad x r_0 r_2 r_3 + x^2 r_4 r_0 r_2 - x^2 r_4 r_1^2 + 2 x^2 r_2 r_3 r_1 - x^2 r_3^2 r_0 + x^2 r_2^3 \\
\text{denom} &= x^2 r_4 r_2 - x^2 r_3^2 - x r_1 r_4 + x r_2 r_3 + r_3 r_1 - r_2^2
\end{aligned} \tag{1.12}$$

There are more solutions available, including Pade[3,3]. In consideration of expeditious use of space, these other general results are posted in appendix A.

On many occasions it is desirable to predict the value of the next term of an infinite series which hitherto is known only to the order of  $n+m$ . This can be done by adding in to the right hand side of equation (2) the additional term of  $r_{(m+n+1)}x^{(m+n+1)}$ . Then multiply the right hand side and the LHS by  $(1 + b_1 \cdot x + b_2 \cdot x^2 + \dots + b_m \cdot x^m)$ . We end up with a Pade approximant prediction (PAP) of what  $r_{(n+m+1)}$  should equal:

$$r_{(n+m+1)} \approx - ( b_1 \cdot r_{(n+m)} + b_2 \cdot r_{(n+m-1)} + b_3 \cdot r_{(n+m-2)} + \dots + b_m \cdot r_{(n+1)} ) . \tag{1.13}$$

There are various examples, for instance in electrodynamics, where it is desirable to get an estimate of the term of order  $(n+m+1)$  since calculating the next term exactly becomes extremely time-consuming.

Let us now continue discussing the material towards which this dissertation is targeted. At the end of this introduction, an overview will be given of the contents of the three areas of discourse towards which the progression of chapters of this dissertation are directed. These three areas were introduced in the beginning of the text. First in the following chapters, integral equations will be discussed. Second, ordinary quantum mechanical perturbation theory will be discussed. And third, QCD and inclusively the strong coupling constant in high energy physics will be studied.

The integral equations discussed include the linear Fredholm integral equations of the second kind, nonlinear quasi-Fredholm integral equations, and the nonlinear H-

function integral equation. Linear Fredholm integral equations have a well developed formal solution. However, there are specific cases in which the formal solution is devastated by catastrophic singularities. Generating an infinite series for the solution and taking a sequence of diagonal Padé approximants (Pade[n,n]) bear convergent numerical predictions which often avoid this catastrophe.

The nonlinear H-function integral equation is a partial simplification of the radiative transfer diffusion equation which is explained in the text by Chandrasekhar.[4] The insights involved in solving such an equation will be useful in diffusive scattering studies of radiation penetrating through biological materials.

The second area of discourse, spectrum related calculations, will be covered in Chapter 6. In Chapter 6, it will be explicitly shown how it is possible to go to higher order perturbation theory with the basic tools published and taught by Merzbacher and Liboff [5.a] in non-relativistic quantum mechanics. A second way to do higher order perturbation theory will also be demonstrated which is simpler than ordinary perturbation theory (the Raleigh Schrödinger procedure) but which involves an input of iterative substitutions for the energy shifts within the essential perturbative summation calculation machinery. The first and immediately important results desired are the corrected energy spectra. Moreover, the corrected eigenstates can be estimated in a functional form.

The issue of why the methods utilizing matrix formalism (e.g. diagonalizing a 60 by 60 Hamiltonian matrix) are not the superior method for calculating spectra of particles in all nonrelativistic binding systems will also be addressed in Chapter 6. In brief, these

matrix formalism techniques are completely numerical. The scaling parameter of the perturbation term has to be set numerically, eliminating any opportunities for concisely constructing a symbolic approximation of the eigenvalues as a function of the adjustable perturbation parameter. There is a true advantage in having a symbolic expression which approximates the new energy levels to high precision. Constructing a perturbation series which is explicitly dependent on the symbolic perturbation scale makes it possible to gain such an advantage.

In the discussion of using perturbation theory to make predictions, there is always the danger that the perturbation term of the Hamiltonian is too large for a meaningful convergent prediction of the new physical solutions. Padé approximants can be used to salvage the series to get a meaningful prediction of the new physical solution. These partial fractions can be used even when the magnitude of perturbation has significantly exceeded the scale limit of perturbations bearing finite behavior.

After evaluating one or more of the new corrected energy levels of the energetically perturbed particle, it is relatively easy to find the corrected eigenstate of this particle described by the new Hamiltonian (or Lagrangian). The second mentioned method for doing higher order perturbation theory provides the mathematical mechanism for generating the corrected eigenstate.[5.b] The unperturbed eigenstates are written here as  $u_n^0$ , where  $n$  stands for the  $n$ -th energy level. The corrected eigenstate is written as  $u_n$ . The way to find  $u_m$  is:

$$u_m = C \left[ u_m^0 + \sum_{n \neq m} \frac{u_n^0 \cdot Q_{nm}}{(l_m - l_n^0)} + \sum_{n \neq m} \sum_{p \neq m} \frac{u_n^0 \cdot Q_{np}}{(l_m - l_n^0)} \cdot \frac{Q_{pm}}{(l_m - l_p^0)} + \dots \right] \quad (1.14)$$

The development of this solution can be recognized from treating the perturbation term as the inhomogeneous term in a linear differential equation and the unperturbed Hamiltonian with the state (or Lagrangian with field) minus the corrected eigenvalue with the state (or Lagrangian with field) as the main operator from which the essential Green's function is built. By using the Green's function and the homogeneous term, the corrected eigenstates  $u_n$  are built up. If the convergence of the right hand side of equation (1.14) is in jeopardy, then it is extremely convenient to take the Pade[n,m] approximant of the perturbation series. In most instances the best result occurs when  $m$  equals  $n$  or  $n+1$ .  $n$  plus  $m$  should equal the order of the perturbation scale parameter of the largest order available term in equation (1.14). There is an example in the appendix (See appendix B. See newstat3.ms ) in which a quartic harmonic oscillator is studied. In brief, the potential  $V \cdot x^4$  is added to the Hamiltonian of a harmonic oscillator. The graphical results of the correction of the ground state of the energetic system  $((-d^2/dx^2 + 2 \cdot x^2) + V \cdot x^4) \Psi$  are displayed in figures (2) and (3). These results for the corrected ground eigenstate are very reasonable. Over all, they are modestly successful. The point of this is that it is no more difficult in terms of writing and executing software to calculate these corrections to the eigenstate than it is to find the eigen-energy of that state. This could serve as a tool to qualitatively inspect the change in the spatial form of the eigenstate as the magnitude of the perturbing term is increased without spending much CPU time to create the new eigenstates.



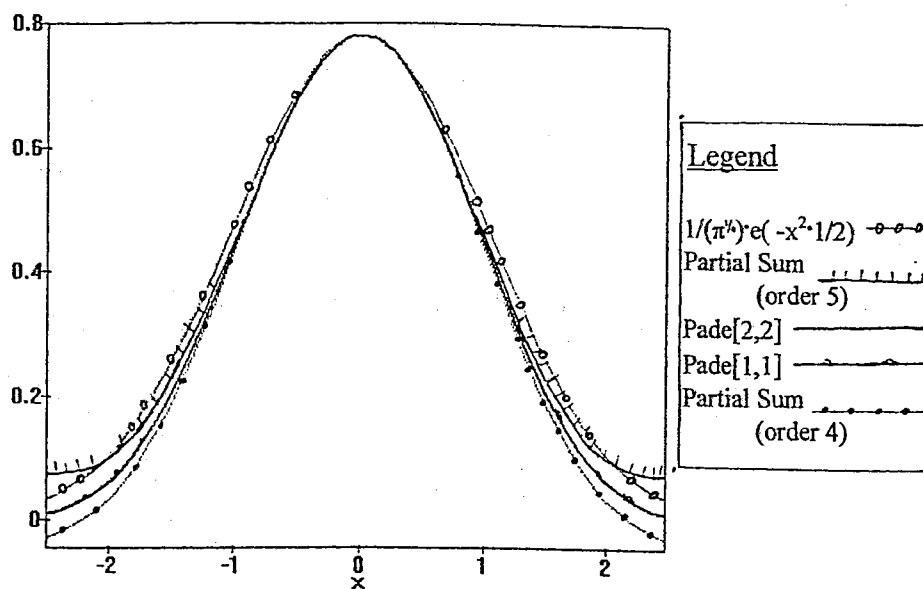


**Figure 1.2)** Comparison of the harmonic oscillator's ground state (spatial form of  $1/(\pi^4) \exp(-x^2/2)$ ) to the fourth order series expression of the corrected ground state and the actually expected wave form of the corrected ground state.-

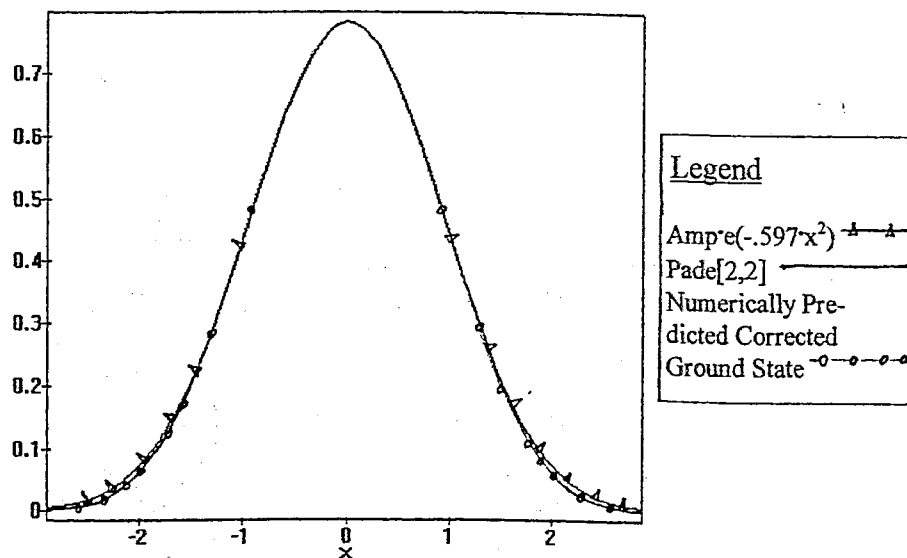


**Figure 1.3)** Comparison of  $\text{amp} \cdot \exp(-x^2 \cdot 0.597)$  to the numerically predicted corrected ground state and to the Pade[2,2] prediction for the ground state, which has the form  $1/(\pi^4) \exp(-x^2/2)$ . ('amp' is an adjustable quantity.)

### **A Cause for Using Padé Approximant Predictions in QCD.**

The area of field theory which includes Quantum Chromodynamics and Quantum Electrodynamics shall be covered in Chapter 7. Any perturbative series in quantum chromodynamics is very difficult to work with in the sense that a large or medium numerical value for  $\alpha_s$  would result in a critically divergent series. Furthermore, it is not known precisely just how large  $\alpha_s$  can be in order to generate a partial sum in a convergent form out to seventh or eighth order of the infinite series. Asymptotic formulas are understood for  $\alpha_s$  of QCD. But, this is only a limited form of aid. PAP's can be helpful in providing a reasonable estimate of the value of the next term in a QCD. This is useful for calculating a higher precision estimate of a perturbative QCD partial sum out to one order higher than has been done presently by analytical means. As was initially announced, the QCD beta function will be given special attention.

### **Summary.**

This completes the overview of the contents of the three areas of discourse of this work. In terms of operation overhead, it is of significance that a mere pentium 120 with only 24 megabytes of RAM was used for the tedious numerical calculations as well as for the involved symbolic information processing. These conventionally tedious numerical calculations and the involved symbolic processing are discussed in Chapters 2 through 6. No more than twenty minutes of CPU time were required to solve as reliable approximation the H-function equation for radiative scattering in chapter 3. No more than seven minutes of CPU time were required for the quantum mechanical calculations involving

fifth order perturbation theory in chapter 6. Indeed, the computations done here in are not exhaustive of computer operation power or of CPU time.

## Chapter 2

### Linear Fredholm Integral Equations

#### Mathematical Justification of the Fredholm Series

In this chapter Fredholm integral equations of the second kind will be studied and solved in application to various examples. The linear Fredholm integral equation of the second kind can be expressed as follows:

$$f(x) = g(x) + \lambda \int_a^b G(x, y) \cdot f(y) \cdot dy \quad (2.1)$$

The objective is to solve equation (2.1) for  $f(x)$ .  $G(x, y)$  is the kernel of this linear integral equation. There is an available formal solution for  $f(x)$ , which is known as the Fredholm solution [6.a]. Although this solution is formally correct, the calculations involved in generating a particular Fredholm solution as one particular function of  $x$  and  $\lambda$  are very lengthy and rather tedious. In this chapter, the effectiveness of using Padé approximants to solve the Fredholm integral equations will be demonstrated. Furthermore, the smaller required computation time of Padé approximants and the smaller amount of difficulty of calculating Padé approximants will be contrasted with the tediousness and occasional technical difficulties of carrying out the formalism required to generate the particular Fredholm solution for particular equations.

If  $\lambda$  is small enough for many cases, equation (2.1) can be solved to sufficient precision by guessing a solution and placing this guess into the right hand side of (2.1). This results in an improved guess for the solution  $f(x)$ . This type of iteration could be continued indefinitely, resulting in the infinite series  $\sum_i r_i(x) \cdot \lambda^i$ , where  $\lambda$  is the expansion pa-

parameter. The name of this is the Neumann series. Let us start the iteration with the initial guess of  $g(x)$  for  $f(x)$  (of equation (2.1)).

$$\begin{aligned} f_0(x) &= g(x) \\ f_1(x) &= g(x) + \lambda \cdot \int_a^b G(x,y) \cdot g(y) \cdot dy \end{aligned} \quad (2.2)$$

Next,  $r_1(x)$  through  $r_N(x)$  are symbolically expressed.

$$r_1(x) = (f_1(x) - f_0(x)) / \lambda = \int_a^b G(x,y) \cdot g(y) \cdot dy \quad (2.3)$$

$$f_2(x) = g(x) + \lambda \cdot \left[ \int_a^b G(x,y) \cdot g(y) \cdot dy + \lambda \cdot \int_a^b G(y,z) \cdot g(z) \cdot dz \right] \cdot dy.$$

$$r_2(x) = (f_2(x) - f_1(x)) / (\lambda^2) = \int_a^b G(x,y) \cdot \int_a^b G(y,z) \cdot g(z) \cdot dz \cdot dy \quad (2.4)$$

Clearly,  $r_N(x) = (f_N(x) - f_{N-1}(x)) / (\lambda^N)$ ,

$$\begin{aligned} \text{specifically: } r_N(x) &= \int_a^b dy_1 \int_a^b dy_2 \dots \int_a^b dy_{(N-1)} \int_a^b dy_N \\ &G(x, y_1) \cdot G(y_1, y_2) \cdot \dots \cdot G(y_{N-2}, y_{N-1}) \cdot G(y_{N-1}, y_N) \cdot g(y_N), \end{aligned}$$

$$\text{and } f_N(x) = \sum_{i=0}^N r_i(x) \cdot (\lambda)^i \quad (2.5)$$

The Neumann series has just been formally demonstrated.

It can be easily demonstrated that this Neumann series will accurately generate the solution to the Fredholm equation if  $|\lambda|$  small enough. The question arises of whether a real solution to equation (2.1) exists for all real values of  $\lambda$ . There is one unusual condition where (2.1) very likely does not have a non-zero solution. It can be seen that when  $\lambda$

of the equation  $f(x) = g(x) + \lambda \cdot \int_a^b G(x,y) \cdot f(y) \cdot dy$  equals an eigenvalue of the kernel op-

erator  $fG(x,y)dy$ , then this equation (2.1) very likely does not have a finite solution in the case other than where  $g(x)$  equals 0. Eigenvalues and eigensolutions are discussed in various texts [6.b]. Such eigenvalues, however are only a set of isolated points on the continuous spectrum of possible real values for  $\lambda$ .

In order to find out whether there exist real solutions for (2.1) when  $\lambda$  is large, a discussion of a numerical technique is useful. We can change the expression

$\int_a^b G(x,u) \cdot f(u) \cdot du$  into the discrete sum expressed as:

$$(\sum_{i=0,k} G(x[n],z[i]) \cdot y(z[i])) \cdot (b-a)/k, \text{ where } k \text{ is large.} \quad (2.6)$$

As  $k$  approaches infinity, expression (2.6) approaches equality to the RHS of (2.1).

Moreover, the following equation,

$$y(x[m]) = g(x[m]) + \lambda \cdot (\sum_{i=0,k} G(x[m],z[i]) \cdot y(z[i])) \cdot (b-a)/k \quad (2.7)$$

approaches equivalence to the equation (2.1) as  $k$  approaches infinity. By taking into consideration equation (2.7), it is completely reasonable to write out the next set simultaneous expressions of (2.7). These simultaneous equations are to be used to find the solution for  $y(x[0]), y(x[1]), \dots, y(x[k-1]), y(x[k])$ .

(Note that  $k$  does not stand for solution function here.)

$$\begin{aligned} y(x[k]) &= g(x[k]) + \lambda \cdot (\sum_{i=0,k} G(x[k],z[i]) \cdot y(z[i])) \cdot D \\ y(x[k-1]) &= g(x[k-1]) + \lambda \cdot (\sum_{i=0,k} G(x[k-1],z[i]) \cdot y(z[i])) \cdot D \\ y(x[k-2]) &= g(x[k-2]) + \lambda \cdot (\sum_{i=0,k} G(x[k-2],z[i]) \cdot y(z[i])) \cdot D \\ &\vdots \\ y(x[1]) &= g(x[1]) + \lambda \cdot (\sum_{i=0,k} G(x[1],z[i]) \cdot y(z[i])) \cdot D \\ y(x[0]) &= g(x[0]) + \lambda \cdot (\sum_{i=0,k} G(x[0],z[i]) \cdot y(z[i])) \cdot D. \end{aligned} \quad (2.8)$$

Here,  $z[j] \equiv x[j]$ .  $x[0]=a$ .  $x[k]=b$ .  $D=(b-a)/k$ .

The set of algebraic values  $[y(x[0]), y(x[1]), \dots, y(x[k-1]), y(x[k])]$  taken together comprise an estimate for the solution  $f(x)$  of (2.1). Going along with this discussion, as  $k$  approaches infinity,  $y(x[q])$  approaches  $f(x)$  of (2.1). Note:  $0 \leq q \leq k$ . Equations (2.8) in principle can be solved mathematically by using Cramer's law. By considering the form of the solution using Cramer's law, it is clear that if all of the coefficients in equations (2.8) are real, then the solution of  $y(x[0]), y(x[1]), \dots, y(x[k-1]), y(x[k])$  exists. Moreover, this solution then is real, given that  $x[j]$  is real. This equation (2.8) will be reviewed later in the discussion of the numerical methods for solving the Fredholm equation. It has now been established that a real valued solution exists for the linear Fredholm equation of the second kind when  $|\lambda|$  is small as well as when  $|\lambda|$  is large. Only for a very small isolated set of eigenvalues might a solution for  $f(x)$  not exist.

It is good to know of the existence of a solution for the above equation even when  $\lambda$  is large. Padé approximants are never able to generate accurate approximations of complex functions represented by an infinite series given by solely real terms. This becomes very apparent by reviewing equations (1.3) and (1.4) of Chapter 1 and the solutions of equations (1.3) and (1.4). An example of a real series which represents a complex function is:

$$\log(1-x) = -x - x^2/2 - x^3/3 - x^4/4 - x^5/5 - x^6/6 - x^7/7 - x^8/8 + \dots \quad (2.9)$$

If  $x$  is less than 1, then  $\log(1-x)$  is real. Or else,  $\log(1-x)$  is complex. Padé approximants perpetually give real full value predictions. For example, we see that  $\text{Pade}[2,3] = 60.0$ ,  $\text{Pade}[5,6] = -7.30667$ , and  $\text{Pade}[8,9] = -3.19488$  when  $x=1.2$  in  $\log(1-x)$ . The actual  $\log(1-(1.2))$  equals  $-1.6094379 + 3.1415927i$ . Clearly, the Padé approximants come

nowhere close to the correct answer. However, it is clear that the Padé approximants do not converge to any definite functional value of 1.2 as  $n$  of  $\text{Pade}[n,n+1]$  approaches plus infinity. Padé approximants fail here, and they indicate they are failing by refusing to converge to any one particular value. There are numerous other examples of real series which represent complex numbers as a function of large  $x$ . In all of these known examples, the Padé approximants openly advertise the non-applicability by refusing to converge to any one particular value for a given  $x$ .

On the other hand, if  $|x|$  is less than 1, then  $\log(1-x)$  is real and the Padé approximants give reliable, converging answers. Consider  $\log(1-x)$  when  $x = .8$ . The partial sum to order 4 equals -1.39307 when  $x = .8$ .  $\text{Pade}[2,2]$  and the actual  $\log(1-x)$  equal -1.56422 and -1.60944 respectively.  $\text{Pade}[2,2]$  is much closer to the correct value than the partial sum of  $\log(1-x)$ . In brief summary, Padé approximants converge to a definite real value for the series of  $\log(1-x)$  around 0 when  $|x|$  is less than 1, and Padé approximants fail to converge to any definite numerical value when  $x$  is greater than 1, where  $\log(1-x)$  is complex.

It is transparent that the solution of the Fredholm integral equation of the second kind (where all parameters of the equation are real) must be real in order for Padé approximants to be a legitimate approximation to this solution. The discussion of the simultaneous equations (2.8) made it evident that the solutions of Fredholm integral equations exist and are real. The fact that integral equations are real and exist in the example of the previous paragraph very strongly suggest the following assertion:



**Padé approximants of sequentially higher order will approach the correct solution of the Fredholm integral equation of the second kind.** (Assertion #1)

There are five conditions which should be met. If not all of these five conditions are met, then Assertion # 1 *somewhat likely* does not hold. Before going through this list, a definition for scaleable infinity is needed. A scaleable infinite kernel is a kernel  $G(x,y)$  which

results in the following two integrals being finite:  $\int_a^b |G(x,y)| \cdot dy$  being less than Infinity and

$\int_a^b G(x,y) \cdot g(y) \cdot dy$  is less than Infinity. Here is the list of five conditions required for Assertion #1 one to hold:

sertion #1 one to hold:

- 1.) *The upper and lower limits of integration must be real.*
- 2.) *It must be true that the upper and lower limits of integration are finite.*
- 3.) *Either the kernel must remain finite within the range of upper and lower limits of integration, or the kernel must be a kernel of scaleable infinity.*
- 4.) *The initial term  $g(y)$  of equation (2.1) must remain finite within the range of upper and lower limits of integration for  $y$ .*

5.) *In the RHS expression  $g(x) + \lambda \int_a^b G(x,y) \cdot f(y) \cdot dy$ ,  $\lambda$ ,  $a$ ,  $b$ ,  $g(x)$ , and  $G(x,y)$  are*

*required to be real.  $g(x)$  and  $G(x,y)$  must be real when  $x$  and  $y$  are real. Padé approximants might function successfully in some examples where  $G(x,y)$  is complex, but not in all such examples.*

This list shall be called the *five-fold statement*. If some of the conditions of the five-fold statement are not met in a Fredholm equation, then this particular equation shall be described for convenience as being a renegade Fredholm equation.

If these five conditions are met, then it is almost guaranteed that  $\text{Pade}[n,n+1]$  and  $\text{Pade}[n,n]$  will converge to the correct 'functional' solution of the Fredholm equation. There are boundless groups of examples where this five-fold statement is verified by fact. The author and others of professional acquaintance have not found any one example which contradicts the five-fold statement. In this chapter, five major examples will be given of integral equations. Padé approximants are completely successful in these examples. These five examples do fulfill the requirements of the five conditions.

It is occasionally possible that Padé approximants can be applied to the Neumann series even if not all of the five conditions are met. As a warning, remember that it is easy to find various Neumann series which fail the five-fold statement and which also are unfruitful for Padé approximants. When  $\Lambda$  is greater than  $1/\pi$  in (2.10), the equation (2.10) does not have a real solution.

$$f(x) = 1/(1+x \cdot x) + \lambda \cdot \int_{-\infty}^{\infty} \frac{1}{(1+(x+y)^2)} \cdot f(y) \cdot dy \quad (2.10)$$

As a matter of fact, the formal solution of (2.10) is  $\sum_{n=1}^{\infty} n/(x^2+n^2) \cdot (Lp)^{(n-1)}$ . It is obvious that this formal solution represents non-real values when  $\Lambda$  is greater than  $1/\pi$ . When  $\Lambda \cdot \pi = 11/10$ , there is no convergence to an answer with Padé approximants:  $\text{Pade}[2,3] = .943260$ ;  $\text{Pade}[3,3] = -.969773$ ; and  $\text{Pade}[3,4] = -.104308$ . (See pole1.ma in dir lintg) This equation is a particular case of equation (2.1). Condition 2.) of the five-

fold statement is not complied with, making this equation vulnerable to the lack of a real solution. The proof of existence of the real solution to the Fredholm integral equation does not apply to equation (2.10) because limits  $a$  and  $b$  of the discretely expressed equations (2.8) are required to be finite real numbers for equations (2.8) to be relevant to the discussion of the Riemann sum approximation of the integral.

Sometimes though, these renegade examples which defy condition 2.) of Fredholm equations are successful. Consider the following case:

$$f(x) = \frac{1}{2} \cdot \frac{1}{(1+1/2 \cdot x^2)} + \lambda \cdot \int_{-\infty}^{\infty} \frac{1}{(1+y^2) \cdot (1+x^2)} \cdot f(y) \cdot dy . \quad (2.11)$$

The solution to this example is  $f(x) = 1/2/(1+1/2 \cdot x^2) + \frac{1}{2} \cdot \pi \cdot \lambda / (1 - \pi/2 \cdot \lambda) \cdot 1/(1+x^2)$ ,

even if  $\lambda$  is larger than the radius of convergence. On a rather random basis, one sees that renegade Fredholm equations sometimes bear real valued functions and at other times complex functions as solutions. On the other hand, there are many examples such as the case of (2.10) and the example  $\ln(1+x)$  where Padé approximants will not work, especially if  $\lambda$  is large.

In this section only the Fredholm equations which follow the five-fold statement will be discussed. Equations which follow the five-fold statement shall be freely called by adjective "adherent" in the rest of this thesis. Likewise, the compiled results in the end of this chapter come solely from equations complying to the five-fold statement. We remember that  $f(x)$  can be expressed formally as the Neumann series  $\sum_{i=0}^{\infty} r_i(x) \cdot (\lambda)^i$ .  $|r_i(x)|$

does happen to have an upper bound. Remember that  $rN(x)$  equals:

$$\int_a^b dy_1 \int_a^b dy_2 \dots \int_a^b dy_{(N-1)} \int_a^b dy_N G(x,y_1) \cdot G(y_1,y_2) \cdot \dots \cdot G(y_{N-2}, y_{N-1}) \cdot G(y_{N-1},y_N) \cdot g(y_N).$$

An upper bound to this quantity is:

$$|r_j(x)| \leq (\text{Max}\{G(x,y),x,y\})^j \cdot \text{Max}\{g(y),y\} \cdot (b-a)^j. \quad (2.12)$$

If there is a weak infinity, then the inequalities of (2.13) apply:

Break  $G(x,y)$  into two functions.  $G(x,y) = H(x,y) \cdot R(x,y)$ .  $H(x,y)$  is finite.

$R(x,y)$  is of scaleable infinity.

$$|r_j(x)| \leq (\text{Max}\{H(x,y),x,y\})^j \cdot \text{Max}\{g(y),y\} \cdot (b-a)^j \cdot |\text{Int}[R(x,y),\{y,a,b\}]|$$

so long as  $R(x,y) \neq 0$  anywhere in  $\{a,b\}$ .

$$|r_j(x)| \leq (\text{Max}\{H(x,y),x,y\})^j \cdot \text{Max}\{g(y),y\} \cdot (b-a)^j \cdot \text{Int}[|R(x,y)|,\{y,a,b\}]$$

$$\text{if } R(x,y) = 0 \text{ somewhere in } \{a,b\}. \quad (2.13)$$

Furthermore, it is clear that it is very unlikely for  $r_j(x)$  to suddenly turn into zero.  $r_j(x)$  does not ever turn into zero if  $G(x,y)$  does not change sign in  $y,\{a..b\}$  and if  $g(y)$  does not change sign in  $y,\{a..b\}$ . A lower bound for  $r_j(x)$  is:

$$|r_j(x)| \geq \text{Min}\{G(x,y),x,y\}^j \cdot \text{Min}\{g(y),y\} \cdot (b-a)^j \quad (2.14)$$

Inequalities (2.12), (2.13), and (2.14), imply that *adherent* Neumann series tend to asymptotically either evolve into a geometric series or into something very similar to a geometric series such as (geometric series  $\cdot (N^{\text{integer}} + \text{constant})$ ). If  $G(x,y)$  and  $g(y)$  are positive definite (including the possibility that  $G(x,y)$  is of scaleable infinity), then it is inevitable that the given adherent Neumann series evolve into a geometric series or into something very similar to a geometric series such as (geometric series  $\cdot (N^{\text{integer}} + \text{constant})$ ). Geo-

metric series are very well known. Let us suppose that  $r_j(x)$  of the Neumann series is expressible as  $(C_1(x) \cdot a_1^j + C_2(x) \cdot a_2^j + \dots + C_m(x) \cdot a_m^j)$ , where  $m \neq \text{infinity}$ . Regardless of the magnitude of the  $\lambda$ , the Neumann series of last statement represents the function  $C_1(x)/(1 + a_1 \cdot \lambda) + C_2(x)/(1 + a_2 \cdot \lambda) + \dots + C_m(x)/(1 + a_m \cdot \lambda)$ . Naturally, Neumann series that are very similar to a geometric series will have solutions that have a structural form which is very similar to  $C_1(x)/(1 + a_1 \cdot \lambda) + C_2(x)/(1 + a_2 \cdot \lambda) + \text{etc.}$ , at least when  $\lambda$  is within the radius of convergence. Therefore, if  $G(x,y)$  and  $g(y)$  of an adherent series do not change sign with respect to  $y$  in the range  $\{a..b\}$ , then it only makes sense that the solution can be approximated by partial fractions with ever increasing success.

Truly, the Neumann series whose  $r_j(x)$  equals

$$(C_1(x) \cdot a_1^j + C_2(x) \cdot a_2^j + \dots + C_m(x) \cdot a_m^j)$$

is exactly solvable with the Padé approximants  $\text{Pade}[m-1,m]$  and  $\text{Pade}[m,m]$  and  $\text{Pade}[m,m+1]$  and  $\text{Pade}[m+1,m+1]$  and so forth. The coefficients  $r_j(x)$  represent exactly the correct function which the complete summation of the above Neumann series equals when  $\lambda$  is small. See the reference Phys. Rev. E [7], which gives the formal foundation of the complete success of reproducing and additive combination of plural geometric series with Padé approximants.

Let us also consider the case of  $r_j(x) = (C_1(x) \cdot a_1^j + C_2(x) \cdot j \cdot a_1^j + C_3(x) \cdot j^2 \cdot a_1^j + \dots)$ . When the coefficients equal  $(C_1(x) \cdot a_1^j + C_2(x) \cdot j \cdot a_1^j + C_3(x) \cdot j^2 \cdot a_1^j + \dots)$ , the function represented by this series is also possible to find exactly by taking Padé approximants of the series. For a certain large but finite  $M$ , the expressions  $\text{Pade}[M,M+1]$  and  $\text{Pade}[M+1,M+1]$  and  $\text{Pade}[M+1,M+2]$  and so forth will evaluate perfectly the  $f(x)$  repre-

sented by the series. The reason for this is a very direct implication of the discussion of geometric series provided in the Phys. Rev. E reference [7].

### Presentation of Results.

Now that Padé approximants have been demonstrated as being a very strong candidate for finding the solutions of Fredholm integral equations which adhere to the five-fold statement, it is time to show various examples of integral equations, the Neumann series of these Fredholm equations, and the Padé approximants for the solutions of these integral equations. In the rest of the second chapter, five particular Fredholm examples will be studied. Immediately below, is given the subsequent kernels of these five integral equations.

$$G1(x,y) = (x \cdot y)^2.$$

$$G2(x,y) = (x \cdot y)^2 + (x \cdot y)^4.$$

$$G3(x,y) = (x \cdot y)/(1 + (x+y)/2).$$

$$G4(x,y) = (x \cdot y) \cdot (1 + (x+y)/4)^{1/3}.$$

$$G5(x,y) = Ei(|x-y|).$$

Tables 1.) through 3.) show the results of various approaches to solving the equation  $f(x) = x + \lambda \cdot \int_0^1 (x \cdot y)^2 f(y) \cdot dy$ . Our  $G(x,y)$  equals  $(x \cdot y)^2$  here. When  $G(x,y)$  equals

$G1(x,y)$ , 'functio[x,lam]', the closed form solution for  $f(x)$  is  $x + x^2 \cdot 5/2 \cdot \lambda / (5 - \lambda)$ .

**Table 2.1)**Results of  $G(x,y) = (x \cdot y)^2$ .

x	$\lambda$	PT[4]	Pade[1,2]	Pade[2,1]	Pade[2,2]	functio[x,lam]
0.2	0.1	.2010204	0.20100503	0.201020408	0.201020408	0.201020408
0.2	0.3	.2031908	0.20304569	0.203191489	0.203191489	0.203191489
0.2	0.5	0.20555	0.20512821	0.205555556	0.205555556	0.205555556
0.2	0.7	0.2081172	0.20725389	0.208139535	0.208139535	0.208139535
0.2	0.9	.2109116	0.20942408	0.210975610	0.210975610	0.210975610
0.2	1.1	0.2139524	0.21164021	0.214102564	0.214102564	0.214102564
0.2	2	0.2312	0.22222222	0.233333333	0.233333333	0.233333333
0.2	6	0.4184	0.28571429	-0.1	-0.1	-0.10000
0.2	12	1.2992	0.5	0.114285714	0.114285714	0.114285714

**Table 2.2)**Results of  $G1(x,y) = (x \cdot y)^2$ .

x	$\lambda$	PT[4]	Pade[0,1]	Pade[1,1]	Pade[1,2]	functio[x,lam]
0.8	0.1	0.816326	0.81632654	0.816326531	0.816326531	0.816326531
0.8	0.3	0.851053	0.85106384	0.851063830	0.851063830	0.851063830
0.8	0.5	0.8888	0.88888889	0.888888889	0.888888889	0.888888889
0.8	0.7	0.929875	0.93023257	0.930232558	0.930232558	0.9302325581
0.8	0.9	0.974585	0.97560977	0.975609756	0.975609756	0.975609756
0.8	1.1	1.023238	1.02564104	1.025641026	1.025641026	1.025641026
0.8	2	1.2992	1.33333334	1.333333333	1.333333333	1.333333333

0.8	6	4.2944	-4.0000001	-4.	-4.	-4.
0.8	8	7.4048	-1.3333335	-1.3333333	-1.3333333	-1.3333333
0.8	12	18.3872	-0.5714287	-0.5714285	-0.5714285	-0.5714285

Table 2.3)

Results of  $G1(x,y) = (x \cdot y)^2$ .

x	$\lambda$	PT[4]	Pade[0,1]	Pade[1,1]	Pade[1,2]	functio[x,lam]
2.	0.1	2.10204	2.10526316	2.102040816	2.102040816	2.102040816
2.	0.3	2.31908	2.35294118	2.319148936	2.319148936	2.319148936
2.	0.5	2.555	2.66666667	2.555555556	2.555555556	2.555555556
2.	0.7	2.81172	3.07692308	2.81395349	2.81395349	2.81395349
2.	0.9	3.09116	3.63636364	3.09756098	3.09756098	3.09756098
2.	0.1	3.39524	4.44444444	3.41025641	3.41025641	3.41025641
2.	2	5.12	101.010	5.333333333	5.333333333	5.333333333
2.	6	23.84	-1.	-28.	-28.	-28.
2.	8	43.28	-0.6666667	-11.333333	-11.333333	-11.333333
2.	12	111.92	-0.4	-6.5714286	-6.5714286	-6.5714286

Tables 2.4) through 2.6) show the results of various approaches to solving the

equation  $f(x) = x + \lambda \cdot \int_0^1 ((x \cdot y)^2 + (x \cdot y)^4) \times f(y) \cdot dy$ . Our  $G(x,y)$  equals  $G2(x,y)$ , which



equals  $(x \cdot y)^2 + (x \cdot y)^4$  here. When  $G(x,y)$  equals  $G_2(x,y)$ , 'functio[x,lam]', the closed form solution for  $f(x)$  is  $x + B_{(1)}(\lambda) \cdot x^2 + B_{(2)}(\lambda) \cdot x^4$ .  $B_{(i)}(\lambda)$  equals  $(\lambda \cdot d\{i\} + \lambda^2 \cdot p\{i\}) / (a_{(i)} + b_{(i)} \cdot \lambda + c_{(i)} \cdot \lambda^2)$ .

**Table 2.4)**

Results of  $G(x,y) = (x \cdot y)^2 + (x \cdot y)^4$ .

x	$\lambda$	PT[4]	Pade[1,2]	Pade[2,1]	Pade[2,2]	functio[x,lam]
0.2	0.1	0.20105801	0.2010580143	0.2010580142	0.2010580143	0.2010580143
0.2	0.3	0.20338084	0.2033810707	0.2033810702	0.2033810718	0.2033810718
0.2	0.5	0.20602666	0.2060298342	0.2060298298	0.2060298443	0.2060298443
0.2	0.7	0.20906169	0.209080091	0.2090800711	0.2090801362	0.2090801362
0.2	0.9	0.212563	0.2126331202	0.2126330562	0.2126332654	0.2126332654
0.2	1.1	0.21661852	0.2168273967	0.2168272265	0.2168277837	0.2168277837
0.2	2	0.24463071	0.2517068237	0.251701417	0.2517191991	0.2517191991
0.2	6	0.93779474	0.1298624528	0.1297650737	0.1300903226	0.1300903226

**Table 2.5)**

Results of  $G(x,y) = (x \cdot y)^2 + (x \cdot y)^4$

x	$\lambda$	PT[4]	Pade[1,2]	Pade[2,1]	Pade[2,2]	functio[x,lam]
0.8	0.1	0.82354303	0.823543046	0.823543045	0.823543045	0.823543045
0.8	0.3	0.87535527	0.875360552	0.875360544	0.875360547	0.875360547
0.8	0.5	0.93454966	0.934622478	0.934622405	0.934622437	0.934622437
0.8	0.7	1.0026402	1.003062157	1.003061831	1.003061975	1.003061975
0.8	0.9	1.0813891	1.082996378	1.082995328	1.082995791	1.082995791
0.8	1.1	1.1728071	1.177593433	1.177590631	1.177591864	1.177591864
0.8	2	1.8073649	1.969494306	1.969404224	1.969443581	1.969443581

0.8	6	17.629385	-0.83783352	-0.83953130	-0.83881290	-0.83881290
0.8	6	184.27079	-0.21517544	-0.21807626	-0.21691315	-0.21691315

Table 2.6)

More results of  $G(x,y) = (xy)^2 + (xy)^4$

x	$\lambda$	PT[ 4]	Pade[1,2]	Pade[2,1]	Pade[2,2]	functio[x,lam]
2.0	0.1	2.3786623	2.378662623	2.378662643	2.378662635	2.378662635
2.0	0.3	3.2151339	3.215221196	3.215223119	3.215222349	3.215222349
2.0	0.5	4.175243	4.176452426	4.176469535	4.176462695	4.176462695
2.0	0.7	5.2843612	5.291384196	5.291460749	5.291430193	5.291430193
2.0	0.9	6.5720219	6.598799388	6.59904599	6.598947726	6.598947726
2.0	1.1	8.0719208	8.151709253	8.152367254	8.152105495	8.152105495
2.0	2	18.560607	21.26398424	21.2851619	21.276796	21.2767962
2.0	6	283.04706	-26.7017264	-26.2993680	-26.451613	-26.451613
2.0	9	1099.2202	-19.3586745	-18.8739908	-19.0518519	-19.0518519
2.0	12	3074.638	-17.5413438	-16.8463607	-17.093010	-17.093010

Next, tables are given of the  $f(x)$  solutions where  $G(x,y)$  is set as  $G3(x,y)$  and then as  $G4(x,y)$ .

$$G3(x,y) = (x \cdot y)/(1 + (x + y)/2).$$

$$G4(x,y) = (x \cdot y) \cdot (1 + (x+y)/4)^{1/4}.$$

The fourth column of Tables 2.7) through 2.8) is labeled as 'Fredholm Solu'. The values of the fourth column were obtained by using a formal Fredholm integral equation solution

as given in the text by Mathews and Walker [6.b]. Truncating the numerator and denominator components was inevitable.

**Table 2.7)**

Results when this kernel is  $G(x,y) = x \cdot y / (1 + (x+y)/2)$

x	La	Pade[3,3]	Fredholm Solu.	Pade[3,4]	Pade[4,3]	Partl. Sum(7th)
2	.2	.209444959	.209447337	.209444959	.209444959	.209444959
2	.6	.230801551	.230824825	.230801551	.230801551	.230801478
2	.8	.242937544	.242980808	.242937544	.242937544	.242936972
2	1.0	.256230540	.256301372	.256230540	.256230540	.256227687
2	1.5	.295756953	.295937944	.295756953	.295756953	.295701612
2	2.0	.347648840	.348021053	.347648840	.347648840	.347169427
2	2.5	.418781733	.419471364	.418781733	.418781733	.416072018
2	3.0	.522288136	.523507587	.522288136	.522288136	.510369763
2	3.5	.686771350	.688920771	.686771349	.686771349	.641382308
2	4.0	.988597736	.992578504	.988597736	.988597736	.824763068
2	4.5	1.723037450	1.731688626	1.723037450	1.723037450	1.081608474
2	4.95	4.9190256	4.9485086	4.9190256	4.9190256	1.398385
2	5.25	-23.51430444	-23.67199915	-23.5143047	-23.5143047	1.66756407
2	5.45	-4.901950234	-4.937097054	-4.901950245	-4.90195025	1.87799188
2	5.7	-2.480207897	-2.499516114	-2.480207901	-2.48020790	2.18117346
2	6	-1.566373370	-1.579769179	-1.566373372	-1.56637337	2.61260900
2	7	-.717464252	-.725586120	-.717464253	-.717464253	4.75525166

2	5.197	1713.845	1722.8284	1713.8438	1713.8437	1.6161504
2	5.198	-4325.64762	-4368.55155	-4325.65459	-4325.65470	1.6171044

Table 2.8)

Results when the kernel is:  $G_4(x,y) = (x \cdot y) \cdot (1 + (x+y)/4)^{(1/2)}$

x	La	Pade[3,3]	Fredholm Solu.	Pade[3,4]	Pade[4,3]	Pt. Sum(7)
.2	.1	.207431617	.207431369	.207431617	.207431617	.207431617
.2	.3	.224154144	.224151730	.224154144	.224154144	.224154139
.2	.5	.243919600	.243912286	.243919600	.243919600	.243919271
.2	.8	.281377248	.281355562	.281377248	.281377248	.281360858
.2	1.2	.354655293	.354593465	.354655293	.354655293	.354123100
.2	1.8	.586942002	.586709853	.586942002	.586942002	.564191676
.2	2.2	1.052608132	1.051982257	1.052608132	1.05260813	.848367842
.2	2.58	4.413194958	4.409538238	4.413194958	4.41319496	1.33439330
.2	2.64	8.952364069	8.944505104	8.952364069	8.95236407	1.43985646
.2	2.67	18.45412287	18.43716605	18.45412287	18.4541229	1.49623399
.2	2.68	28.56573659	28.53865773	28.56573660	28.5657366	1.51559240
.2	2.69	63.20939388	63.14420356	63.20939388	63.2093939	1.53524040
.2	2.694	122.7838494	122.6407043	122.7838494	122.783849	1.54318160
.2	2.70	-296.631043	-296.559456	-296.631043	-296.631042	1.55518207
.2	2.75	-10.0597911	-10.0506349	-10.0597911	-10.0597911	1.65944106
.2	2.8	-5.11332430	-5.10843595	-5.11332430	-5.11332430	1.77167973
.2	2.9	-2.57549830	-2.57283689	-2.57549830	-2.57549830	2.02238932
.2	3.0	-1.71970859	-1.71780031	-1.71970859	-1.71970859	2.31224235
.2	3.5	-.642941483	-.641961379	-.642941483	-.642941483	4.56544993
.2	4.0	-.393339633	-.392550771	-.393339633	-.393339633	8.94246821

It is significant to note that the Fredholm formal solution is useless in finding the solution to the Fredholm integral equation in which  $(E_i |x-y|)$  serves as the kernel  $G(x,y)$ . The reason is that  $G(x,x)$  equals infinity. The numerator and denominator of the Fredholm

solution both become a collection of infinities [6]. Due to this failure, there is no Fredholm solution column in Table 2.9) and in Table 2.10).

Table 2.9)

Results when  $G(x,y)$  is  $Ei(|x-y|)$

x	Lam	Seria(ord5)	Pade[2,3]	Pade[3,2]	Pade[2,2]
.2	-2.09	18.340754525	2.318179190	2.318096492	2.362954069
.2	-1.99	15.603592781	1.990174197	1.990108969	2.027162828
.2	-1.89	13.270037379	1.667131299	1.667077716	1.699048643
.2	-1.79	11.291168861	1.320900088	1.320853858	1.349914408
.2	-1.69	9.622323568	.908506593	.908463983	.936774927
.2	-1.59	8.222895481	.344757396	.344713982	.375308207
.2	-1.49	7.056138076	-.593341676	-.593394444	-.553816537
.2	-1.39	6.088966172	-2.795127212	-2.795222310	-2.719113628
.2	-1.34	5.670838047	-5.836192323	-5.836379393	-5.681921379
.2	-1.315	5.476621127	-9.344593075	-9.344930402	-9.062801227
.2	-1.29	5.291757775	-18.374303249	-18.375240542	-17.58790727
.2	-1.275	5.185165431	-36.822684621	-36.825798158	-34.25628334
.2	-1.24	4.948531221	37.017542031	37.015481719	38.991500002
.2	-1.19	4.638155932	11.381135887	11.381025580	11.486444978
.2	-1.09	4.104870577	5.723787227	5.723777550	5.733771458
.2	-.990	3.671480382	4.242134286	4.242132350	4.244326319
.2	-.790	3.035854927	3.120396382	3.120396246	3.120589255
.2	-.490	2.464054761	2.466993833	2.466993831	2.466998947
.2	-.290	2.230310578	2.230410886	2.230410886	2.230411087
.2	-9e-5	2.061735303	2.061735377	2.061735377	2.061735378
.2	.110	1.933325456	1.933325667	1.933325667	1.933325667
.2	.310	1.831102714	1.831195307	1.831195307	1.831195235
.2	.510	1.745773071	1.747402105	1.747402105	1.747401498
.2	.710	1.666385998	1.677045227	1.677045226	1.677042930
.2	.910	1.573993598	1.616905440	1.616905435	1.616899540
.2	1.11	1.435309769	1.564762978	1.564762966	1.564750881

For Table 2.10) let  $G(x,y)$  equal  $Ei(|x-y|)$ .  $x$  equals .6 here.

Table 2.10)

Results when  $G(x,y) = Ei(|x-y|)$ 

x	Lam	Seria( ord5 )	Pade[2,3]	Pade[3,2]	Pade[2,2]
.6	-1.69	19.996901720	-3.795400749	-3.798071519	-4.439191961
.6	-1.59	16.505757149	-4.978610463	-4.981205278	-5.586034634
.6	-1.49	13.616222660	-7.238984701	-7.242017914	-7.949226574
.6	-1.39	11.241556142	-13.032371071	-13.037682151	-14.31596451
.6	-1.34	10.222705503	-21.361524975	-21.371912448	-23.97630833
.6	-1.315	9.751427961	-31.166218472	-31.185035552	-36.10655325
.6	-1.29	9.304157181	-57.064642506	-57.118239797	-72.70931766
.6	-1.275	9.046888766	-112.756737525	-112.94643477	-184.1894497
.6	-1.24	8.477553364	90.246348097	90.150410162	72.197437162
.6	-1.19	7.735041962	25.665805931	25.660283629	24.398926316
.6	-1.09	6.473318181	10.815080174	10.814598385	10.692874199
.6	-.990	5.465659950	6.998405796	6.998311081	6.972371474
.6	-.790	4.033918126	4.261025220	4.261018778	4.258885608
.6	-.490	2.835433636	2.843321011	2.843320909	2.843268990
.6	-.290	2.392868412	2.393137398	2.393137396	2.393135448
.6	-.009	2.100497580	2.100497780	2.100497780	2.100497776
.6	.1100	1.895674823	1.895675390	1.895675390	1.895675395
.6	.3100	1.744400324	1.744648142	1.744648141	1.744648771
.6	.5100	1.624517830	1.628875488	1.628875477	1.628880659
.6	.7100	1.508911711	1.537411391	1.537411331	1.537430494
.6	.9100	1.348704017	1.463387760	1.463387565	1.463435807
.6	1.110	1.056451538	1.402283414	1.402282933	1.402380088

For the above Fredholm equation where  $G(x,y) = Ei(|x-y|)$ , more than one numerical test was done on properly functioning numerical source code in the Maple programs `mistaky6.ms` and `chek6rhs.ms`. A text book entitled Integral Equations [7.b] discusses this particular integral equation.

## Chapter 3

### The Radiative Transfer Equation and the H-function

#### Mathematical Introduction, Showing Recursive Relation

In this chapter, radiative scattering off of a semi-infinite, plane-parallel, isotropically scattering material medium for the transmission of light shall be considered for the most significant application of extracting solutions to integral equations in this dissertation. Much of the material discussed here is also covered in publication [8]. The intensity of *diffusively scattered* electromagnetic radiation is expressed as  $I(\tau, \cos(\phi))$ . The integro-differential equation which describes this diffusively scattered penetration was developed by Chandrasekhar in [9.a]. In the work discussed here, only the example of a isotropically scattering material medium was considered.

The differentio-integral equation which expresses the change in intensity with respect to depth of penetration in the material medium is:

$$u \frac{dI(\tau, u)}{d\tau} = I(\tau, u) + \frac{w}{2} \int_{-1}^1 I(\tau, u') \cdot du' + \text{damped Amp} e^{\tau/u_0} \quad (3.1)$$

Already this equation has been selected for modification for the isotropic condition. By the use of the conversion factor  $H(u)$  and  $F$  on equation (1-3), we indirectly end up with the

integral equation: 
$$H(u) = 1 + 1/2 \cdot \omega \cdot H(u) \int_0^1 \frac{1}{(u+u')} \cdot H(u') \cdot du' \quad (3.2)$$

$H(u)$  is related to  $I(0, u, u_0)$  as:  $I(0, u, u_0) = 1/4 \cdot \omega \cdot F \cdot u_0 / (u+u_0) \cdot H(u) \cdot H(u_0)$ . See reference [9.b].  $u_0$  is  $\cos(\phi)$  of the incoming plane wave. In equations (3.1) and (3.2),  $u$  is equivalent to  $\cos(\phi)$ , and  $\tau$  is related to penetration depth through a direct proportionality. The

more creative and mathematically inclined reader might move to linearly transform (3.1) into a linear Fredholm integral equation of the second kind. However, if this person chooses a good transforming function, the Fredholm equation to solve will involve a formidably difficult singularity within the kernel. This is a much more detrimental situation than the one imposed by a 'scaleable infinity' from chapter 2.

A solution to the H-function is proposed to be in the form of the following partial sum:  $H_{(n)}(x, W_2) = g_0[x] + W_2 \cdot g_1[x] + (W_2)^2 \cdot g_2[x] + \dots + (W_2)^n \cdot g_{\{n\}}[x]$ ,

$$\text{where } W_2 = \omega/2. \quad (3.2f)$$

The RHS of (3.2f) is to be plugged into (2-3). All of the coefficients of particular integer powers of  $\omega$  are match in order to construct a complete successive set of recursive equations. These recursive steps and assignments to  $g_{\{m\}}[x]$  are given on the next several lines.

Let us begin an iteration for a recursion.  $g_0[x]$  equals 1 of equation (3.2).  $G[u, y]$  is built to equal  $1/(u+y)$ .

The following steps amount to a recursive iteration.

$$\begin{aligned} g_1[x] &= x \cdot g_0[x] \cdot \int_0^1 g_0[y] \cdot G[x, y] \, dy \\ g_2[x] &= x \cdot g_0[x] \cdot \int_0^1 g_1[y] \cdot G[x, y] \, dy + x \cdot g_1[x] \cdot \int_0^1 g_0[y] \cdot G[x, y] \, dy \\ g_3[x] &= x \cdot g_0[x] \cdot \int_0^1 g_2[y] \cdot G[x, y] \, dy + x \cdot g_1[x] \cdot \int_0^1 g_1[y] \cdot G[x, y] \, dy + \\ &\quad x \cdot g_2[x] \cdot \int_0^1 g_0[y] \cdot G[x, y] \, dy \end{aligned} \quad (3.3)$$

In repetitive generality, it is clear that:



$$\begin{aligned}
g_{\{n+1\}}[x] = & x \cdot g_0[x] \cdot \int_0^1 g_n[y] \cdot G[x,y] dy + x \cdot g_1[x] \cdot \int_0^1 g_{\{n-1\}}[y] \cdot G[x,y] dy + \dots \\
& x \cdot g_{\{n-1\}}[x] \cdot \int_0^1 g_1[y] \cdot G[x,y] dy + x \cdot g_{\{n\}}[x] \cdot \int_0^1 g_0[y] \cdot G[x,y] dy. \quad (3.4)
\end{aligned}$$

In specific application to the H-function,  $g_0[x]$  and  $g_1[x]$  are set as:

$$g_0[x] \equiv 1 \text{ and } g_1[u] \equiv u \log[(1+u)/u].$$

Furthermore,  $f(y) = \log((1+y)/y)$ , and  $g_1[y] = y \cdot f[y]$ .

The following review steps can be re-stated as a recursive iteration.

$$g_1[x] = x \cdot \int_0^1 1 \cdot G[x,y] dy, \text{ one term.}$$

$$g_2[x] = x \cdot \int_0^1 y \cdot f(y) \cdot G[x,y] dy + x \cdot (x \cdot f[x]) \cdot \int_0^1 1 \cdot G[x,y] dy, \text{ two terms.}$$

$$\begin{aligned}
g_3[x] = & x \cdot \int_0^1 y \cdot 1 \cdot \int_0^1 z \cdot f[z] \cdot G[y,z] dz \cdot G[x,y] dy + x \cdot \int_0^1 y \cdot f[y] \cdot \int_0^1 1 \cdot G[y,z] dz \cdot G[x,y] dy + \\
& x \cdot (x \cdot f[x]) \cdot \int_0^1 (y \cdot f[y]) \cdot G[x,y] dy + x \cdot x \cdot \int_0^1 (y \cdot f[y]) \cdot G[x,y] dy \cdot \int_0^1 1 \cdot G[x,y] dy + \\
& x \cdot x \cdot (x \cdot f[x]) \cdot \int_0^1 1 \cdot G[x,y] dy \cdot \int_0^1 1 \cdot G[x,y] dy, \text{ five terms.} \quad (3.5)
\end{aligned}$$

This can be re-stated at a more simplistic level as:

$g_0$  has 1.  $g_1$  has  $G$ .  $G(x,y)$  has  $G$ .

$g_1[x] \rightarrow 1 \cdot G$ .

$g_2[x] \rightarrow G \cdot G + G \cdot G \rightarrow 2 \cdot G^2$ .

$g_3[x] \rightarrow (2 \cdot G^2) \cdot G + G \cdot G \cdot G + (2 \cdot G^2) \cdot G \rightarrow 5 \cdot G^3$ .

$g_4[x] \rightarrow (2 \cdot 1 \cdot (5 \cdot G^3) + 2 \cdot G \cdot (2 \cdot G^2)) \cdot G \rightarrow (10+4) \cdot G^3 \cdot G = 14 \cdot G^4$ .


The magnitude recursion relation to use is:

$$g_{\{n+1\}}[x] \rightarrow g_0 \cdot g_{\{n\}}[y] \cdot G + g_{\{1\}}[x] \cdot g_{\{n-1\}}[x] \cdot G + g_2[x] \cdot g_{\{n-2\}}[x] \cdot G + \dots + g_{\{n-1\}}[x] \cdot g_{\{1\}}[x] \cdot G + g_{\{n\}}[x] \cdot g_0 \cdot G. \quad (3.6)$$

If the recursion relation for term counting is carried out several hundred times on code on a PC, then it becomes evident inductively that  $g_{[N+1]}/g_{[N]}$  approaches the value 4 as  $N$  becomes large. Restated, this means that the number of terms in the expression for  $g_n[x]$  grows approximately as  $C \cdot 4^n$  when  $n$  is very large. *The significance of this is that if the inductively discovered premise of  $C \cdot 4^n$  growth is true, then  $g_{\{n\}}[x]$  asymptotically grows as a geometric series.* Furthermore, by considering also the fact that  $G(x,y)$  in this chapter remains finite (except in the one unusual case where external  $x$  of  $G(x,y)$  equals 0), it is possible to conclude that  $g_{\{n\}}[x]$  does not grow faster than portrayed by an appropriate upper bound of the following form:

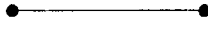
$$\text{Large } C \cdot n^{jj} \cdot 4^n. \quad (3.7)$$

$jj$  is a non-negative constant integer.

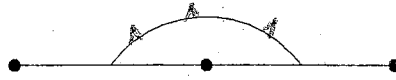
It was explained in Chapter 2 that a series which has the asymptotic form of (3.7) is an extremely strong candidate for successful estimates to the full value of the  $g$ -series through the use of Padé approximants. The  $g$ -series, of course, is  $H\text{func}(u,w) = \sum g_{\{n\}} \cdot w^n$ . The recursion relation (3.5) can be used to establish upper bounds on the magnitude  $g_{\{n\}}(u)$ . Indeed, the maximum possible growth of approximately  $4^n$  w.r.t.  $n$  was observed. There is a convenient way to keep track of the rate of  $g_{\{n\}}$  through the construction of analogous diagrams which represent  $g_{\{n\}}(x)$ . These diagrams follow rules which can be viewed as a simplification of the Feynman rules for the diagrams which describe the self-energy of a fermion.  $G(u,u')$  can be treated as the "interaction gauge boson" propagator, which is represented by the wavy line . A vertex is a point at which a  $\Psi(u)^*$

couples with a  $G(u,u')$  propagator and a plane wave state  $\Psi(u')$ .  $\Psi(u)^*$  is used to represent  $u^{-1}$ , or  $u \cdot g_0$  in the H-function expansion.  $\Psi(u')$  is used to represent 1, or  $g_0$ . Now, the first three diagrams represent  $g_0$ ,  $g_1(u)$ , and  $g_2(u)$ .

$g_0$  is depicted as



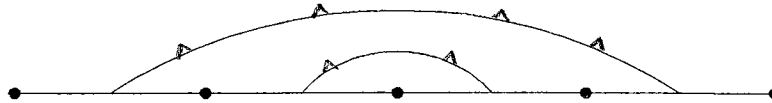
$g_1(u)$  is depicted as





$g_2(u)$  is depicted as



plus



Thus  $g_2(u)$  is depicted by 2 sub-diagrams. Unlike in the Feynman rules for QED, the wavy line  cannot cross over another wavy line  on the planar region of illustration.

By continuing with the same rules, the reader should with mild effort be able to see that  $g_3(u)$  is depicted by 5 sub-diagrams.  $g_4(u)$  is depicted by 14 sub-diagrams. It becomes clear that the number of sub-diagrams grows exactly at the same rate as the number of terms of  $g\{n\}$ , as shown in recursion (3.6). Those readers interested in the growth of the number of terms of  $g_{\{n\}}(u)$  and in the number of diagrams should view appendix D.

CONTINUE.

Let us consider the first few iterations.

$$g_0=1 .$$

$$f(u)= \ln(1+u) - \ln(u) .$$

$$g_1(u)= u \cdot f(u) .$$

$$g_2(u) = 2 \cdot \ln(2) - u \cdot \ln(2) \cdot \ln\left(\frac{u+1}{u-1}\right) - u \cdot \operatorname{dilog}\left(\frac{u+1}{u-1}\right) + u \cdot \operatorname{dilog}\left(\frac{u+1}{u}\right) + u \cdot \operatorname{dilog}\left(\frac{u}{u-1}\right). \quad (3.8)$$

$g_3(u)$  is not known with easily manageable known analytical functions. Subsequently, it will be even harder to calculate  $g_4(u)$ ,  $g_5(u)$ ,  $g_6(u)$ , et cetera. In the next several statements, an algorithm for construction  $g_3(u)$ ,  $g_4(u)$ , et cetera with a polynomial fitting method is described.

The approach used to calculate the  $g_3(u)$  useful for research of this dissertation was one of polynomial approximation of  $g_2(u)$ . In the research pertinent to Chapter 3, the polynomial for approximation is denoted as  $\operatorname{polfg}_2(u)$ . There where imposed 20 simultaneous matchups between  $\operatorname{polfg}_2(u)$  and  $g_2(u)$ , such that  $\operatorname{polfg}_2(.02) = g_2(.02)$ ,  $\operatorname{polfg}_2(.08) = g_2(.08)$ ,  $\operatorname{polfg}_2(.1) = g_2(.1)$ , and so on all the way up to  $\operatorname{polfg}_2(.95) = g_2(.95)$ , and  $\operatorname{polfg}_2(1.0) = g_2(1.0)$ .  $\operatorname{polfg}_2(u)$  is a nineteenth order polynomial for which each of the twenty coefficients are to be determined by the 20 simultaneous matchups. In fact twenty simultaneous equations determine the coefficients to  $\operatorname{polfg}_2(u)$ .  $\operatorname{polfg}_2(u)$  equals  $\sum_i (c_{4_i} \cdot u^i)$ .  $c_{4_i}$  is obtained numerically. However, the expression of  $\operatorname{polfg}_4(u)$  is a fairly accurate closed form symbolic expression in function of  $u$ . When  $u \geq 0$  and  $u \leq 1$ , the expression  $\operatorname{polfg}_2(u)$  gives a fairly accurate representation of  $g_2(u)$ . This is especially true because  $g_2(u)$  does not have any singularities in the range  $0 < u \leq 1$ . In the study of continuous functions, Weierstrauss proved that there does exist a sequence of polynomials of  $x$  which successfully approximates any given singularity free function of  $x$  [10, Weierstrauss ref.]. An immediate implication of the Weierstrauss theorem is that the expression  $\operatorname{polfg}_2(u) = \sum_i^{36} c_{4_i} \cdot u^i$  would be even more accurate than the above 19th order represen-

tation for  $\text{polfg2}(u)$ . Numerically, it was found that the difference between a 15 order and 19 order polynomial representation of  $g_2(u)$  when  $0 < u \leq 1$  was negligible *within  $10^{-8}$  percent*. Clearly for the purposes of approximating  $g_n(u)$ , there would be no significant improvement numerically in using the 35th order polynomial representation of  $g_2(u)$  over the 19th order representation.

Once the coefficients of  $\text{polfg2}(u)$  have been found, it is time to insert this into the equation of recursion:

$$g_3[x] = x \cdot g_0[x] \cdot \int_0^1 \text{polfg2}[y] \cdot G[x,y] dy + x \cdot g_1[x] \cdot \int_0^1 g_1[y] \cdot G[x,y] dy + x \cdot \text{polfg2}[x] \cdot \int_0^1 g_0[y] \cdot G[x,y] dy. \text{ See equations (3.3).}$$

$g_3(x)$  also is a very difficult expression to work with.  $\text{polfg3}(u)$  is designated as the polynomial representation of  $g_3(u)$ , which has turned into a transcendental function.  $\text{polfg3}(u)$  is taken out to the 19th order. In exactly the same manner that the coefficients of  $\text{polfg2}(u)$  were determined by  $g_2(u)$ ,  $\text{polfg3}(u)$  is also developed by matching  $\text{polfg3}(u)$  to  $g_3(u)$  for 20 different values of  $u$  in the linearly set interval within  $0 < u \leq 1$ . Once  $\text{polfg3}(u)$  is known explicitly as a function of  $u$ ,  $\text{polfg3}(u)$  is plugged in as  $g_3(u)$  into the recursion formula (4-3) used to generate  $g_4(u)$  from  $g_3(u)$ ,  $g_2(u)$ ,  $g_1(u)$ , and  $g_0$ . This time a long, unwieldy expression for  $g_4(u)$  is obtained. It is then imperative to obtain a polynomial expression  $\text{polfg4}(u)$  for the transcendental function  $g_4(u)$ . And, the whole process discussed in the beginning of this paragraph is repeated in order to generate  $g_5(u)$ . Next in turn  $g_6(u)$  is calculated.  $g_7(u)$ ,  $g_8(u)$ , and  $g_9(u)$  were also found. In table 3.1) are shown various values of  $g\{n\}(u)$ .

**Table 3.1)**

Example of the Values of  $g_{\{n\}}(u)$  for Three Values of  $u$

u	.2	.8	.9
g1(u)	.358351893845610	.648744172973062	.672492961647198
g2(u)	.275237355339286	.719900556021486	.764383975398485
g3(u)	.287877433553651	.950733073664056	1.02713349849796
g4(u)	.357372704916896	1.37630275650370	1.50657478108083
g5(u)	.493004968258362	2.11079374260696	2.33454751520814
g6(u)	.729201449707502	3.36926942602789	3.75753189158554
g7(u)	1.13238361159873	5.53857831222114	6.21921399540239
g8(u)	1.82224587124395	9.31253656724590	10.5169867574193
g9(u)	3.01278816189040	15.9409717133517	18.0904289321405

It should be noticed that  $g_{\{n\}}(u)$  is growing approximately at a geometric rate with respect to  $u$ .

Below are shown the excellent results for the calculations of H-functions out to 9th order.  $Hfun9(u, W_2)$  shall be defined as the following expression:

$$g_0 + g_1(u)W_2 + g_2(u)W_2^2 + \dots + g_9(u)W_2^9, \text{ where } W_2 = \omega/2. \quad (3.9)$$

This is a partial sum of the H-function. In the research involved in presenting the results for H-function calculations, Padé approximants were taken of  $Hfun9(u, w_2)$ . The most interesting results are the comparison of Pade[4,5], Pade[5,4],  $Hfun9(u, w_2)$  and established numerical results of H-funct( $u, w_2$ ) as presented in Chandrasekhar's text [11].

The reader might question the purpose of reproducing Chandrasekhar's results. The point is that a tremendously large range of H-function values can be calculated very quickly with algorithms presented in this chapter added with the last step of carrying out

Padé approximants. Chandrasekhar's approach is more intensive of computer CPU work time. For example somebody might want to reliably calculate  $H(.223, w_2)$  out to eight significant figures. It is more accurate to calculate the partial sum directly and then take the Padé approximants than it would be to interpolate  $H(.223, w_2)$  from the previously available data of  $H(.20, w_2)$  and  $H(.225, w_2)$ .

In the future, the author hopes to do more difficult cases of the H-function in cases where equation (3.1) has an anisotropic contribution to the Kernel of the integral term.

### Results of Series Iteration and Padé Approximants

In this section, tables are given in which evaluations of the H-function as a function of  $u$  and  $w$  are listed. Ninth order partial sums obtained through the use of the iterated  $g\{n\}$ 's are also listed. For the sake completeness, Table 3.1) on the previous page lists  $g_1(u)$ ,  $g_2(u)$ ,  $g_3(u)$ , through  $g_9(u)$  for a few values of  $u$ . Table 3.9) lists the corresponding values when  $u=1.0$ .

One example which demonstrates the numerical/semi-analytical results shall be given. The tables of this chapter were built from the information of examples such as this case when  $u=0.2$ . When  $u=.2$ , the ninth order partial sum equals:

$$\begin{aligned}
 & 1 + (\ln(1.2) - \ln(0.2)) \cdot W + (2 \cdot \ln(2) - 0.2 \cdot \ln(2) \cdot \ln((1.2)/(0.2-1)) - 0.2 \cdot \text{dilog}((1.2)/(0.2-1)) + \\
 & 0.2 \cdot \text{dilog}((1.2)/0.2) + 0.2 \cdot \text{dilog}(0.2/(0.2-1)) ) \cdot W^2 + .2878774335536509 \cdot W^3 + \\
 & .3573727049168958 \cdot W^4 + .4930049682583625 \cdot W^5 + .72920144970750169 \cdot W^6 + \\
 & 1.132383611598726 \cdot W^7 + 1.82224587124395 \cdot W^8 + 3.01278816189041 \cdot W^9. \quad (3.10)
 \end{aligned}$$

The best off-diagonal Padé approximant of the ninth order partial sum is:

Padé[4,5]:=

$$\frac{(1 - 3.9585037921261 \cdot (w/2) + 5.1170726839235 \cdot (w/2)^2 - 2.3777169816148 \cdot (w/2)^3 + 2.8346980726021 \cdot (w/2)^4)}{(1 - 4.3168556859718 \cdot (w/2) + 6.3887887391104 \cdot (w/2)^2 - 3.7668690168198 \cdot (w/2)^3 + 0.76025376791391 \cdot (w/2)^4 + (-1) \cdot 0.025121992194445 \cdot (w/2)^5)}$$

(3.11)

Table 3.2) uses information based on the simple 'number crunching' of (3.10) and (3.11).

**Table 3.2)**

Comparison of the Established Numerically Labored Values of the H-function to Padé Approximants.

u	w	Partl Sum	Padé[4,5]	Padé[5,4]	Book Value*
.2	0.2	1.038917	1.038917	1.038917	1.03892
.2	0.3	1.0611464	1.0611464	1.0611464	1.06115
.2	0.4	1.0857798	1.0857806	1.0857806	1.08578
.2	0.5	1.1134523	1.1134608	1.1134608	1.11349
.2	0.6	1.1451004	1.1451632	1.1451632	1.14517
.2	0.8	1.2268261	1.2286126	1.2286101	1.2286
.2	0.9	1.2826089	1.2910541	1.2910254	1.2914
.2	0.95	1.3162682	1.3352346	1.3351214	1.3373
.2	.975	1.3349166	1.3641043	1.3638625	1.3703
.2	1.0	1.3549552	1.4013931	1.400834	1.4503

\* Note that the book values listed in Tables 3.2) through 3.6) can be found on page 125 of Chandrasekhar's text Radiative Transfer [9.a].



**Table 3.3)**

Table of Percent Error of the Predictions from the Book Values.

u	w	Er Partl Sum	Er Pade[4,5]	Er Pade[5,4]
.2	0.2	-0.00028876	-0.000288761	-0.000288761
.2	0.3	-0.00033926	-0.000339255	-0.000339255
.2	0.4	-0.000018420	k0.000055260	0.000055260
.2	0.5	-0.0033858	-0.0026224	-0.0026224
.2	0.6	-0.0060777	-0.00059380	-0.00059380
.2	0.8	-0.14438	0.0010256	0.00082207
.2	0.9	-0.68074	-0.026785	-0.029007
.2	0.95	-1.5727	-0.15445	-0.16291
.2	0.975	-2.5822	-0.45214	-0.46979
.2	1.0	-6.5741	-3.3722	-3.4107

**Table 3.4)**

Comparison of Padé Approximants to the Respective Book Values.

u	w	Partl Sum	Pade[4,5]	Pade[5,4]	Book Value
.5	0.2	1.0611766	1.0611766	1.0611766	1.06117
.5	0.3	1.0975588	1.0975589	1.0975589	1.09756
.5	0.4	1.139189	1.1391915	1.1391915	1.14266
.5	0.5	1.1877068	1.1877338	1.1877338	1.18776
.5	0.6	1.2456059	1.2458041	1.2458041	1.24581
.5	0.8	1.4074908	1.4132035	1.4131974	1.4132
.5	0.9	1.5276527	1.5550945	1.555016	1.5560
.5	0.95	1.6034178	1.6661202	1.6657843	1.6718
.5	0.975	1.6463203	1.7442425	1.7434834	1.7621
.5	1.	1.6930899	1.8525719	1.8506767	2.0128

**Table 3.5)**

Table of Percent Error of the Predictions from the Book Values.

u	w	Er Partl Sum	Er Pade[4,5]	Er Pade[5,4]
.5	0.2	0.00062195	0.00062195	0.00062195
.5	0.3	-0.00010933	-0.00010022	-0.00010022
.5	0.4	-0.30377	-0.30355	-0.30355
.5	0.5	-0.0044790	-0.0022058	-0.0022058
.5	0.6	-0.016383	-0.00047359	-0.00047359
.5	0.8	-0.40399	0.00024767	-0.00018398
.5	0.9	-1.8218	-0.058194	-0.063239
.5	0.95	-4.0903	-0.33974	-0.35983
.5	0.975	-6.5705	-1.0134	-1.0565
.5	1.0	-15.884	-7.9605	-8.0546

**Table 3.6)**

Example "3.6"

u	w	PT	Pade[4,5]	Pade[5,4]	book valu
.8	0.2	1.0731869	1.0731869	1.0731869	1.07319
.8	0.3	1.117626	1.1176262	1.1176262	1.11763
.8	0.4	1.1693468	1.1693512	1.1693512	NotInRec
.8	0.5	1.2308361	1.2308834	1.2308834	1.23091
.8	0.6	1.3059536	1.3063032	1.3063032	1.30631
.8	0.8	1.5255334	1.535742	1.5357329	1.5358
.8	0.9	1.6961324	1.7459466	1.7458195	1.7474
.8	0.95	1.8062481	1.9219448	1.9213674	1.9313

.8	0.975	1.8693207	2.0525244	2.0511619	2.0833
.8	1.	1.9385969	2.2437188	2.2400986	2.5527

Table 3.7)

Table of Percent Error of the Predictions from the Book Values

u	w	Er Partl Sum	Er Pade[4,5]	Er Pade[5,4]
.8	0.2	-0.00028886	-0.00028885	-0.00028885
.8	0.3	-0.0003579	-0.00034000	-0.00034000
.8	0.4	-----	-----	-----
.8	0.5	-0.00600369	-0.002161	-0.002161
.8	0.6	-0.02728	-0.00052	-0.00052
.8	0.8	-0.668485	-0.0037765	-0.0043691
.8	0.9	-2.93394	-0.083175	-0.090449
.8	0.95	-6.4750	-0.48440	-0.51430
.8	0.975	-10.271	-1.4772	-1.5426
.8	1.0	-24.057	-12.104	-12.246

Table 3.8)

Example when  $u = .9$ 

u	w	PT	Pade[4,5]	Pade[5,4]	hbook
.9	0.2	1.0760988	1.0760988	1.0760988	1.07610
.9	0.3	1.122536	1.1225362	1.1225362	1.12254
.9	0.4	1.1768049	1.1768099	1.1768099	NotInRec
.9	0.5	1.2416375	1.2416917	1.2416916	1.24171
.9	0.8	1.5567244	1.5684491	1.5684391	1.5685
.9	0.9	1.7416792	1.7991723	1.7990297	1.8008
.9	0.95	1.8617356	1.9959527	1.9952943	2.0065
.9	0.975	1.9306907	2.1441549	2.1425814	2.1795
.9	1.0	2.0065636	2.3646482	2.3603886	2.7306

**Table 3.9)**List of  $g_n(1.0)$  when  $n = \{1, 2, 3 \dots 9\}$ .

	When $u=1$ .
g1	.693147180559945
g2	.804053834654890
g3	1.09662773728995
g4	1.62698942254175
g5	2.54414533551182
g6	4.12534574676417
g7	6.87024271658987
g8	11.67869437787
g9	20.17878923532

## Chapter 4

### Analysis of a Nonlinear Integral Equation

In this chapter another nonlinear integral equation will be solved through a method iteration. The series generated by these iterations will be further investigated with the use of Padé approximants in almost the same manner that was done in Chapter 3. The results of the inspection of the overall results of using Padé approximants for the examples of Chapter 3 are almost as impressive as the accuracy demonstrated in Chapter 3 with Padé approximants.

The form of the integral equation to be investigated in Chapter 4 is that of an integral term whose Kernel is coupled with the solution two-fold. The form appears as:

$$f(x) = g(x) + \lambda \int_a^b G(x, y) \cdot f(y) \cdot f(y) \cdot dy \quad (4.1)$$

Two particular examples of equation (4.1) shall be studied through the use of iterated series solutions in this chapter. Although the author does not know of any physical applications for this equation, it is interesting from a mathematical point of view the nature of the solution (or 2 solutions) of equation (4.1). Perhaps equation (4.1) is similar enough to the physically interesting equation (3.1) in order to lead also to illumination and assistance in some mathematical physics applications. The highest value of content in Chapter 4 is that it demonstrates the effectiveness of using Padé approximants for evaluating with much more precision the solution of (4.1) than one obtains by use of the series solution alone. This chapter serves as a nonlinear anecdotal note to the first area of thrust of this dissertation, solutions to integral equations.

Two particular examples of equation (4.1) are: the case where

$$g(x) = 1 \text{ and } G(x,y) = (xy)^2$$

and the case where  $g(x) = 1$  and  $G(x,y) = 1/(1+(x+y)/2)$ .

The algorithm for determining the detailed structure of the iterated series estimation of the nonlinear integral equation is very similar to the algorithm used to generate the series of the H-function in Chapter 3. In the next paragraph, the coefficients of the series  $\sum g_{1(x)} \Lambda^n$  shall be presented. And then, the rest of this chapter shall be devoted to the solutions and improved estimates of the solutions to the two examples where  $G(x,y)$  equals  $(xy)^2$  and  $G(x,y)$  equals  $1/(1+(x+y)/2)$ , respectively.

Note that  $g_0[x]$  equals  $g(x)$  of equation (4.1).

The following steps amount to a recursive iteration.

$$g_1[x] = \int_0^1 g_0[y] \cdot g_0[y] \cdot G(x,y) dy$$

$$g_2[x] = \int_0^1 (2 \cdot g_0[y] \cdot g_1[y]) \cdot G(x,y) dy$$

$$g_3[x] = \int_0^1 (2 \cdot g_0[y] \cdot g_2[y] + 1 \cdot g_1[y] \cdot g_1[y]) \cdot G(x,y) dy$$

$$g_4[x] = \int_0^1 (2 \cdot g_0[y] \cdot g_3[y] + 2 \cdot g_1[y] \cdot g_2[y]) \cdot G(x,y) dy \quad (4.2)$$

$$g_5[x] = \int_0^1 (2 \cdot g_0[y] \cdot g_4[y] + 2 \cdot g_1[y] \cdot g_3[y] + 1 \cdot g_2[y] \cdot g_2[y]) \cdot G(x,y) dy$$

The higher  $g_n[x]$  follow the pattern of iteration demonstrated here.

Nonlinear integral equation (4.1) in the example where  $g(x) = 1$  and  $G(x,y) = (xy)^2$  has the closed form solution of  $f(x,\lambda) = 1 + B(\lambda)x^2$ .

$$\text{Note: } B(\text{Lam}) = (-7 \cdot (2/5 - 1/\text{Lam}) + \text{Sqrt}[49 \cdot (2/5 - 1/\text{Lam})^2 - 4 \cdot 7/3]) / 2. \quad (4.3)$$

The series solution of the first example is found by using the recursion relations shown in (4.2). This series solution is to be denoted as  $H(x,\Lambda)$ .  $\Lambda$  and  $\lambda$  are interchangeable.

Note  $H(x,\Lambda) = g_0[x] + \Lambda \cdot g_1[x] + \Lambda^2 \cdot g_2[x] + \Lambda^3 \cdot g_3[x] + \Lambda^4 \cdot g_4[x] \dots$ .  $H\{n\}(x,\Lambda)$  is the partial sum taken to the  $n$ th order of  $\Lambda$ . Following the same mode of thought as in chapter 3,  $\text{pade}[3,4]$  is the Padé approximant of  $H_7(x,\Lambda)$  with respect to  $\Lambda$  in form  $\sum a_n \Lambda^n$  up to  $n = 3$  divided by the denominator of  $\sum b_n x^n$  up to  $n = 4$ . Likewise,  $\text{pade}[4,4]$  is the Padé approximant of  $H_8(x,\Lambda)$  with respect to  $\Lambda$ . The tables in the rest of this chapter serve to catalog my fairly successful results of doing the iteration of (4.2) and then applying Padé approximants.

**Table 4.1)**

Comparison when  $G(x,y) = (x \cdot y)^2$

x	$\lambda$	$H_6(x,\lambda)$	$H_8(x,\lambda)$	$\text{pade}[3,3]$	$\text{pade}[3,4]$	$\text{pade}[4,4]$	exact
.2	-1.40	.98995478	.98983706	.987537	0.987536	0.987536	.98753629
.2	-3.0	1.3022639	2.3765350	.979862	0.979833	0.979841	.97983855
.2	.75	1.0150371	1.0151287	1.01516	1.01517	1.01517	1.0151658
.2	1.18	1.0349451	1.0375611	1.04331	1.04466	1.04554	1.0488258

These results for the first example, where  $G(x,y)=(x \cdot y)^2$  do show successful application of Padé approximants to reliably calculating the solution from the iterated serial coefficients of (4.2). The second example ( $G(x,y)=1/(1+(x+y)/2)$ ) is very similar to the first example.

However, there is no well known closed form solution to equation (4.1) in the second example. Most probably it is not known. In this example Padé approximants of sequentially higher order converge to the same result. These common answers of convergence and the similarity of the particular integral equation of example 2 to that of the very successful example 1 make the reliability of the numerical results of example 2 very plausible.

Let us inspect numerical results of the second case, where  $G(x,y) = 1/(1+(x+y)/2)$ . As in Table 4.1),  $H\{n\}(x,\Lambda)$  is the partial sum of  $H(x,\Lambda)$  taken to the  $n$ th order of  $\Lambda$ .

**Table 4.2)**

The second case, where  $G(x,y) = 1/(1+(x+y)/2)$

x	$\lambda$	$H6(x,\lambda)$	$H10(x,\lambda)$	pade[4,4]	pade[4,5]	pade[5,4]	pade[5,5]
.4	.300	1.3139270	1.3231612	1.3256556	1.3256664	1.3279408	1.3258301
.2	.200	1.1853851	1.1858020	1.1858196	1.1858197	1.1858209	1.1858203
.4	-.70	1.1668171	3.9694534	.58944410	.58946170	.58933952	.58926976
.2	-.80	1.9485188	14.974905	.49563233	.49568671	.49535798	.49515534
.5	-.900	3.2598878	44.740611	.48200072	.48207240	.48145696	.48101183



Clearly, Table 4.1) demonstrates complete success of the application of Padé approximants. The results of Table 4.2) suggest very strongly the success of Padé approximants when  $G(x,y) = 1/(1 + (x+y)/2)$ .

## Chapter 5

### Numerical Results of the Asymptotic Padé Approximant Predictions

In this chapter, Asymptotic Padé Approximant Predictions will be introduced.

Numerical results of Asymptotic Padé Approximant Predictions of different series and the procedure involved will be discussed only in this chapter. First the procedure and formulas involved in making the Asymptotic Padé Approximant Predictions are discussed. Then the results of the Asymptotic Padé Approximant Predictions for the series of the H-function are presented. And finally, the results of the Asymptotic Padé Approximant Predictions for the Taylor series of  $\ln(1+x)/x$  is presented.

In addition to the use of Padé approximants and Padé Approximant Predictions, Dr. Mark Samuel rather recently has developed an improved method for estimating the successive terms of an infinite series. The predicted next successive term of this proposed method is called the Asymptotic Padé Approximant Prediction (APAP). With his initial desire to test APAP's and with the assistance of the author of this text, Asymptotic Padé Approximant Predictions have been successfully applied to many series entailing the inclusion of at least several terms for analysis of a desired mathematical function. The (APAP) procedure relevant for this dissertation text first involves making a Padé Approximant Prediction (PAP) for  $r_{n+1}$  based on the information available in the precise partial sum  $r_0 + r_1 \cdot x + r_2 \cdot x^2 + \dots + r_{n-1} \cdot x^{(n-1)} + r_n \cdot x^n$ . (cf. (1.13).) After predicting  $r_{n+1}$ , it is then necessary to predict the relative error (in decimal form) of the (PAP) in order to carry out the Asymptotic Padé approximant prediction. The Asymptotic Padé approximant prediction is defined in terms of the quantity 'arr' by:

$$\tilde{r}\{n+m+1\} = r\{n+m+1\}/(1+arr) , \quad (5.1)$$

where  $r\{n+m+1\}$  is the PAP of the partial sum  $r_0 + r_1 \cdot x + r_2 \cdot x^2 + \dots + r_{n+m-1} \cdot x^{(n+m-1)} + r_{n+m} \cdot x^{(n+m)}$  and  $\tilde{r}\{n+m+1\}$  is the APAP.

The Asymptotic Padé Approximant Prediction has proven to be very helpful in prediction of the terms  $g\{N\}[u]$  of the H-function series (See equation (3.2f)). For the H-function, the formula for  $arr$  for the Padé approximant prediction  $[n,m]$  of equation (5.1) and  $\tilde{r}\{n+m+1\}$  is :

$$arr = -1 \cdot m! \cdot B \cdot (B+1) \cdot (B+2) \cdot (\dots) \cdot (B+m-1) / (L[n,m]^{(2m)}), \quad (5.2)$$

where  $arr$  is the relative error (i.e., the PAP minus exact  $r(n+m+1)$ , all divided by  $r(n+m+1)$ ) and where

$$L[n,m] = n+m + a \cdot m + b . \quad (5.3)$$

References [16] and [8] also explain in further depth the appropriate formula for 'arr'.

For the important functional examples of  $H(1.0,w)$  and  $H(0.8,w)$ , the constants  $B$ ,  $a$ , and  $b$  were first determined by examining the numerical values of  $g1[u_h]$ ,  $g2[u_h]$ , through  $g7[u_h]$ , where  $u_h$  equals either 1.0 or 0.8 for purposes of this chapter.  $B$ ,  $a$ , and  $b$  were secondly determined by comparing the values of  $g1[u_h]$ ,  $g2[u_h]$ ,  $g3[u_h]$ , etc. to the PAP results of the following equations [17]:

$$g\{n+2\}[u] = (g\{n+1\}[u])^2 / g\{n\}[u] , \quad \text{Padé approximant prediction } [n,1], \quad (5.4)$$

$$g\{n+3\}[u] = \frac{2 \cdot g\{n\}[u] \cdot g\{n+1\}[u] \cdot g\{n+2\}[u] - g\{n-1\}[u] \cdot (g\{n+2\}[u])^2 - (g\{n\}[u+1])^3}{((g\{n\}[u])^2 - g\{n-1\}[u] \cdot g\{n+1\}[u])} ,$$

$$\text{Padé approximant prediction } [n,2], \quad (5.5)$$

with  $g\{j\}[u]=0$  for  $j < 0$ . ( The method for generating (5.4) and (5.5) is discussed with (1.13) in chapter 1. )

We then evaluated the complete set of quantities  $B$ ,  $a$ , and  $b$  of 'arr' for the PAPs of  $H[1.0,w]$  for moderately sized  $n$  and for small  $m$  and determined that 'arr' is given by the error formula in equation (5.1) with  $B=1.34$ ,  $a=-0.5$ , and  $b=1.6$ . This determination of  $B$ ,  $a$ , and  $b$  of  $L[n,m]$  was done almost completely by considering examples of  $L[n,1]$  (where  $m=1$ ) and forcing ( 'arr' +1 ) to equal  $(\text{PAP } g\{n+1+1\}[1.0]) / \check{g}\{n+1+1\}[1.0]$  for moderately sized values of  $n$ .  $\text{PAP } g\{n+1+1\}[1.0]$  is calculated by (5.4). We then used  $\check{g}\{n+1+1\}[1.0]$ , applied the PAP again to obtain  $g\{n+1+2\}[1.0]$ , and then applied the correction again after invoking equation (5.1) in order to obtain the APAP  $\check{g}\{n+1+2\}[1.0]$ . This process can be continued indefinitely.

$B$ ,  $a$ , and  $b$  were evaluated a second time, this time for  $H[0.8,w]$ . The determination of  $B$ ,  $a$ , and  $b$  of  $L[n,m]$  was done completely by considering examples of  $L[n,2]$  (where  $m=2$ ) and forcing ( 'arr' +1 ) to equal  $g\{n+2+1\}[0.8] / \check{g}\{n+2+1\}[0.8]$  for those positive  $n$ 's which satisfy the inequality  $0 < n+m < 8$ . Again,  $B$ ,  $a$ , and  $b$  were found to equal 1.34, -0.5, and 1.6 respectively. We then used  $\check{g}\{n+2+1\}[0.8]$ , applied the PAP again to obtain  $g\{n+2+2\}[0.8]$ , and then applied the correction again after invoking equation (5.1) in order to obtain the APAP  $\check{g}\{n+2+2\}[0.8]$ . This process can be continued indefinitely.

In the immediately following section, three tables are presented which display the successful results of using Asymptotic Padé Approximant Predictions to calculate the H-function  $H(u_h, w)$  as a function of  $w$  for the two selected choices of  $u_h$ .  $u_h=0.8$ , and

$u_h=1.0$ . In Tables 5.1) through 5.3),  $u$  equals 0.8. In Table 5.1),  $H(.8,w)$  functions obtained with ordinary Padé approximants and the APAP applied to obtain  $g\{8\} [.8]$  in order to generate the partial sum  $PtSum[8]$  are presented.

**Table 5.1)**

$H(.8,w)$  Functions obtained with ordinary Padé Approximants and with the Assistance of APAPs in  $PtSum[8]$

w	Pade[34]	Pade[43]	PtSum[8]	Hbook
0.2	1.0731869	1.0731869	1.0731869	1.07319
0.3	1.1176262	1.1176262	1.1176254	1.11763
0.5	1.2308825	1.2308823	1.2307752	1.23091
0.8	1.5352571	1.5351955	1.5213527	1.5358
0.9	1.7415087	1.7410548	1.6840653	1.7474
0.95	1.9061789	1.9048033	1.786618	1.9313
0.975	2.0203374	2.0178139	1.8445209	2.0833
1.0	2.1718993	2.1670136	1.9074508	2.5527

Table 5.2 shows the improvement in the calculation of  $H(.8,w)$  which results from generating a higher order partial sum via APAP's and then taking the Padé Approximants of these higher order (11th) partial sums.

**Table 5.2)**

Higher order Padé Approximants computed with the help of APAP's

w	Pade[4,4]	PtSum(8)	Pade[5,6]	Pade[6,5]	Hbook
0.2	1.0731869	1.0731869	1.0731869	1.0731869	1.07319
0.3	1.1176262	1.1176254	1.1176262	1.1176262	1.11763
0.5	1.2308828	1.2307752	1.230883	1.230883	1.23091
0.8	1.5353623	1.5213527	1.5355933	1.535593	1.5358
0.9	1.7423191	1.6840653	1.7447578	1.744752	1.7474
0.95	1.9087094	1.786618	1.9179995	1.9179702	1.9313
0.975	2.0250684	1.8445209	2.0446932	2.0446207	2.0833
1.	2.1812771	1.9074508	2.2265055	2.2263051	2.5527

In Table 5.3 is listed the coefficients  $g_{\{n\}}(0.8)$  for the  $H(.8,w)$  function obtained from the iteration algorithm presented in chapter 3 up to the seventh order. For orders eight and higher,  $g_{\{n\}}(.8)$  is approximated with APAPs.

**Table 5.3)**

The Coefficients  $g_{\{n\}}(0.8)$  for the  $H(.8,w)$  Function obtained from the Iteration Algorithm up to the seventh Order and then the APAP for eighth Order and Beyond

u=.8	Value of $g_{\{n\}}(u)$
$g_1(u)$	.648744172973
$g_2(u)$	.719900556021
$g_3(u)$	.950733073664
$g_4(u)$	1.37630275650

g5(u)	2.11079374261
g6(u)	3.36926942603
g7(u)	5.53857831222
gnu8	9.3096352
gnu9	15.920857
gn10	27.601755
gn11	48.383159

↑ This is the continuation of Table 5.3).

For the APAP of  $g\{n\}[u]$  of  $H(u,w)$ ,  $u$  is set equal to 1.0 in the next three tables.

**Table 5.4)**

$H(1.0,w)$  functions obtained with Padé approximants and from partial sums with seventh order iterations

w	Pade[3,4]	Pade[4,3]	Prtl Sum (7)	Hbook
0.3	1.1268438	1.268438	1.126843	1.126844
0.5	1.251255	1.251254	1.250940	1.251259
0.8	1.597426	1.597457	1/571937	1.598219
0.9	1.842901	1.842344	1.748239	1.850098
0.95	2.045295	2.043641	1.857371	2.077123
0.975	2.189267	2.1861712	1.918297	2.270984
1.0	2.385145	2.378988	1.983958	2.907809

In Table 5.5), for orders eight and higher,  $g\{n\}(1)$  is approximated with the Asymptotic Padé Approximant Prediction (APAP).

**Table 5.5)**

Coefficients  $g\{n\}(1)$  for  $H(1)$  functions obtained from the iteration algorithm given Chapter 3 up to the seventh order.

	u= 1.0			u= 1.0
g1(u)	0.693147		gnu9	20.178
g2(u)	0.804054		g9(u)	20.164 **
g3(u)	1.096628		gn10	35.257
g4(u)	1.626989		gn11	62.263
g5(u)	2.544145		gn12	110.84
g6(u)	4.125346		gn13	198.62
g7(u)	6.870243		gn14	357.89
gnu8	11.67867		gn15	647.94
g8(8)	11.678690 **		gn16	1177.9

\*\* Note that the precise numerical values of  $g8(u)$  and  $g9(u)$  were not used in any calculations in this chapter, although they were used to find Pade[4,5] and Pade[5,4] in chapter 3 for cases which include  $u=.8$  and then  $u=.9$  as contributing formal parameters for the H-function.



Now let us consider  $H(1.0,w)$ . Note  $u = 1.0$  here.

**Table 5.6)**

$H(1,w)$  functions computed Pade[3,4] and from the APAP and Asymptotic Padé assisted Partial Sum (PS) Methods

w	Pade[3,4]	(APAP)	(PS)	Hbook
0.3	1.126844	1.12684	1.12684	1.126844
0.5	1.251255	1.25126	1.25094	1.251259
0.8	1.597526	1.59797	1.57195	1.598219
0.9	1.842901	1.84833	1.74826	1.850098
0.95	2.045295	2.07339	1.85740	2.077123
0.975	2.189267	2.26728	1.91833	2.270984
1.0	2.385145	2.68543	1.98399	2.907809

The next series to analyze is the taylor series generated from  $\text{Log}[1+x]/x$  w.r.t.  $x$ .

This material is from a Mathematica file developed for use for research related to this material. For the series of  $\ln[1+x]/x$ , the predicted error from the APAP was found to equal:

$$\text{arr} = -1 \cdot m! \cdot B \cdot (B+1) \cdot (\dots) \cdot (B+m-1) / (L[n,m]^{(2-m)}), \quad (5.6)$$

where  $L[n,m] = n+m + a \cdot m + b$ . For the series examined,  $B$  is to be set equals to 1.

For the series examined,  $a+b$  is to be set equal to 1. The APAP in turn, equals

$r\{n+m+1\}/(1+\text{arr})$ . For  $\text{Log}[1+x]/x$ ,  $r[n]$  equals  $(-1)^n \cdot 1/(n+1)$ .

Tables 5.7a) demonstrates the success of the Asymptotic Padé Approximant Prediction in predicting the value of the next  $r\{j\}$  of the series of  $\ln(1+x)/x$  when  $m$  equals 2. Tables 5.7b) and 5.7c) demonstrate simple numerical calculations for the function  $\ln(1+x)/x$  which involve the Asymptotic Padé Approximant Prediction[k,2], where  $k+2+1=n$ .

**Table 5.7a)**

Comparison of Predictions of  $r[n]$

Value of n	Actual $r[n]$	Asymptotic Padé Approximant Prediction	Padé Approximant Prediction
9	-0.1	-0.0999719	-0.0999228
10	0.0909091	0.0908941	0.0908642
11	-0.0833333	-0.0833248	-0.0833058
12	0.0769231	0.076918	0.0769054
13	-0.0714286	-0.0714254	-0.0714168
14	-0.0625	-0.0624987	-0.0624943
15	0.0588235	0.0588226	0.0588194
16	-0.0555556	-0.0555549	-0.0555526
17	0.0526316	0.0526311	0.0526293
18	-0.05	-0.0499997	-0.0499983

**Table 5.7.b)**

x	-0.400	-0.8
Pade[2,3]	1.27705628	2.0033670
Asymptotic Pade Prediction generated Partial Sum[7]	1.27694742	1.94134577
Asymptotic Pade Prediction generated Partial Sum[13]	1.27706117	1.99951063
APAP assisted Pade[5,6]	1.27706141	2.0103378
APAP assisted Pade[6,7]	1.27706145	2.01150116
Log[1+x]/x	1.27706406	2.01179739

**Table 5.7.c)**

x	-0.9 is x	-0.95 is x
Ordinary Pade[2,3]	2.49623305	2.92618057
Asymptotic Pade Prediction generated Partial Sum[7]	2.26720653	2.47380541
Asymptotic Pade Prediction generated Partial Sum[13]	2.4514217	2.79046662
APAP assisted Pade[5,6]	2.53954412	3.05131006
APAP assisted Pade[6,7]	2.55499994	3.12352367
Log[1+x]/x	2.55842788	3.15340239

We have looked at the results which use the **Asymptotic Padé Approximant Prediction**[k,2], where  $k+2+1=n$ .

**Table 5.8)**

Comparison of predictions of  $r[n]$  in the Case when APAP[n,1] is used

Value of n	Actual $r[n]$	Asymptotic Padé Approximant Prediction	Padé Approximant Prediction
6	.14285714286	.14285714286	0.138888889
8	0.11111111111	0.11111111111	0.10937500
9	-0.1	-0.1	-0.0999228
10	0.0909091	0.0909091	0.0908642
11	-0.0833333	-0.0833333	-0.0833058
12	0.0769231	0.0769231	0.0769054
13	-0.0714286	-0.0714286	-0.0714168
14	-0.0625	-0.0625	-0.0624943
15	0.0588235	0.0588235	0.0588194
16	-0.0555556	-0.0555556	-0.0555526
17	0.0526316	0.0526316	0.0526293
18	-0.05	-0.05	-0.0499983

We have looked at the results which use **Asymptotic Padé Approximant Prediction**[k,1], where  $k+1+1=n$ . From table 5.8), we can infer that APAP's can be evaluated successively to generate amazingly accurate terms of the partial sum which represents  $\text{Log}(1+x)/x$ . The numerical value of Pade[j,m] is identical to the numerical value of the Asymptotic Padé Approximant Prediction assisted Pade[j,m] in the case

where  $\text{APAP}[j+m-2, 1]$  is used for the highest order term serving as input in the calculation of  $\text{Pade}[j, m]$ .

This new method of Assymptotic Padé Approximant Predictions have not been formally explained. However, the numerical results in tables 5.7) and 5.8) are worthy of consideration. Furthermore, in consideration of the review of tables 5.2) and 5.6), it becomes apparent that the use of APAPs in the improvement in the accuracy of the estimation of the values of the H-function is quite worthy of consideration.

## Chapter 6

### The Quartic Harmonic Oscillator and Perturbation Theory

#### 1. Overview.

In this chapter, lower energy perturbation theory of simple quantum mechanical systems will be studied. In order to find the correct spectral energies of attractive cores, perturbation theory will be carried out to the fifth order in various systems which comprise either a one-body problem with external field or a two-body problem reducible to a one-body problem. Two different procedures for generating perturbative series to evaluate the corrected energy of a given system will be discussed. These two methods are: the Raleigh Schrödinger procedure of perturbation theory for generating a perturbative series and a procedure for generating an elegant implicit perturbative series. The elegant implicit perturbative series shall be referred to as the Walker Green's function Series. (See section 4 below, page 82.)

Two mathematical types of examples will be examined: They are the one-dimensional harmonic oscillator with a supplemental quartic term, and the spherical harmonic oscillator with an extra quartic term. These two types of examples will be elaborated upon before a complete discussion of the results is given.

#### 2. The Nature of Perturbation Theory.

The spherical harmonic oscillator is especially interesting. We shall study the three lowest energy levels in the two orbital configurations in which  $l = 0$  and  $l = 1$ . Those simple quantum systems with a spherical attractive potential given in general as

$$V(r) = r^2 + b \cdot r^4 + c \cdot r^6 + d \cdot r^8 \quad (6.1a)$$

can be evaluated with relative ease for their spectral energy levels by using the methods demonstrated in this chapter. In principle, the methods used to find the energy levels for spherical systems of the potential

$$V(r) = r^2 + V' \cdot r^4 \quad (6.1b)$$

are equally valid in the semi-analytical evaluation of the energy levels of systems with

$$V(r) = r^2 + b \cdot r^4 + c \cdot r^6 + d \cdot r^8. \quad (6.1c)$$

A quicker yet reliable way to find the spectra of such spherical system could be useful for the careful and the time-efficient modeling of the spectrum of a Shell Model form core before applying a spherical symmetry breaking perturbation to a particle bound in a core styled after the Nuclear Shell Model [12].

Now we shall consider the two types of examples of Hamiltonian systems selected for extensive examples in this chapter. Before discussing the 1-dimensional and spherical types of examples of Hamiltonian systems, the author would like to point out that Carl Bender and Tai Tsun Wu have done substantial work in the perturbative evaluation of the spectrum of the quartic harmonic oscillator [12.b][12.c]. Some of the material in this chapter (involving the Raleigh Schrödinger procedure and especially the Taylor series representation of the Walker Green's Function) is similar in many respects to Carl Bender's work on the perturbative representation for the quartic harmonic oscillator. However, the algorithms presented in this chapter for carrying out the Raleigh Schrödinger procedure of perturbation theory and the procedure for the construction of and optimizing of the 'Walker Green's function series' are general enough to be easily applicable to harmonic oscillator systems in which the perturbation is  $V' \cdot r^6$  or  $V' \cdot r^8$  or

even  $V \cdot (r^4 + c \cdot r^6) \dots$ . Furthermore, the method which is based on the construction of and optimizing of the 'Walker Green's function Series' can be applied to three dimensional examples of quantum systems (with more than variable) for which the algebraic approach of references [12.b] and [12.c] is not an effective vehicle for the computation of the perturbative coefficients. The algebraic approach developed by Bender and Wu is designed to work with only one spatial variable rather than two or three variables. The 'Mathews and Walker' text inspired results (See [5.b].) in this chapter for the ground state energy of the quartic harmonic oscillator are very good. The lowest energy results are extremely close algebraically to those of the perturbative series formulated and worked out in ref. [12.b]. See section # 6, page 111 for a comparison.

The 1-dimensional quartic harmonic oscillator example has a non-relativistic Hamiltonian of the following form:

$$\hat{H} = (-d^2/dx^2 + x^2) + V' \cdot x^4. \quad (6.2)$$

The first part  $(-d^2/dx^2 + x^2)$  has well known eigenstates and a well known spectrum of eigenvalues. The perturbation is  $V' \cdot x^4$ . The eigenvalues for the energies of the Hamiltonian including  $V' \cdot x^4$  are known numerically as a function of  $V'$ , but not in closed analytical form. ( It is well known that if  $V' = 0$ , then  $E(n) = 2 \cdot n + 1$ . ) By carrying out fifth order perturbation theory, one can find a polynomial of the form  $(2 \cdot n + 1) + r_1 \cdot (V') + r_2 \cdot (V')^2 + r_3 \cdot V'^3 + r_4 \cdot V'^4 + r_5 \cdot (V')^5$  in order to approximate what the eigenenergies are as a function of  $n$  and the magnitude of the perturbing  $V'$  factor. Such an approximation is valid only when  $V' \ll (2 \cdot n + 1)$  for a given integer  $n$ . The Padé approximants Pade[2,2], Pade[2,3], and Pade[3,2] have been applied to the expression  $(2 \cdot n + 1) + r_1 \cdot (V') + r_2 \cdot (V')^2$



$+ r_3 \cdot V'^3 + r_4 \cdot V'^4 + r_5 \cdot (V')^5$ . It will be demonstrated through the comparison of the Padé approximants to carefully worked out numerical data that Padé approximants are a very efficient and effective way of finding the eigenstates of the quartic one-dimensional harmonic oscillator.

The spherical quartic harmonic oscillator as a Hamiltonian of the form

$$H = (-1 \cdot \nabla^2 + r^2) + V' \cdot r^4. \quad (6.2b)$$

By carrying out fifth order perturbation theory for the expression in (6.2b) where  $V' \cdot r^4$  is the perturbing element, one can find another polynomial of the  $(2 \cdot n + 1) + r_1 \cdot (V') + r_2 \cdot (V')^2 + r_3 \cdot V'^3 + r_4 \cdot V'^4 + r_5 \cdot (V')^5$  in order to approximate what the eigenenergies are as a function of the quantum number  $n$  and of the magnitude of the perturbing  $V'$  factor.

The numerical calculation of the *eigenenergies* of the spherical harmonic oscillator with  $V' \cdot r^4$  is difficult. Whereas all of the work for the Padé approximants and one-dimensional *eigenenergies* are done with Maple source code, the high precision *numerical* calculation of the *eigenenergies* of the quartic harmonic oscillator has to usually be done with well designed numerical source code. This is done much better through the use of C or Fortran compilations than with the use of the Maple command package. This situation clearly illustrates that it is desirable to even have an approximate formula for the corrected eigenenergies of the modified (quartic in this chapter) spherical harmonic oscillator. This approximate formula obviously is to be a closed-form function of  $V'$ . In spite of nontrivial difficulties, there is a numerical plot in the section entitled '**Results of Calculations**' (section # 5) of the corrected eigenenergies provided for the case when  $n=1$  and  $l=0$  (the ground state level in the spherical potential) and for the case

when  $n=1$  and  $l=1$  (the lowest level for spin 1). Indeed, it is desirable to have a tool or algorithm from which one can quickly picture the dependence of spherically attractive spectrum as a function of the perturbation magnitude  $V'$ .

Now a brief review of *eigenenergies* of matrices is given. The eigenvalues of a Hamiltonian can be written as  $\hat{H}(x) \Psi_n = E_n \Psi_n$ . The operator  $\hat{H}(x)$  usually is  $-d^2/dx^2 + V(x)$ . A reasonable approximation of the matrix representation of  $\hat{H}(x)$  for many one-body problems can be written as an  $N \times N$  matrix where  $N = 11$ . In the perturbation theory of nearly harmonic systems, the part  $-d^2/dx^2 + x \cdot x$  is the operator whose eigenfunctions comprise the basis for the matrix representation of the total Hamiltonian.  $\hat{H}$ , which is in the oscillator's diagonal representation, is constructed from this. The

perturbation  $V \cdot x^4$  is represented in matrix form by  $Q(n,m)$ . Let  $Q(n,m) = \langle \Psi_n | V' | \Psi_m \rangle$ .

(6.3)

Through review, the following 3 by 3 matrix representation becomes transparent:

$$\hat{V}' = \begin{bmatrix} Q(0,0) & Q(0,1) & Q(0,2) \\ Q(1,0) & Q(1,1) & Q(1,2) \\ Q(2,0) & Q(2,1) & Q(2,2) \end{bmatrix}$$

and

$$\hat{H}_0 = \begin{bmatrix} E_0 & 0 & 0 \\ 0 & E_1 & 0 \\ 0 & 0 & E_2 \end{bmatrix}$$

(6.4)

$$\Psi_1 = \begin{bmatrix} 1 \\ 0 \\ 0 \end{bmatrix}, \quad \Psi_2 = \begin{bmatrix} 0 \\ 1 \\ 0 \end{bmatrix}, \quad \Psi_3 = \begin{bmatrix} 0 \\ 0 \\ 1 \end{bmatrix}.$$

(6.5)

In (6.4) and (6.5),  $\hat{H}_0$ ,  $\Psi_1$ ,  $\Psi_2$ , and  $\Psi_3$  are clearly in the diagonalized representation with respect to the operator  $\hat{H}_0$ .  $E_0$  is the unperturbed ground state eigenenergy.  $E_1$  is the second eigenenergy, or first excitation level. If we include the perturbation  $\hat{V}'$ , then  $\hat{H}_0 + \hat{V}'$  must of course be considered and diagonalized for eigenvalues.

Thus for an 11 by 11 matrix representation,  $H_0(i,j) = \delta(i,j) \cdot E_{0j}$ .  $E_{0j}$  is the  $j^{\text{th}}$  level

eigenenergy of  $\hat{H}_0$ .  $V'(i,j) = \left\langle \Psi_i \left| \hat{V}' \right| \Psi_j \right\rangle$ . For the examples in this chapter, the

maximum  $i$  equals 11, and  $j$  goes to 11. For the spherically distributed examples \*\*,

$$V'(i,j) = \int_0^{\infty} \exp\left(-\frac{1}{2}r^2\right) \cdot sHle(r,i) \cdot (V'r^4) \cdot sHle(r,j) \cdot \exp\left(-\frac{1}{2}r^2\right) dr \quad (6.5b)$$

With this notation, we can write the following matrix equation:

$$H_0(i,j) \cdot \Psi_{j(k)} + V'(i,j) \cdot \Psi_{j(k)} = (E_0 + \Delta E) \cdot \Psi_{i(k)} \quad (6.6)$$

The required task is to find the eigenvalues of the matrix equation (6.5), where the eigenvalues are  $(E_{0j} + \Delta E_j)$ .  $\Delta E_j$  is the correction in energy due to the perturbation. The larger maximum  $i$  and maximum  $j$  are for this matrix equation (6.5), the more accurate the values of  $E_{0j} + \Delta E_j$  will be as estimates of the actual eigenenergies of the Hamiltonian operator  $\hat{H}_0 + \hat{V}'$ . It is the matrix equation (6.6) which was solved for most of the perturbed harmonic oscillator examples of this chapter. Most of these examples were double-checked by diagonalizing and solving the 9 by 9 matrix representation, the 10 by 10 matrix representation, and the 11 by 11 representation. The lowest three eigenvalues of the these three representations all mutually agreed to precision of at least 5 significant figures.

\*\* Note:  $sHle(r,j) \equiv r^j \cdot \exp(-r^2/2) \cdot \text{Laguerre}(r^2)$ , when  $l = 0$ .

This matrix diagonalization procedure for equation (6.6) involves solving the secular equation of a sufficiently large matrix so as to require the numerical solving of the secular equation. The processes of repeatedly generating the secular equation for different values of  $V'$  (of the perturbant) by taking the determinant of such an  $n$  by  $n$  matrix equation and then solving the secular equation take a not so small amount of computer time. This ever repeating demand for central processing time is a strong source of motivation for finding a method which finds a reliable closed-form approximation of the eigenenergies of a quantum mechanical system as a function of the magnitude of coefficient  $V'$  of the perturbing potential. The Raleigh Schrödinger procedure combined with the use of Padé approximants is very suitable for fulfilling this role for cases in which the coefficient  $V'$  is small or of intermediate magnitude. The  $V'$  polynomial expressions available from non-degenerate perturbation theory alone is not reliable when  $V'$  is of intermediate magnitude.

This reality of naive perturbation theory giving us meaningful information only when  $V'$  is very small can be seen from the following results. Non-degenerate fifth order perturbation theory was individually applied by the author to the 1-dimensional harmonic oscillator with  $V' \cdot x^4$  added in. The author found from careful calculation that the ground state energy of this quartic harmonic oscillator is expressed as the following Naive Perturbation Series:

$$E_5(V') := 1 + 3/4 \cdot V' - 1.312500000000 \cdot V'^2 + 5.203125000000 \cdot V'^3 + (-1) \cdot 30.56103515625000 \cdot V'^4 - 10023.08297538757 \cdot V'^5. \quad (6.7)$$

$V'$  is the perturbative expansion parameter. When  $V'$  equals .1, the first three terms grow progressively smaller. However, the last two terms,  $30.56 \cdot V'^4$  and  $-10023 \cdot V'^5$ , progressively grow larger in magnitude. It is clear from inspection and the properties of asymptotic series that when  $V'$  is in the order of magnitude of .2 or .1 or smaller that useful information for the energy level estimate can be directly obtained from only the first 3 terms. As is immediately above written, these first three terms are:

$1 + 7.7500000000 \cdot V' - 1.3125000000 \cdot V'^2$ . DPade22\_1 and DPade23\_1 are Padé approximants of the series presented in (6.7). DPade22\_1 means Pade[2,2] of (6.7).

Next, DPade22\_1, DPade23\_1, and DPade32\_1 are written out.

$$\text{DPade22}_1 := \frac{(1 + 8.132560483870968 \cdot V + 10.20640120967742 \cdot V^2)}{(1 + 7.382560483870968 \cdot V + 5.981980846774194 \cdot V^2)} ; \quad (6.8)$$

$$\text{Dpade23}_1 := \frac{(1 - 853.0243826429354 \cdot V - 3477.479218453888 \cdot V^2)}{(1 - 853.7743826429354 \cdot V - 2835.835931471687 \cdot V^2 + 1001.094946384912 \cdot V^3)} ; \quad (6.9a)$$

$$\text{DPade32}_1 := \frac{(1 - 1020.37612983630 \cdot V - 4838.47742459 \cdot V^2 - 1708.059074996 \cdot V^3)}{(1 - 1021.126129836 \cdot V - 4071.320327 \cdot V^2)} . \quad (6.9b)$$

Nondegenerate fifth order perturbation theory was applied to the 1-dim harmonic oscillator with  $V' \cdot x^4$  added in. The first excitation energy of this harmonic plus quartic oscillator is expressed as the following Naive Perturbation Series:

$$E_5(V') := 3 + 15/4 \cdot V' - 10.31250000000 \cdot V'^2 + 61.17187500000 \cdot V'^3 - 533.66455078125 \cdot V'^4 + (-1) \cdot 1006630.1143169 \cdot V'^5 . \quad (6.10)$$

When  $V'$  here equals .1, the first three terms grow progressively smaller. However, the last two terms,  $533.6 \cdot V'^4$  and  $-1006630 \cdot V'^5$ , grow progressively larger in magnitude. It is clear from inspection and the properties of asymptotic series that when  $V'$  is in the order of magnitude of .2 or .1 or smaller that useful information for the energy level estimate can be directly obtained from only the first 3 terms. As is immediately written above, these first three terms are:  $3 + 3.7500 \cdot V' - 10.3125000 \cdot V'^2$ . DPade22\_3 and DPade23\_3 are Padé approximants of the series expressed in equation (6.10), the case of the first excitation. DPade22\_3 means Pade[2,2] of (6.8). Next, DPade22\_3 and Dpade23\_3, and DPade32\_3 are written out.

$$\text{DPade22}_3 := \frac{(3 + 37.16183035714287 \cdot V + 74.39732142857151 \cdot V^2)}{(1 + 11.13727678571429 \cdot V + 14.31501116071430 \cdot V^2)}; \quad (6.11)$$

$$\text{DPade23}_3 := \frac{(3 - 14882.42427584945 \cdot V - 92240.54171072470 \cdot V^2)}{(1 - 4962.058091949817 \cdot V - 24540.83712197096 \cdot V^2 + 13598.58108638621 \cdot V^3)} \quad (6.12a)$$

$$\text{DPade32}_3 := \frac{(3 - 17732.28186947236 \cdot V - 127542.5165228015 \cdot V^2 - 70673.92380614 \cdot V^3)}{(1 - 5912.010623157456 \cdot V + (-1) \cdot 35120.72139532036 \cdot V^2)} \quad (6.12b)$$

On the next page, a table is given in which  $E(V)$  of the quartic oscillator is evaluated as a function of  $V$ .

**Table 6.1)**

When  $n = 0$ , the Ground State Level.

A Table in which  $E(V)$  of the quartic oscillator is evaluated as a function of  $V$  by NPT partial sums, Padé approximants, and by the numerical spectrum search explained with equations (6.4) and (6.5).

V	seri3	seri4	seri5	Pade[2,2]	Accurate Value (*)	Pade[2,3]
.1	1.0670781	1.06402202	.963791191	1.06520567	1.0652857	1.0657139
.2	1.1391250	1.09022734	-2.1171592	1.11745262	1.1182933	1.1218277
.3	1.2473594	.999814990	-23.356277	1.16125079	1.1640550	1.1749381
.4	1.4230000	.640637410	-101.99573	1.19875340	1.2048479	1.2279363
.5	1.6972656	-.21279907	-313.43414	1.2313168	1.2419573	1.2824305
.8	3.4240000	-9.0938000	-3293.4576	1.30775761	1.3376248	1.4649341
1.	5.6406250	-24.920410	-10048.003	1.34629859	1.3925661	1.6109689
1.2	9.0010000	-54.370363	-24995.008	1.37801754	1.4425051	1.7855402

(\*) Note that the 'Accurate Value' is found by diagonalizing an  $11 \times 11$  matrix (or better).

**Table 6.2)**

When  $n = 1$ , the first excited level.

A Table in which  $E(V)$  of the quartic oscillator is evaluated as a function of  $V$

V	seri3	seri4	seri5	Pade[2,2]	Accurate Value	Pade[2,3]
.1	3.3330469	3.2796804	-6.7866207	3.3055207	3.306903	3.3116866
.2	3.8268750	2.9730117	-319.14863	3.5284374	3.5394276	3.5741362
.3	4.8485156	.52583276	-2445.5853	3.7026702	3.7337016	3.8338461

.4	6.7650000	-6.896813	-10314.789	3.8433961	3.9031801	4.1087816
.5	9.9433594	-23.41068	-31480.602	3.9596626	4.0547397	4.4101973
.6	14.750625	-54.412301	-78329.97	4.0574218	4.1925630	4.7481120
.7	21.553828	-106.57903	-169290.90	4.1408038	4.3194790	5.1335601
.8	30.720000	-187.86900	-330040.42	4.2127809	4.4375323	5.5801733
.9	42.616172	-307.52114	-594712.54	4.2755527	4.5482651	6.1059375
1.0	57.609375	-476.05518	-1007106.2	4.3307842	4.6509386	6.7357008

Padé[2,2] for the lowest energy, or DPade22\_1, DPade23\_1, and the lowest

numerical eigenvalue of  $\begin{bmatrix} H_{11} & H_{12} & \dots \\ H_{21} & H_{22} & H_{32} \\ \vdots & H_{32} & \ddots \end{bmatrix}$ , which represents  $\hat{H}_{\text{total}}$ . Likewise, DPade22\_3

representing Padé[2,2] of the 1st excitation, DPade23\_3, and the 2nd lowest eigenvalue

of  $\begin{bmatrix} H_{11} & H_{12} & \dots \\ H_{21} & H_{22} & H_{32} \\ \vdots & H_{32} & \ddots \end{bmatrix}$ . Clearly, the Padé approximants get very close to the correct answer

when  $V'$  is less than or equal to 0.5. On the other hand, when  $V'$  equals 0.5, the fourth

order and fifth order Naive Perturbation Theory series (NPT) fails miserably. Indeed,

solving the secular equation of an  $N_i$  by  $N_i$  matrix is the most reliable (where  $N_i$  is a large

+ integer). However, the unwieldiness of an  $N_i$  by  $N_i$  matrix should be considered. Given

a particular value for  $V'$ , algorithmically setting up and solving the large secular equation

for such an  $N_i$  by  $N_i$  matrix is much more time consuming than numerically evaluating the

Padé[2,2] and Padé[2,3] partial fractions by substituting for  $V'$ .

Clearly, the thought of doing higher order perturbation theory is convenient in an

academic computational setting. However, there is one source of concern for applying

ordinary non-relativistic perturbation theory to various simple attractive potential



systems. There are examples in which the coefficients of the Naive Perturbation Theory (NPT) series grow at a rate which is faster than that of geometric growth. For the sake of discussion, a Naive Perturbation Theory series of simple Hamiltonian operator plus perturbation shall be expressed as

$$\sum_n r_n \cdot V^n \quad (6.13)$$

In some challenging examples,  $r_n$  grows as quickly as  $(n!)$  in magnitude or almost as quickly as  $n$ -factorial as  $n$  progresses in size. In the ‘anharmonic’ oscillator examples of this chapter (e.g. quartic harmonic and even octant harmonic),  $r_n$  grows approximately as quickly as  $(n!)$ , for all eigenenergy levels. In Chapter 2 there was written assertion #1 for Fredholm integral equations. The requirement for the reliable application of assertion #1 and thereby Padé approximants on integral equations requires that the Neumann series asymptotically grow as a geometric series. A geometrically evolving NPT series can be successfully analyzed and estimated through the use of Padé approximants due to reasons very similar to the reasons given in Chapter 2 for the justification of assertion #1 (and the five-fold statement of qualification) for the Neumann series of Fredholm integral equations. When  $r_n$  of (6.13) grows in an  $n$ -factorial manner, the claim of the previous sentence for the reliability of Padé approximants can no longer be applied with deep certainty.

### 3. The Apparent Kinship of some Perturbative Series to Stieljes Series

However, there still is a very good chance for the *reliable* application of Padé approximants to (6.13). There are three sources of confidence for such reliability:

1) The evidence of success of Padé approximants of all of the NPT series examples included in this chapter when compared to the precise numerical matrix eigenvalues of the Hamiltonian;

2) the fact that these series grow in manner which is very similar to the manner of growth of a Stieltjes series with respect to  $n$ ; and

3) the fact that the Padé Approximants of Stieljes series, which appear similar to the NPT series of this chapter, are inherently reliable, especially for large  $N$  of  $\text{Pade}[N,N]$  and  $\text{Pade}[N,N+1]$ .

Futhermore, if a perturbative series of a function is available up to order  $2 \cdot N + 1$  where  $N$  is very large, then very often it is possible to witness *the convergence of  $\text{Pade}[N,N]$ ,  $\text{Pade}[N,N+1]$ , and  $\text{Pade}[N+1,N]$  to a common value* for sequentially larger values of  $N$ .

Several examples of functions which generate terms that are almost the same as a Stieljes series (Stieljes functions) will be given. Before giving these examples of near-Stieljes functions, the properties of all Stieltjes series in relation to Padé approximants will be reviewed.

The topic of Stieljes series is thoroughly discussed in numerically oriented mathematical text books such as Advanced Mathematical Methods for Scientists and Engineers by Bender and Orzsag [13a]. A Stieltjes series can be precisely expressed as:

$\text{Stiel}(z) = \sum_{n=0}^{\infty} a_n (-x)^n$ .  $a_n$  is equal to  $\int_0^{\infty} \text{fun}(t) \cdot t^n \cdot dt$ , where  $\text{fun}(t)$  in an arbitrary but

well behaved function of  $t$ . Let us define  $\text{Ft}(x)$ :

$$\text{Ft}(x) \equiv \int_0^{\infty} \text{fun}(t) / (1 + x \cdot t) \cdot dt . \quad (6.13b)$$

Padé approximants can be taken of  $\text{Stiel}(x)$  with respect to  $x$ . Chapter 8 of reference [13.a] explains and shows the following bounds on the Padé approximants of  $\text{Stiel}(x)$ :  
 $\text{Pade}[0,1] \leq \text{Pade}[1,2] \leq \text{Pade}[N,N+1] \leq \text{Ft}(x) \leq \text{Pade}[N,N] \leq \text{Pade}[2,2] \leq \text{Pade}[1,1]$  .  
 Chapter 8 explains thoroughly that  $\lim_{n \rightarrow \infty} \text{Pade}[n,n+1] \approx \text{F}(x) \approx \lim_{n \rightarrow \infty} \text{Pade}[n,n]$ . In essence this is saying that  $\text{Pade}[N,N+1]$  and  $\text{Pade}[N,N]$  provide precise lower bound and upper bound values for  $\text{Ft}(x)$  when  $N$  is large.

An additional property of Stieltjes functions, as is explained in reference [13.b], is the fact that  $\text{Pade}[N+1,N]$  is less than  $\text{Pade}[N,N+1]$  of the same Stieltjes series.

Therefore, an extension of the inequality of the previous paragraph is:

$$\text{Pade}[N+1,N] < \text{Pade}[N,N+1] \leq \text{Ft}(x) \leq \text{Pade}[N,N] \leq \text{Pade}[2,2] \leq \text{Pade}[1,1] .$$

Now a particular choice for  $\text{fun}(t)$  of (6.13b) relevant to this chapter shall be given. Let  $\text{fun}(t)$  equal  $\exp(-t)$ . Then  $a_n$  equals  $n!$ . In this case,  $\text{Stiel}(x) = \sum_{n=0}^{\infty} n! (-x)^n$ .

This shows  $n$  factorial growth. Padé approximants are guaranteed to produce

convergently more precise approximations of what  $\text{Ft}(x)$ ,  $\int_0^{\infty} \exp(-t) / (1+x \cdot t) \cdot dt$ ,

actually equals at a given value of  $x$  .

Now that the relevant properties of Stieltjes functions and their Stieltjes series have been discussed, Several examples of functions which generate terms which are almost the same as a Stieltjes series (of Stieltjes functions) will be given. These examples all demonstrate the same patterns of proximity and boundary formation around the correct value as all of the NPT perturbation series (at least those which are so far available) which exist for the quartic harmonic oscillator and the spherical quartic harmonic

oscillator. They also match the pattern of the Padé approximants taken of the NPT perturbation series resulting from the Hamiltonian of a harmonic oscillator plus  $V \cdot x^6$ .

However, the NPT series for  $H_{\text{harmonic}} + V \cdot x^6$  is not shown in length (See appendix c).

The examples included in this paragraph will lead to a strong case for the Source of Confidence clause number 2).

In Mathematica program files developed by the author, series were generated for

the functions  $1/2 + V/5 - 1 \cdot V^2 \cdot (\int_0^{\infty} \text{borr}(V,t) dt)$ ,  $1/2 + V/3 + (-1) \cdot V^2 \cdot (\int_0^{\infty} \text{borr}(V,t) dt)$ ,

and  $1/2 - V/3 - 1 \cdot V^2 \cdot (\int_0^{\infty} \text{borr}(V,t) dt)$ , where  $\text{borr}(V,t)$  was chosen to equal  $\exp(-t)/$

$(1+V \cdot t)$ . In accordance with (6.13b),  $(\int_0^{\infty} \text{borr}(V,t) dt)$  is a Stieltjes function. The Stieltjes

series generated by each of these three exemplary functions is:  $a_q + b_q \cdot V - 1 \cdot V^2 \cdot (1 - 1! \cdot V + 2! \cdot V^2 - 3! \cdot V^3 + \dots)$ , where  $a_q = 1/2$  and  $b_q \in \{1/5, 1/3, -1/3\}$ . Various Padé approximants were

taken of these three series.  $\text{Pade}[n,n]$ ,  $\text{Pade}[n,n+1]$ , and  $\text{Pade}[n+1,n]$  were calculated for the cases  $n=1$ ,  $n=2$ , and  $n=3$ . Plots of the values of  $\text{Pade}[n,n]$ ,  $\text{Pade}[n,n+1]$ , and

$\text{Pade}[n+1,n]$  are given in Figures 6.1), 6.2), and 6.3). The result of these Padé

approximant calculations is that an observed (See Figures 6.1) and 6.2)) pattern is

consistently followed:  $\text{Pade}[n,n] < \text{exact value of function} < \text{Pade}[n+1,n] < \text{Pade}[n,n+1]$ .

$a_q + b_q \cdot V - 1 \cdot V^2 \cdot (1 - 1! \cdot V + 2! \cdot V^2 \dots)$  not a Stieltjes series. However, it is very similar to a

Stieltjes series, which always follows the inequality  $\text{Pade}[N+1,N] < \text{Pade}[N,N+1] \leq$

$\text{Stieltjes\_function}(x) \leq \text{Pade}[N,N]$ . This pattern of inequality is not completely different.

On the next two pages, Figures 6.1), 6.2), and 6.3) are shown. The pattern of  $\text{Pade}[n,n] < \text{exact value of function} < \text{Pade}[n+1,n]$  is clearly manifested.

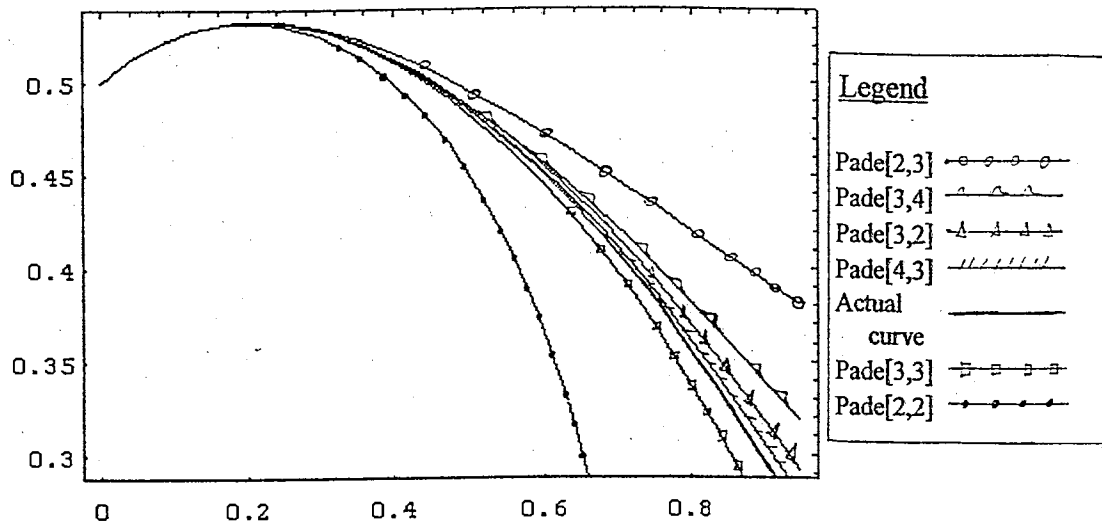


Figure 6.1)

The exact value for  $1/2 + V/3 - V^2 \cdot (1 - 1! \cdot V + 2! \cdot V^2 - 3! \cdot V^3 + \dots)$  and Padé approximants such as  $\text{Pade}[2,2]$ ,  $\text{Pade}[3,2]$ , and  $\text{Pade}[2,3]$

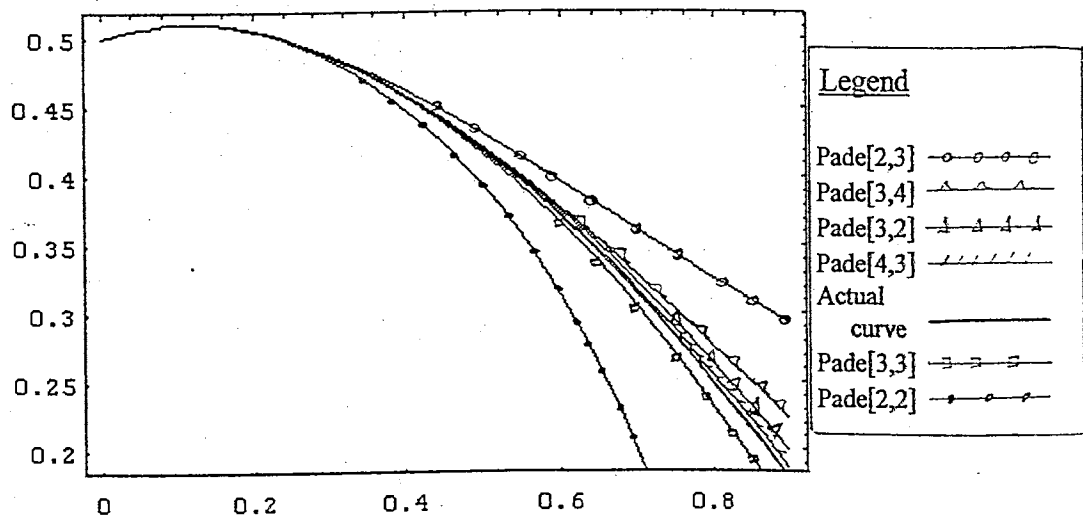


Figure 6.2)

The exact value for  $1/2 + V/5 - V^2 \cdot (1 - 1! \cdot V + 2! \cdot V^2 - 3! \cdot V^3 + \dots)$  and Padé approximants such as  $\text{Pade}[2,2]$ ,  $\text{Pade}[3,2]$ , and  $\text{Pade}[2,3]$

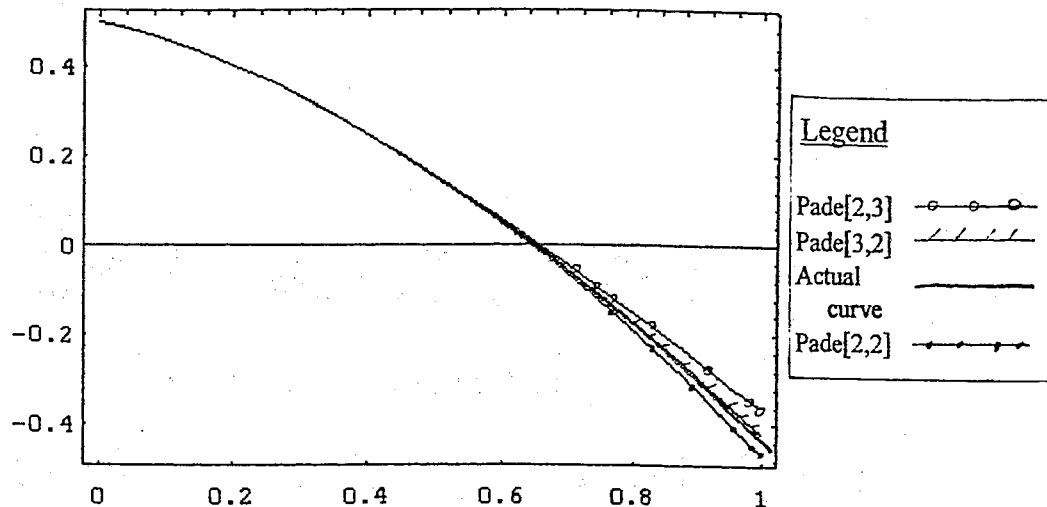


Figure 6.3)

The exact value for  $1/2 - V/3 - V^2 \cdot (1 - 1! \cdot V + 2! \cdot V^2 - 3! \cdot V^3 + \dots)$  and Padé approximants such as Padé[2,2], Padé[3,2], and Padé[2,3]

Tables 6.1), 6.2), and 6.3) completely and unambiguously demonstrate the pattern  $\text{Padé}[n,n] < \text{exact value of energy} < \text{Padé}[n,n+1]$  for the NPT series of the quartic harmonic oscillator. As was earlier explained, Table 6.1) involves the perturbation series of the ground state, and Table 6.2) involves the perturbation series of the first excitation. By inspecting the RHS expressions of (6.9b) and (6.12b), one can see that by substituting small as well as larger positive values of  $V$  that one shall get fruitful values for comparison from Padé[3,2]. Such a comparison within Tables 6.1) and 6.2) will definitely show that also for the quantum mechanical perturbation theory series that the Padé approximants form the following inequality:  $\text{Padé}[n,n] < \text{exact} < \text{Padé}[n+1,n] < \text{Padé}[n,n+1]$ . This exactly the same inequality that exists for the series of

generated by the function  $a_n + b_n - 1 \cdot V^2 \cdot \left( \int_0^{\infty} \frac{\exp(-t)}{(1+V \cdot t)} dt \right)$  with respect to  $V$ .

Padé approximants are reliable and are very accurate at high enough order for the series generated by  $a_n + b_n \cdot V^2 \cdot \left( \int_0^\infty \text{corr}(V,t) dt \right)$ . Since the Padé approximants of the NPT series for the quartic harmonic oscillator have the same bounds ( $\text{Pade}[n,n] < \text{exact} < \text{Pade}[n+1,n] < \text{Pade}[n,n+1]$ ) and since Tables 6.1) and 6.2) demonstrate successful numerical results, source of confidence clause number 2) in reference to the quartic harmonic oscillator is highly plausible. Furthermore, it is highly plausible that Padé approximants are reliable and are very accurate when the order of  $V^n$  is sufficiently high for the NPT series involving the quartic harmonic oscillator.

The virtually guaranteed success of Stieltjes series, the fact that the perturbative quantum mechanical series in this chapter grow approximately at a rate of n-factorial (Many Stieljes series grow at the approximate rate of n-factorial.), and the fact that there exist near-Stieltjes functions which yield the same type of results for Padé approximants as the perturbative quantum mechanical series in this chapter all favor in combined consideration the hypothesis that Padé approximants can be applied to the perturbative quantum mechanical series which represent the spectral energies of the quartic harmonic oscillator. However, the success of all of the examples and calculations of chapter 6 does not prove such a hypothesis; it merely strengthens it.

#### **4. Introduction to Walker Green's Function Series Iteration**

##### **4a. Orientation**

The Raleigh Schrödinger procedure for Perturbation Theory, as used for equation (6.10), is the commonly taught formalism for estimating energy level shifts of one-body

or two-body quantum mechanical systems. There is at least one other formalism which described perturbative energy shifts in term of a series. This formalism is developed from Green's functions generated by unperturbed eigenstates. The proof and formalism are discussed in chapter 10 of Matthew and Walker's mathematical methods text [14].

For very small  $V$ , the following series equation enables us to calculate the corrected energy  $Lam(m, V)$  as a function of  $V$ .

$$Lam(m, V) = L^o(m) + V \cdot G(m, m) + V^2 \cdot \sum_{n \neq m} \frac{G(m, n) \cdot G(n, m)}{Lam(m, V) - L^o(n)} + \\ V^3 \cdot \sum_{n \neq m} \sum_{p \neq m} \frac{G(m, n) \cdot G(n, p) \cdot G(p, m)}{(Lam(m, V) - L^o(n)) \cdot (Lam(m, V) - L^o(p))} + \dots \quad (6.14)$$

*This series is referred to the Walker Green's Function Series in this chapter* <sup>(6)</sup>. It should be noticed that  $Lam(m, V)$  is found on both the right hand side as well as the left hand side of (6.14). This makes it very difficult to solve (6.14), even when (6.14) is written out only to the third order. However, one can make an initial guess to what  $Lam(m, V)/Lo(m)$  should equal. Let "sca" equal the initial guess for  $Lam(m, V)/Lo(m)$  for given  $m$  and  $V$ .  $Lam(m, V)$  can be estimated in terms of this "sca" parameter. This initial estimate of  $Lam(m, V)$  is to be known as  $Lam(m, V, sca)$ :

$$Lam(m, V, sca) = L^o(m) + V \cdot G(m, m) + V^2 \cdot \sum_{n \neq m} \frac{G(m, n) \cdot G(n, m)}{(sca \cdot L^o(m) - L^o(n))} + \\ V^3 \cdot \sum_{n \neq m} \sum_{p \neq m} \frac{G(m, n) \cdot G(n, p) \cdot G(p, m)}{(sca \cdot L^o(m) - L^o(n)) \cdot (sca \cdot L^o(m) - L^o(p))} + \dots \quad (6.15)$$

Note that  $V \cdot G(m, n) \equiv Q(m, n)$  (6.15f)

in this chapter.  $L^o$  is  $\lambda^o$  in [14], and  $Lam(m, V)$  is  $\lambda(m, V)$  in [14].

<sup>(6)</sup> Note that the Walker Green's Function Series equals the Series in Brillouin Wigner P.T..



**4b. A Scheme for Solving a Truncated Version of Equation (6.15), which is partly catalogued in the Mathews and Walker Text**

There is an iteration algorithm that the author proposes in order to get very accurate values of the estimated  $Lam3(m, V, sca)$ . If  $|V|$  is much less than  $(|G(m, m)| / (\sum_j G(j, m)^2))$ , then let  $sca(n)$  equal  $Lam(m, V, sca(n-1)) / L^o(m)$  in such a way that:

$$Lam3(m, V, sca(s)) = L^o(m) + V \cdot G(m, m) + V^2 \cdot \sum_{n \neq m} \frac{G(m, n) \cdot G(n, m)}{(sca(s-1) \cdot L^o(m) - L^o(n))} + V^3 \cdot \sum_{n \neq m} \sum_{p \neq m} \frac{G(m, n) \cdot G(n, p) \cdot G(p, m)}{(sca(s-1) \cdot L^o(m) - L^o(n)) \cdot (sca(s-1) \cdot L^o(m) - L^o(p))} \quad (6.16)$$

The RHS of (6.16) needs to be calculated. Next,  $Lam3(m, V, sca(s))$  needs to be re-expressed as a Taylor series expanded with respect to  $V$  up to the third order. This is  $Series(Lam3(m, V, sca(s)), V, 3)$ . Subsequently, the ratio

$$sca(s+1) = Series(Lam3(m, V, sca(s)), V, 3) / L^o(m) \quad (6.17)$$

needs to be found. Then one should calculate  $Series(Lam3(m, V, sca(s+1)), V, 3)$  by using equation (6.15). Again subsequently, the ratio

$$sca(s+2) = Series(Lam3(m, V, sca(s+1)), V, 3) / L^o(m)$$

needs to be found. This iteration should be carried out at least two times. Four times is completely sufficient. This method of subsection 4b.) is very effective for finding the corrected energy  $Lam(m, V)$  and is within the requirements for the approximate convergence of a truncated perturbative series, so long as if the following two conditions are met: A.) the initial guess for the scaling factor  $sca(\text{first})$  needs to be reasonably close to the correct choice for  $sca(n)$ ; and B.)  $(V)^2 \cdot \sum_j G(j, m)^2$  needs to be much less than

$V \cdot |G(m,m)|$ . Condition B.) can be re-stated as  $V \ll |G(m,m)| / (\sum_j G(j,m)^2)$ . The

choice  $sca(\text{first}) = 1$  is to be avoided. A good starting choice for  $sca(n)$  is  $sca(1) = (L^\circ(m) + V \cdot G(m,m)) / L^\circ(m)$ , presuming that  $V \ll |G(m,m)| / (\sum_j G(j,m)^2)$ .

From ordinary perturbation theory, as is discussed in the **two texts** by Merzbacher [15.a] and Liboff [15.b], the corrected energy  $Lam(m,V)$  can also be expressed as:

$$\begin{aligned} Lam(m,V) = & L^\circ(m) + V \cdot G(m,m) + V^2 \cdot \sum_{n \neq m} \frac{G(m,n) \cdot G(n,m)}{L^\circ(m) - L^\circ(n)} + \\ & V^3 \cdot \sum_{n \neq m} \sum_{p \neq m} \frac{G(m,n) \cdot G(n,p) \cdot G(p,m)}{(L^\circ(m) - L^\circ(n)) \cdot (L^\circ(m) - L^\circ(p))} + \\ & (-1) \cdot V^3 \cdot \sum_{n \neq m} \frac{G(m,n) \cdot G(n,m) \cdot G(m,m)}{(L^\circ(m) - L^\circ(n))^2} + V^4 \cdot (5 \text{ terms}) \dots \quad (6.18) \end{aligned}$$

While the RHS of equation (6.18) has five compact summation terms, equation (6.14) has only four compact summation terms. Through analytical review, it can be rediscovered that there is only one compact summation term which has  $V^4$  as a coefficient in (6.14). On the other hand, (6.18) has five compact summation terms (See <sup>s</sup>) which have  $V^4$  as their coefficient. The number of compact summation terms in Naive Perturbation Theory (6.18) which have  $V^n$  as their coefficient grows at least as quickly as the rate of  $2^n$  as  $n$  increases. The number of compact summation terms in Walker Perturbation Theory (6.14) remains constant (one) regardless of how large  $n$  of the  $V^n$  becomes.

For the sake of easy reference, the expression in equation (6.14) shall be called a '*Walker Green's Function Series*'. As has already been briefly explained in the beginning of this chapter on pg. 71, the expression in equation (6.18) is to be called a Naive Perturbation Theory series.

<sup>s</sup> The five compact summation terms for the  $V^4$  contribution are available upon request.

**4c. A Scheme for Solving a more Effective Version of a Truncated Equation (6.15) when only 6 or Less Terms are Available.**

The algorithm discussed in the last two paragraphs is a method for the approximate solving of equation (6.14) when  $V$  is very small. Now an *iterative method* similar to (6.16) and (6.17) shall be introduced and explained for cases where  $V$  is not necessarily so small. Let us look at (6.15) again.

$$\begin{aligned} \text{Lam}(m, V, \text{sca}) = & L^{\circ}(m) + V \cdot G(m, m) + V^2 \cdot \sum_{n \neq m} \frac{G(m, n) \cdot G(n, m)}{(\text{sca} \cdot L^{\circ}(m, V) - L^{\circ}(n))} + \\ & V^3 \cdot \sum_{n \neq m} \sum_{p \neq m} \frac{G(m, n) \cdot G(n, p) \cdot G(p, m)}{(\text{sca} \cdot L^{\circ}(m) - L^{\circ}(n)) \cdot (\text{sca} \cdot L^{\circ}(m) - L^{\circ}(p))} + \dots \end{aligned} \quad (6.15)$$

It is a very useful idea to re-express the RHS of (6.15) as a Padé approximant, where  $V$  is the adjustable expansion parameter. It is straight forward to picture how this would be done on (6.15) when 'sca' is an initial numerical guess. However, a second, third, and maybe a fourth value will be assigned to sca. Just as in (6.16) (found two pages back), sca will serve as the vehicle of iteration in a scheme in which this iterated parameter will be inserted into the RHS of (6.15) several times. The main advancement in this scheme is that the RHS of (6.15) will be replaced by a Padé approximant in which  $V$  is the expansion.

**4d. The Algorithm Required in order to Realize the Concept from Subsection "4c".**

Let us look at the optimization scheme algorithm for the iteration method inspired by (6.16) and (6.17). We recall equation (6.15). For the purposes of the interesting examples in this chapter, (6.15b) needs to be expanded all the way out to the  $V^5$  term.

$$\begin{aligned} \text{Lam5}(m, V, \text{sca}) = & L^{\circ}(m) + V \cdot G(m, m) + V^2 \cdot \sum_{n \neq m} \frac{G(m, n) \cdot G(n, m)}{(\text{sca} \cdot L^{\circ}(m) - L^{\circ}(n))} + \\ & V^3 \cdot \sum_{n \neq m} \sum_{p \neq m} \frac{G(m, n) \cdot G(n, p) \cdot G(p, m)}{(\text{sca} \cdot L^{\circ}(m) - L^{\circ}(n)) \cdot (\text{sca} \cdot L^{\circ}(m) - L^{\circ}(p))} + \dots + V^5 \cdot \sum \sum \sum \sum \dots \end{aligned} \quad (6.15b)$$

We benefit from some specific function definitions:  $\text{Pade22}(f(V), V)$  is the approximant  $\text{Pade}[2,2]$  taken of  $f(V)$ , where  $V$  is the expansion parameter.  $\text{Pade23}(f(V), V)$  is the approximant  $\text{Pade}[2,3]$  taken of  $f(V)$ , where  $V$  is the expansion parameter.

$\text{Pade32}(f(V), V)$  is the Padé approximant  $\text{Pade}[3,2]$ . Now several algorithmic functions shall be introduced. These algorithmic functions serve as the essential operational mechanisms of the optimization scheme algorithm. First note the following two mini-defn's: For almost all examples in chapter 6, it suffices to set 'N' equal to 5. The operational function 'Expand' is defined as  $\text{Expand}[f(V), V, N]$ , where

$$\begin{aligned} \text{Expand}[f(V), V, N] \equiv \\ f(0) + 1 \cdot f'(0) \cdot V + 1/2! \cdot f''(0) \cdot V^2 + \dots + 1/N! \cdot f^{(N)}(0) \cdot V^N. \end{aligned}$$

The task at hand is to establish the equality

$$\text{sca} \cdot L^{\circ}(m) = \text{Pade23}(\text{Lam}(m, V, \text{sca}), V). \quad (6.19)$$

First of all, a fairly good numerical guess for  $\text{sca}$  should be made. A good way to obtain a good guess for  $\text{sca}$  for a harmonic oscillator plus polynomial system is to solve equation (6.15b) in terms of  $\text{sca}$  for the specific case where  $V$  equals  $1/2 \cdot L^{\circ}(m)$ . It is suggested to use the secant method to carry out this root search of  $\text{sca}$ . Next, it is good to plug this numerical guess for  $\text{sca}$  into functional execution equation (6.15b) one additional time.

$$\text{firstpade23}(V, \text{sca}) = \text{Pade23}(\text{Lam5}(m, V, \text{sca}), V) \quad (6.20)$$

$$\text{seri1}(V, \text{sca}) = \text{Expand}[\text{Lam5}(m, V, \text{firstpade23}(V, \text{sca})/L^{\circ}(m)), V, \text{Num}] \quad (6.21)$$

$$\text{seconpade23}(V, \text{sca}) = \text{Pade23}(\text{seri1}(V, \text{sca}), V) \quad (6.22)$$

$$\text{seri2}(V, \text{sca}) = \text{Expand} [\text{Lam5}(m, V, \text{seconpade23}(V, \text{sca})/L^{\circ}(m)), V, \text{Num}] \quad (6.23)$$

$$\text{thirdpade23}(V, \text{sca}) = \text{Pade23}(\text{seri2}(V, \text{sca}), V) \quad (6.24)$$

$$\text{seri3}(V, \text{sca}) = \text{Expand} [\text{Lam5}(m, V, \text{thirdpade23}(V, \text{sca})/L^{\circ}(m)), V, \text{Num}] \quad (6.25)$$

... continue along ...

$$\text{Nthpade23}(V, \text{sca}) = \text{Pade23}(\text{seri}\{N\_minus\_1\}(V, \text{sca}), V) \quad (6.26)$$

$$\text{seriN}(V, \text{sca}) = \text{Expand} [\text{Lam5}(m, V, \text{Nthpade23}(V, \text{sca})/L^{\circ}(m)), V, \text{Num}] \quad (6.27)$$

In order to carry out the optimization scheme algorithm successfully,  $\text{firstpade23}(V, \text{sca})$ ,  $\text{seri1}$ ,  $\text{seconpade23}(V, \text{sca})$ ,  $\text{seri2}$ ,  $\text{thirdpade23}(V, \text{sca})$ ,  $\text{seri3}$ , and  $\text{fourthpade23}(V, \text{sca})$  should be evaluated in sequential order. The idea behind all of this is to find a nearly correct solution to represent  $\text{Lam}(m, V)$  in (6.14).  $\text{Lam}(m, V, \text{sca})$  is a very close approximation to  $\text{Lam}(m, V)$  of (6.14). As is explained in the Mathews and Walker text [14],  $\text{Lam}(m, V)$  also is the correct  $m$ -th level eigenvalue of the Hamiltonian studied, where the perturbing potential of magnitude  $V$  is included.

Next, the results of Calculations which include Padé approximants and optimized Padé approximants is discussed and presented in numerical terms.

## 5. Results of Calculations.

There should be negligible difference between  $\text{thirdpade23}(V, \text{sca})$  and  $\text{fourthpade23}(V, \text{sca})$ , as  $\text{seconpade23}(V, \text{sca})$ ,  $\text{thirdpade23}(V, \text{sca})$ , and  $\text{fourthpade23}(V, \text{sca})$  are designed to be quickly converging to a common answer. It is good for the initial guess of 'sca' to be carefully obtained in manner similar to the procedure described in subsection 4b, which starts in the printed vicinity of equation (6.16). However, even if  $\text{sca} \cdot L^{\circ}(m)$  and  $\text{Pade23}(\text{Lam}(m, V, \text{sca}), V)$  disagree with each

other by as much as 3 percent, the sequence  $\text{seconpade23}(V, \text{sca})$ ,  $\text{thirdpade23}(V, \text{sca})$ , and  $\text{fourthpade23}(V, \text{sca})$  will converge to the same common answer as if the choice of  $\text{sca}$  caused a 1/2 percent initial error. **Eqn (6.19)** alludes to the desire for agreement between  $\text{sca} \cdot L^\circ(m)$  and  $\text{Pade23}(\text{Lam}(m, V, \text{sca}), V)$ . This statement is about to be demonstrated as being realistic in all of the spectral energy calculations presented in this final major section, # 5, of this chapter.

The optimal Padé approximant functions  $\text{firstpade23}(V, \text{sca})$ ,  $\text{seconpade23}(V, \text{sca})$ ,  $\text{thirdpade23}(V, \text{sca})$ , and  $\text{fourthpade23}(V, \text{sca})$  shall be referred to by the names  $\text{firstpade23}(V)$ ,  $\text{OptPade23}(V)$ ,  $\text{OpOptPade23}(V)$ , and  $\text{OpOpOptPade23}(V)$ , respectively in the next few paragraphs. Some of the successful results of the *optimization scheme algorithm* applied to the one-dimensional harmonic oscillator shall now be demonstrated. A table and graphs will be presented in which  $E\text{-corrected}(V, m)$ ,  $\text{seri4}(V, m)$ ,  $\text{Pade}[2,3]$  of  $\text{seri5}(V, m)$ ,  $\text{Pade}[3,2]$  of  $\text{seri5}(V, m)$ ,  $\text{OptPade23}(V)$  at  $m$  and  $\text{OpOptPade23}(V)$  at  $m$ . It will be seen from the numerical data that  $\text{OptPade23}(V)$  and  $\text{OpOptPade23}(V)$  will be even closer to  $E(V, m)$  than  $\text{Pade}[2,3]$  of  $\text{seri5}(V, m)$  is.

Energy level number  $m = 0$  here. (ground)

Naive Perturbation Series:

$$E_5(V) := 1 + 3/4 \cdot V - 1.3125000000000000 \cdot V^2 + 5.2031250000000000 \cdot V^3 + (-1) \cdot 30.561035156250000 \cdot V^4 - 10023.082975388 \cdot V^5. \quad (6.28)$$

$$\text{Lam}(m=0, V, 1.1187) := 1 + .7500000000000000 \cdot V - 1.3497292852074 \cdot V^2 + 5.71457138071564459 \cdot V^3 - 34.521611060067 \cdot V^4 + 262.299588070097 \cdot V^5 \quad (6.29)$$

$$\text{firstpade23}(V, 1.1187) := \frac{(1 + 11.27840723109600 \cdot V + 23.28916552015348 \cdot V^2)}{(1 + 10.52827840723110 \cdot V + 16.74258938203889 \cdot V^2 + (-1) \cdot 4.061013850845145 \cdot V^3)} \quad (\text{cf. 6.20}).$$

$$\text{OpOptPade}[2,3] := \frac{(1 + 11.062298768334 \cdot V + 22.285122511754 \cdot V^2)}{(1 + 10.312298768334 \cdot V + 15.863398843550 \cdot V^2 - 3.5657816931888 \cdot V^3)} \quad (6.30)$$

In equation 6.30b), the Taylor series of OpOptpade[2,3] has been generated with respect to V out to the fifth order.

$$\text{Taylor Series of OpOptPade}[2,3] \approx 1 + .75000 \cdot V - 1.3125 \cdot V^2 + 5.203125 \cdot V^3 + (-1) \cdot 30.16113 \cdot V^4 + 223.8113 \cdot V^5 \quad (6.30b)$$

Now finally let us look in Table 6.3) at the numerical results of the partial fractions OpOptPade[2,3] from (6.30) and OpOptPade[2,2]. The quantity CorrtNum is defined as the precise numerical value of the corrected energy  $E_{[mj]}(V)$  as found by diagonalizing the 10 by 10 matrix representation of  $(\hat{H}_o + \hat{V}) \cdot \hat{V}$ , of course, is either  $V \cdot r^4$  or  $V \cdot x^4$ . CorrtNum is in the fourth column.

**Table 6.3)**

A Table comparing ordinary Padé Approximants to the respective Optimal Padé Approximants

V	DPade[2,2]	OpOptPade[2,2]	CorrtNum	OpOptPade[2,3]	DPade[2,3]
.1	1.06520537	1.065217852	1.0652857	1.065308122	1.06571394
.2	1.11745262	1.117540578	1.1182933	1.118685796	1.1218277
.3	1.16125079	1.161484673	1.1640550	1.165753269	1.17493806

.4	1.19875340	1.199186277	1.20484792	1.209242312	1.22793626
.5	1.2313168	1.231983692	1.24195727	1.250732168	1.28243049
.8	1.30775761	1.309214986	1.33762481	1.371831520	1.46493406
1.0	1.34629859	1.348289097	1.39256605	1.454787979	1.61096887
1.2	1.37801754	1.380516749	1.44250506	1.542612005	1.78554017

Now the partial fractions which represent the optimized Pade[3,3] and the optimized Pade[3,4] are shown. These partial fractions are the best semi-analytical approximations of the ground state energy level presented in this thesis. These partial fractions were difficult to calculate with a PC, so, the optimized Pade[3,3] and optimized Pade[3,4] have not been calculated for any other examples besides the ground state.

$$\text{OptPade}[3,3]: = \frac{(1 + 16.432997853186 \cdot V + 65.231699776538 \cdot V^2 + 52.980300915123 \cdot V^3)}{(1 + 15.682297853186 \cdot V + 54.782476386649 \cdot V^2 + 27.273334557443 \cdot V^3)} ;$$

$$\text{OpOptPade}[3,3]: = \frac{(1 + 16.4215261870 \cdot V + 65.1319296262 \cdot V^2 + 52.85484017 \cdot V^3)}{(1 + 15.67152618701 \cdot V + 54.690784986 \cdot V^2 + 27.202504553 \cdot V^3)} ; \quad (6.31)$$

$$\text{OptPade}[3,4]: = \frac{(1 + 20.98561776412 \cdot V + 115.5690757218 \cdot V^2 + 154.3460752284 \cdot V^3)}{(1 + 20.23561776412 \cdot V + 101.7048623987 \cdot V^2 + 99.42355174470 \cdot V^3 + (-1) \cdot 16.21861239183 \cdot V^4)} . \quad (6.32)$$

In equation 6.32b), the Taylor series of OpOptpade[3,3] has been generated with respect to V out to the sixth order.



$$\begin{aligned} \text{Taylor Series of OpOptPade}[3,3] \approx & 1 + 7.750000000000 \cdot V - 1.31250000 \cdot V^2 + \\ & + 5.20312500 \cdot V^3 - 30.16113274852 \cdot V^4 + 223.8112786 \cdot V^5 + \\ & - 1999.4641 \cdot V^6 \end{aligned} \quad (6.32b)$$

The coefficients of (6.32b) are compared in section # 6 (starting at pg. 108) with the coefficients of the perturbation series algebraically constructed by Bender and Wu for the ground state energy [12.b].

The numerical values of rational fractions (6.31) and (6.32) are listed in the next table.

**Table 6.4)**

A Table showing the Optimal Padé Approximants, in particular OpOptPade[2,2], OpOptPade[2,3], OpOptPade[3,3], and OptPade[3,4], of E(V) when n=0.  
(Note E(V) grows positively with V.)

V	OpOptPade[2,2]	OpOptPade[3,3]	CorrtNum	OptPade[3,4]	OpOptPade[2,3]
.1	1.0652178524	1.0652808767	1.0652857	1.0652874852	1.0653081223
.2	1.1175405783	1.1181837963	1.1182933	1.1183537985	1.1186857964
.3	1.1614846726	1.1635245536	1.1640550	1.1644047064	1.1657532690
.4	1.1991862772	1.203396003	1.2048479	1.2059244869	1.2092423122
.5	1.2319836920	1.238985777	1.2419573	1.2443796126	1.2507321681
.8	1.3092149855	1.326833793	1.3376248	1.3495820325	1.3718315197
1.0	1.3482890967	1.373799514	1.3925660	1.4159944441	1.4547879794
1.2	1.3805167486	1.413985969	1.4425051	1.4820791599	1.5426120052

Energy level number  $m = 1$  here. (first excitation)

Naive Perturbation Series:

$$E5(V) := 3 + 15/4 \cdot V - 103125/10000 \cdot V^2 + (61.171875000\dots) \cdot V^3 + (-1) \cdot 533.6645507812500 \cdot V^4 - 1006630.1143169 \cdot V^5 \quad (6.33)$$

$$\text{Lam}(m=1, V, 1.182) := 3 + (3.7500000\dots) \cdot V - 11.86314860074428 \cdot V^2 + 91.33004682241915 \cdot V^3 - 919.3773392928851 \cdot V^4 + 10799.34913764610 \cdot V^5 \quad (6.34)$$

$$\begin{aligned} \text{firstpade23}(V, 1.182) := & (3 + 51.38565359127636 \cdot V + 165.8842074872459 \cdot V^2) \\ & \hline & (1 + 15.87855119709212 \cdot V + 39.40092969963158 \cdot V^2 + \\ & \quad \quad \quad (-1) \cdot 16.90464026013591 \cdot V^3) ; \end{aligned}$$

$$\begin{aligned} \text{OpOptoPade}[2,3] := & (3 + 46.28303681613 \cdot V + 135.9104699873 \cdot V^2) \\ & \hline & (1 + 14.17767893871 \cdot V + 31.01889132237 \cdot V^2 + \\ & \quad \quad \quad (-1) \cdot 10.42846780116 \cdot V^3) . \quad (6.35) \end{aligned}$$

**Table 6.5)**

Table for the case  $n = 1$  (The level of first excitation).

V	Pade[2,2] (not Opto scheme)	OpOptPad[2,2]	CorrtNum	OpOptPad[2,3]	Pade[2,3]
.1	3.3055207	3.306041716	3.306903	3.307199507	3.3116866
.2	3.5284374	3.531438673	3.5394276	3.543662961	3.5741362
.3	3.7026702	3.709684230	3.7337016	3.750511512	3.8338461
.4	3.8433961	3.855217625	3.9031801	3.944577621	4.1087816
.5	3.9596626	3.976599700	4.0547397	4.134740033	4.4101973
.6	4.0574218	4.079500103	4.1925630	4.326486101	4.7481120
.7	4.1408038	4.167893532	4.3194790	4.523695390	5.1335601

V	Pade[2,2] (not Opto scheme)	OpOptPad[2,2]	CorrtNum	OpOptPad[2,3]	Pade[2,3]
.8	4.2127809	4.244671513	4.4375323	4.729465705	5.5801733
.9	4.2755527	4.311996156	4.5482651	4.946549448	6.1059375
1.0	4.3307842	4.371519961	4.65093864	5.177616202	6.7357008

Next, many graphs will be presented which display the correct spectrum and the very good results from Padé approximants for the one-dimensional quartic harmonic oscillator.

These graphs are presented on the next several pages.

Legend of Figure 6.4					
n=3	OpOptPade[2,3]	— (blue)	n=2	OpOptPade[2,3]	— (cyan)
	Correct Value	— (red)		OpOptPade[2,2]	— (red)
	OpOptPade[2,2]	— (black)			
n=1	OpOptPade[2,3]	— (black)	n=0	OpOptPade[2,3]	— (yellow)
	Correct Value	— (green)		Correct Value	— (yellow)
	OpOptPade[2,2]	— (black)		OpOptPade[2,2]	— (green)

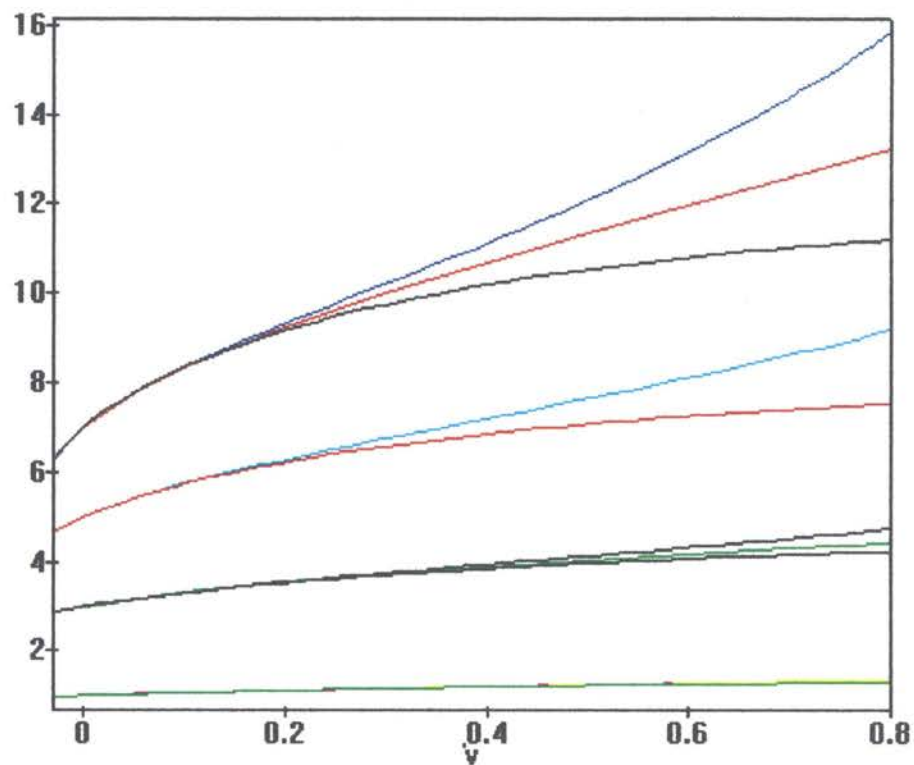













Figure 6.4

Optimal Padé Approximants for the four lowest levels of the 1-dimensional

Legend of Figure 6.5					
n=3	Pade[2,3]		n=2	Pade[2,3]	
	Correct Value			Pade[2,2]	
	Pade[2,2]				
n=1	Pade[2,3]		n=0	Pade[2,3]	
	Correct Value			Correct Value	
	Pade[2,2]			Pade[2,2]	

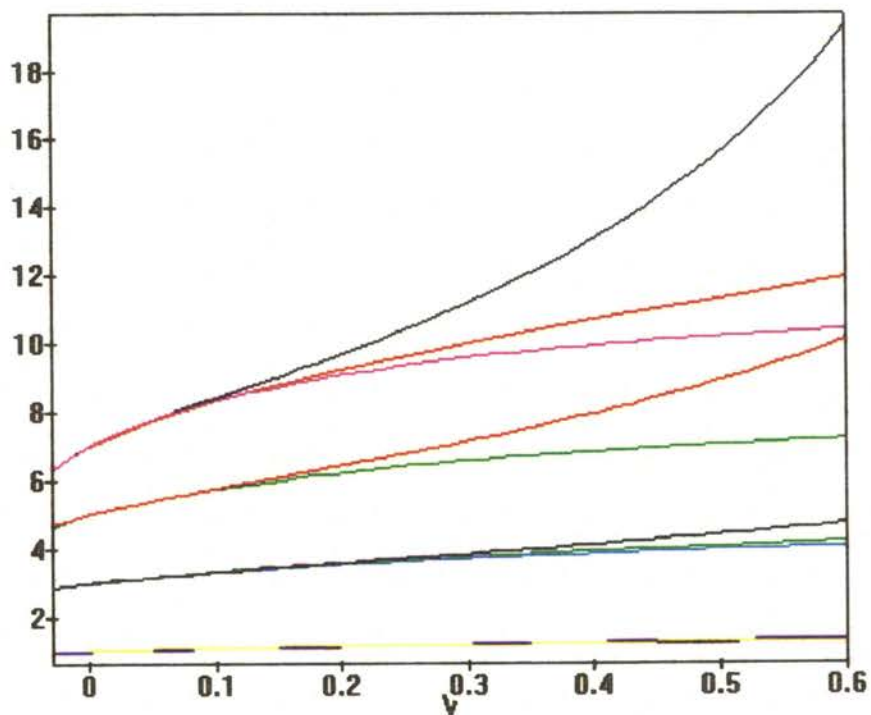








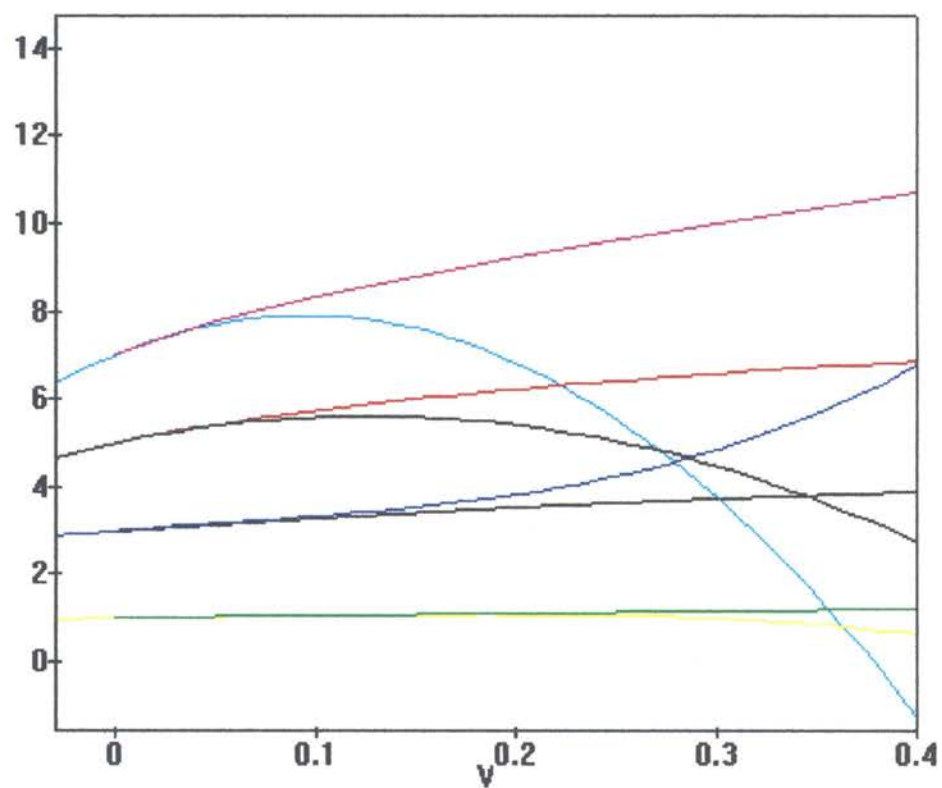


Figure 6.5









Ordinary Padé Approximants for the 4 lowest energy levels of the 1-dimensional Quartic Harmonic Oscillator.

Legend of Figure 6.6					
n=3	NPT Partial Sum		n=2	NPT Partial Sum	
	Correct Value			(order 4)	
				Correct Value	
n=1	NPT Partial Sum		n=0	NPT Partial Sum	
	Correct Value			Correct Value	



**Figure 6.6**

Naive Perturbation Theory Series compared to the correct spectral Energy Levels.

Legend of Figure 6.6					
n=3	NPT Partial Sum		n=2	NPT Partial Sum	
	Correct Value			(order 4)	
				Correct Value	
n=1	NPT Partial Sum		n=0	NPT Partial Sum	
	Correct Value			Correct Value	

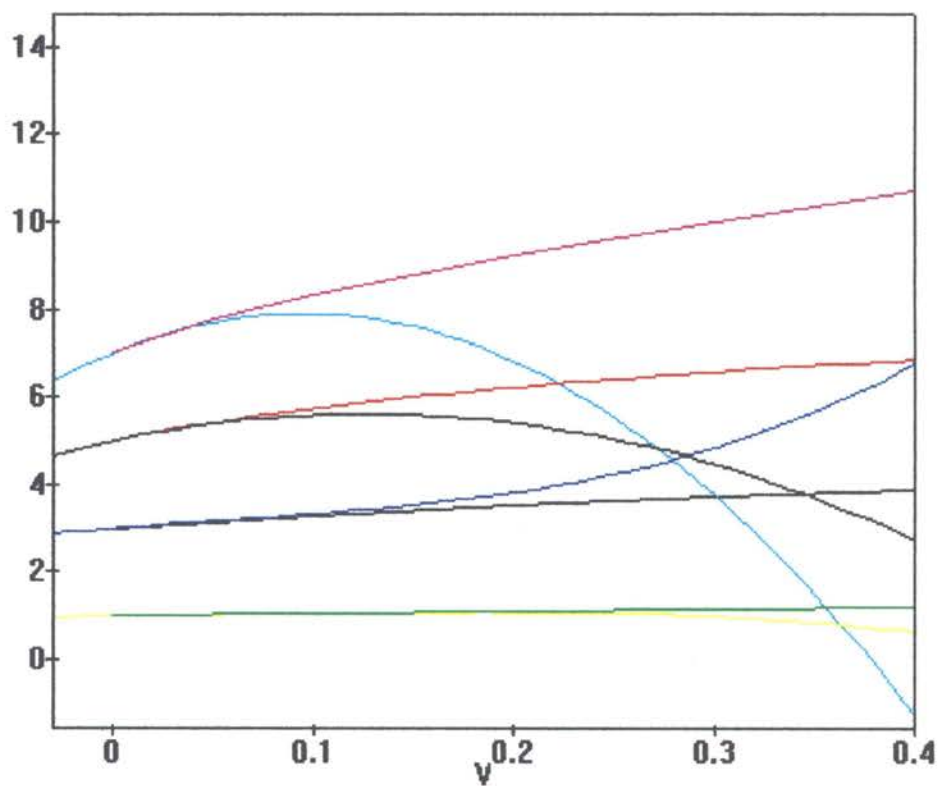


**Figure 6.6**

Naive Perturbation Theory Series compared to the correct spectral Energy Levels.

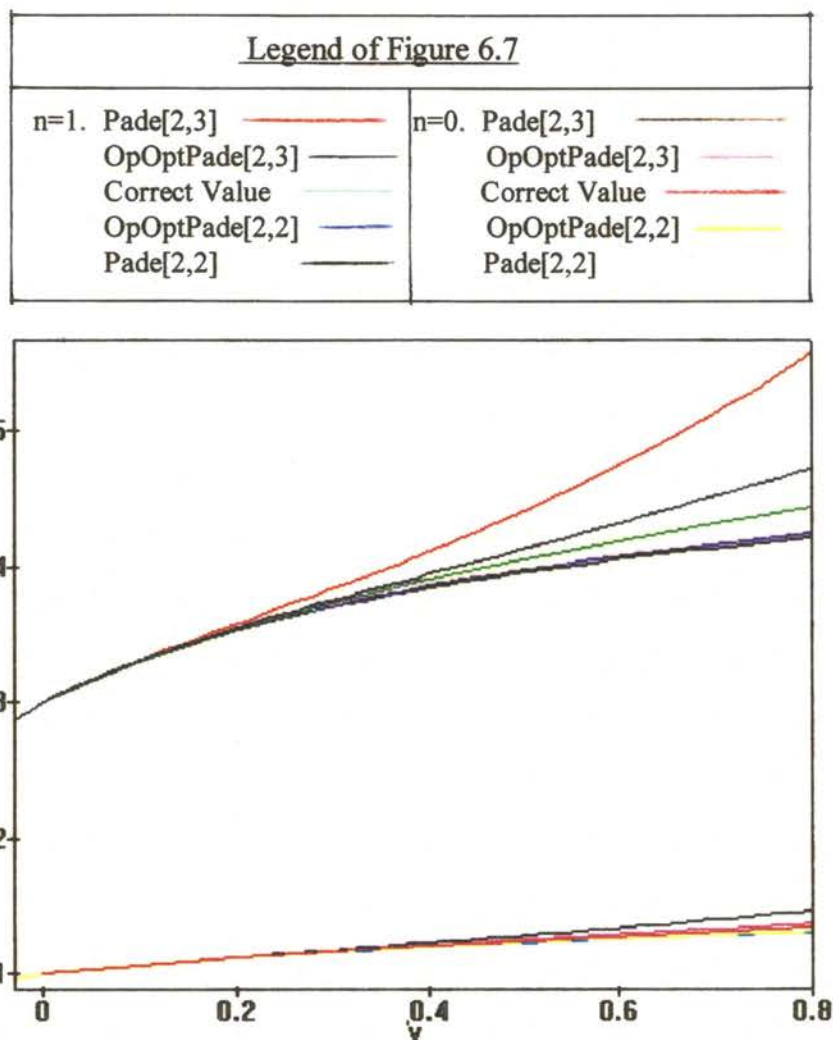


**Figure 6.7**

Pade Spectrum for the two lowest Energy Levels.



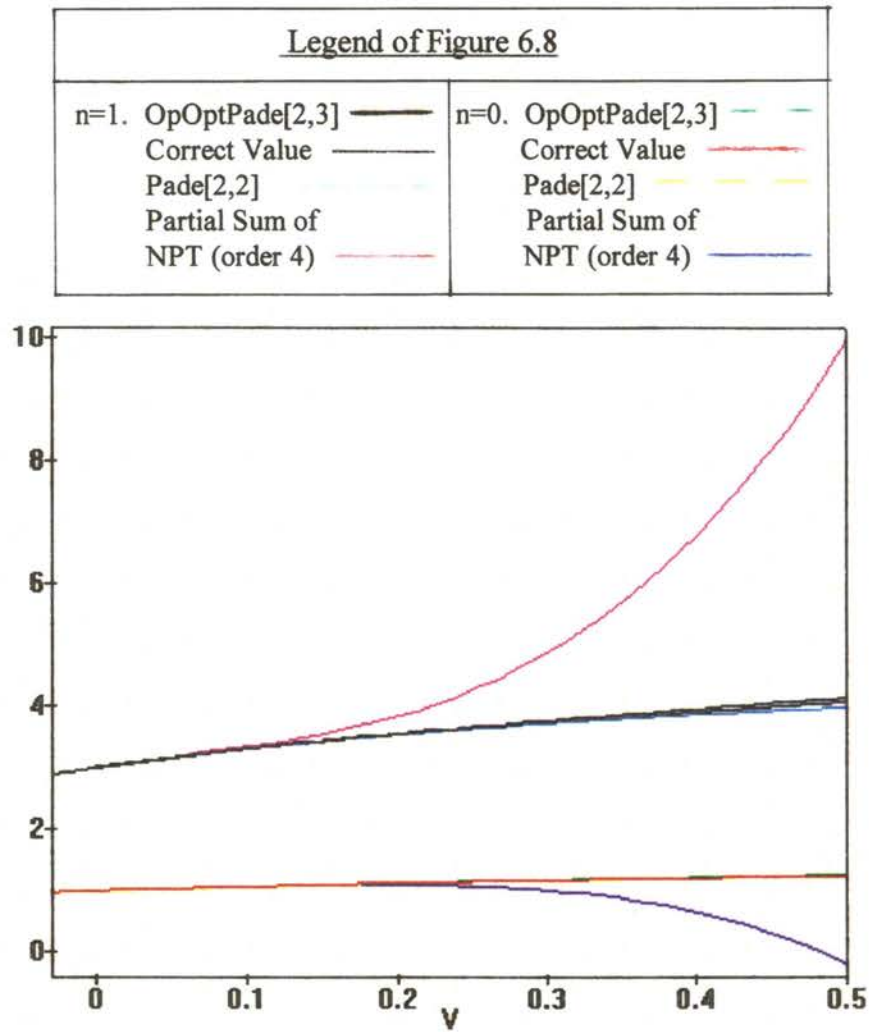


**Figure 6.8**

NPT Partial Sums presented for the two lowest Energy Levels.

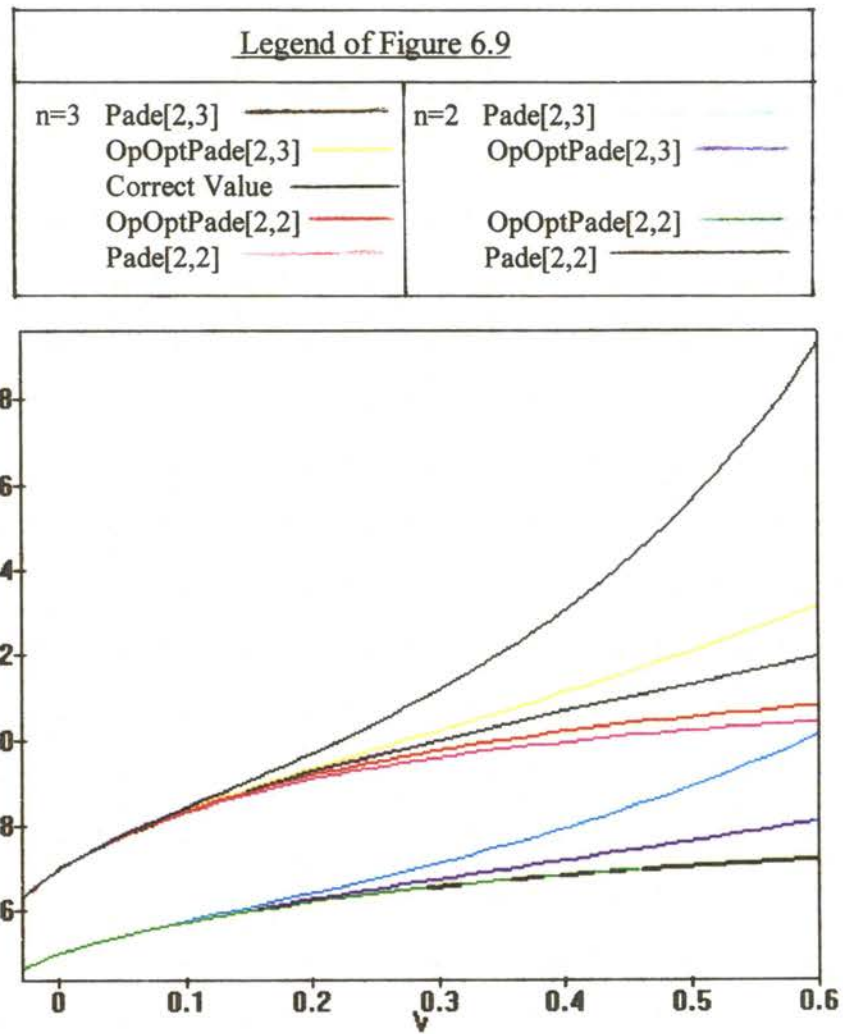


**Figure 6.9**

Padé Spectrum for excitation levels ( $n=2$ ) and ( $n=3$ ).

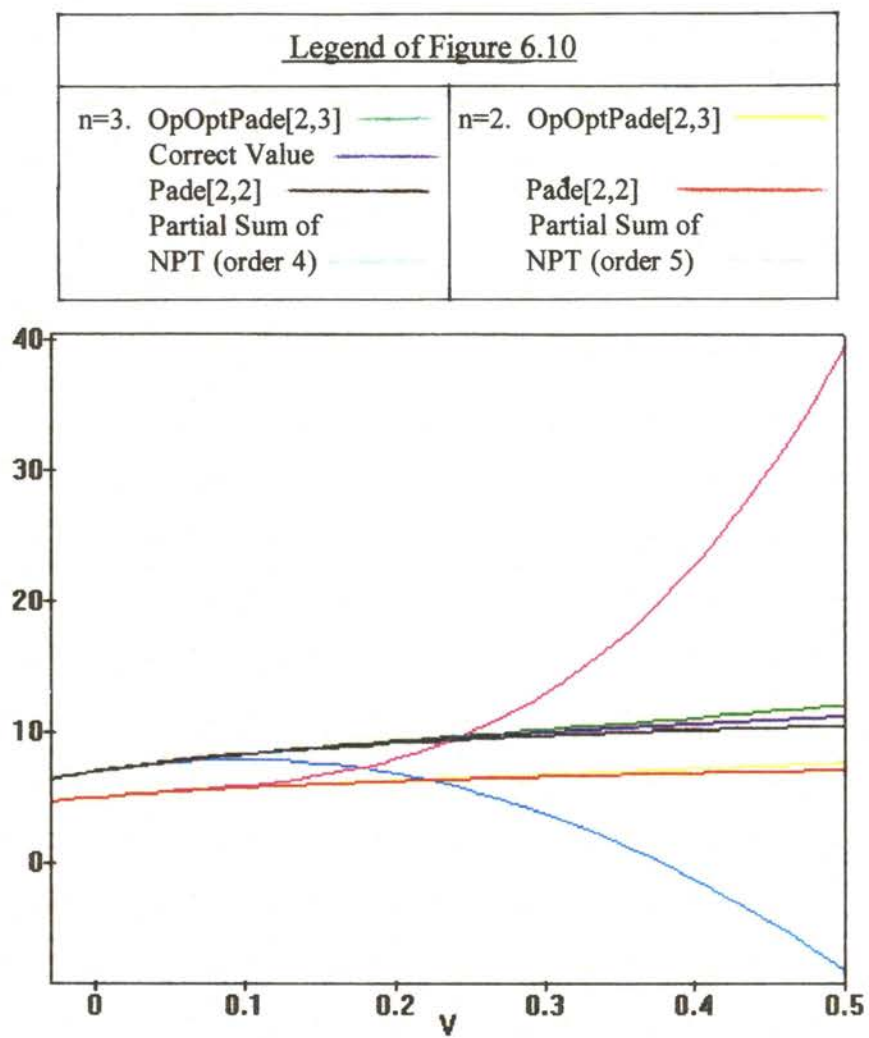


**Figure 6.10**

NPT partial sums presented for 2 upper n's.

The spherical harmonic oscillator spectrum is shown on the next few pages for the three lowest energy levels in the case where orbital angular momentum is  $l = 0$ . We first examine the example of the spherical quartic harmonic oscillator in the case where

orbital angular momentum  $l$  equals zero. Figures 6.11), 6.12), 6.13) and 6.14) are all of the results for the three lowest possible energy levels when  $l$  equals 0. Note that  $T$  is the spectral energy level number of the spherical harmonic oscillator.

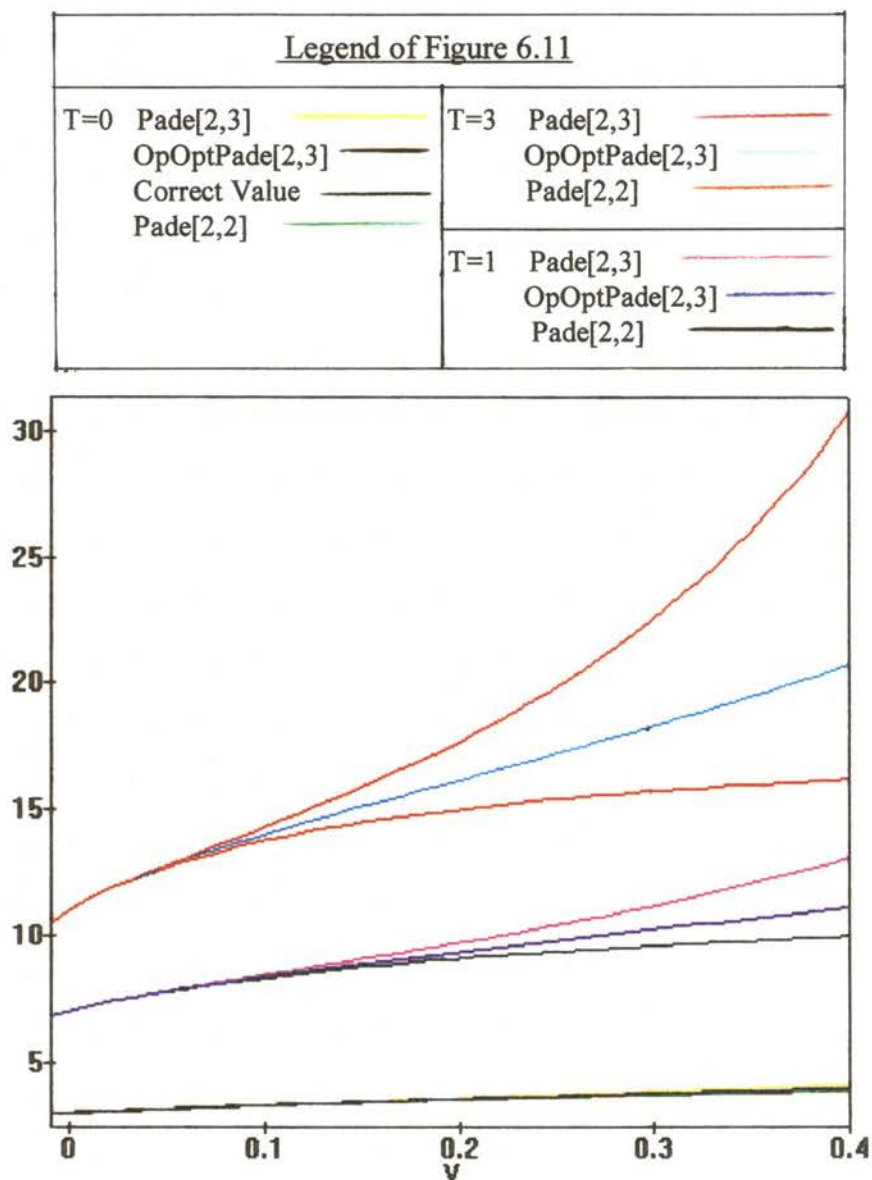


**Figure 6.11**

Padé Spectrum (including Padé approximants) of the 3 lowest energies.

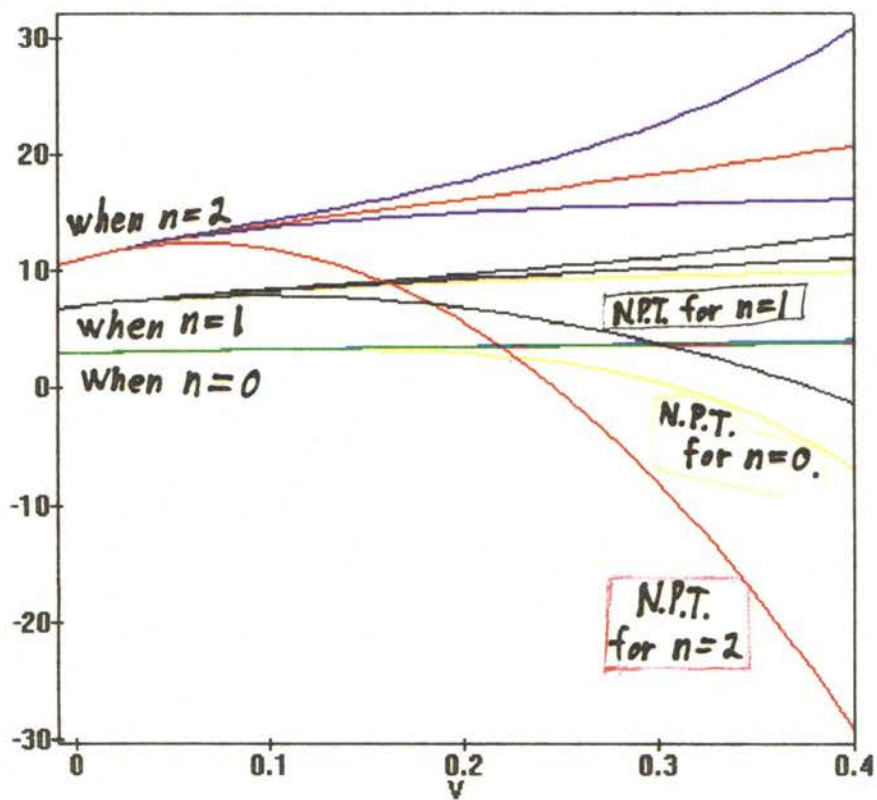
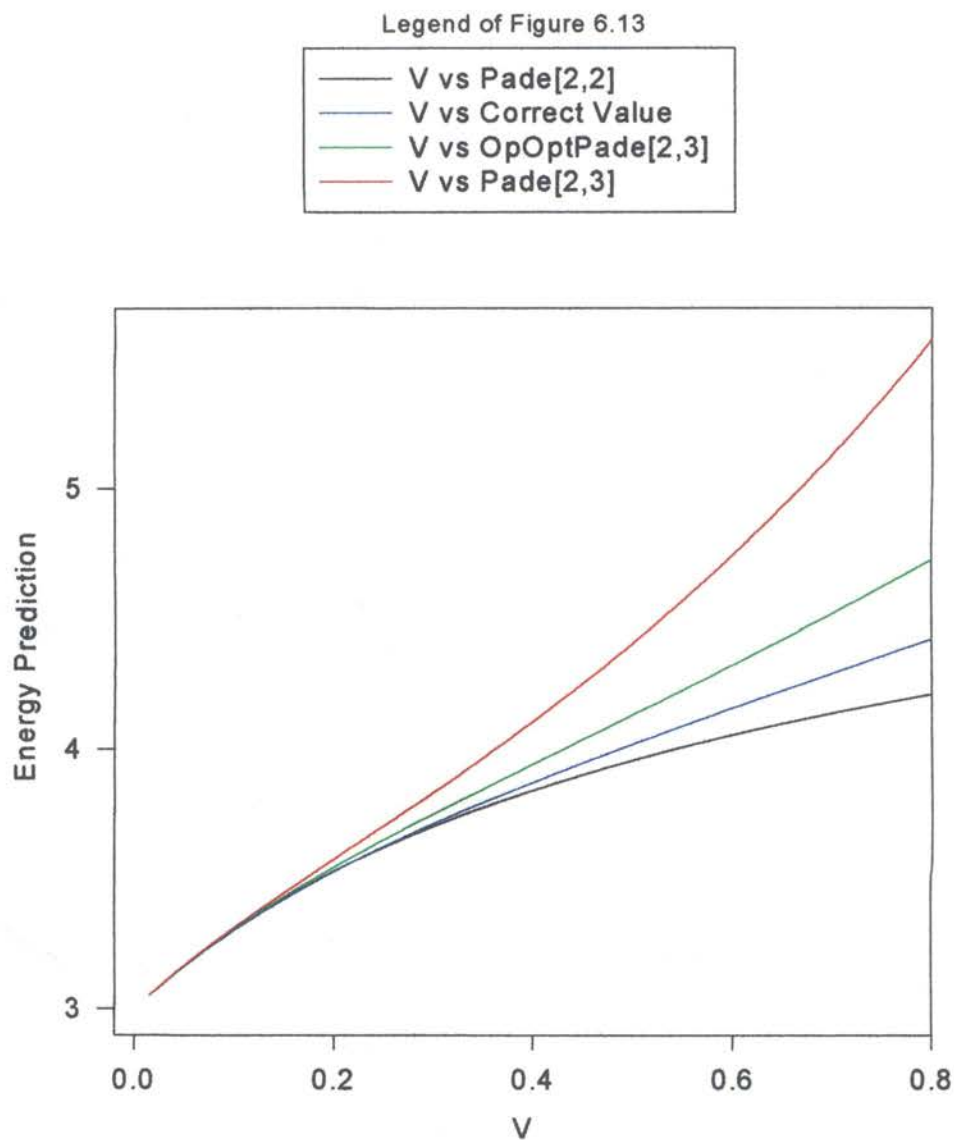


Figure 6.12

Spectrum for the 3 lowest energies including NPT Series as well as Padé approximants.

Now  $T$  is set equal to 1. The choice 1 is the smallest possible choice for  $T$  when the orbital angular momentum is  $l = 0$ . In figure 6.13,  $I$  does still equal zero.



**Figure 6.13**  
Energy Curve for the lowest possible Level when  $l = 0$ , showing Pade[2,2], OpOptPade[2,3], Pade[2,3], and the correct Energy.

Now  $T$  is set equal to 1. The choice 1 is the smallest possible choice for  $T$  when

the orbital angular momentum is  $l = 0$ . In figure 6.13,  $V$  does still equal zero.

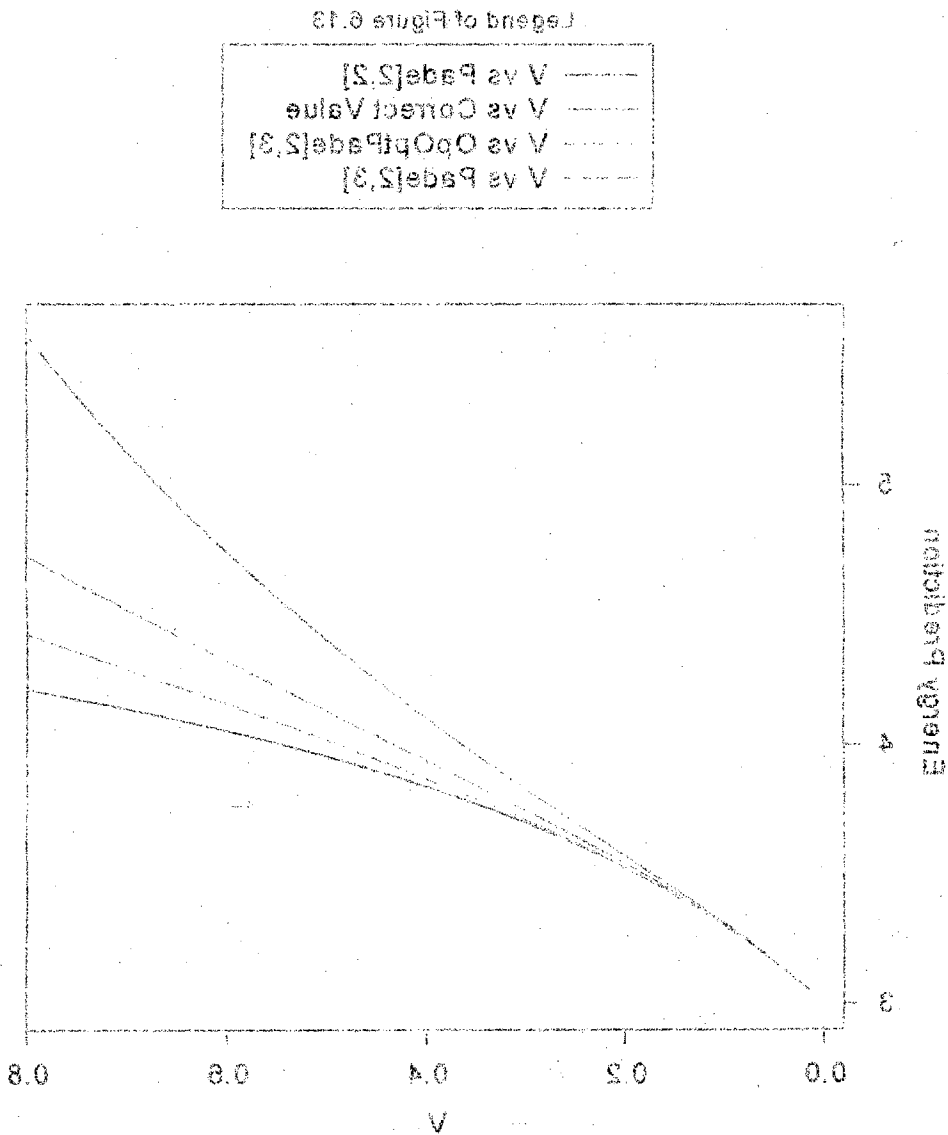
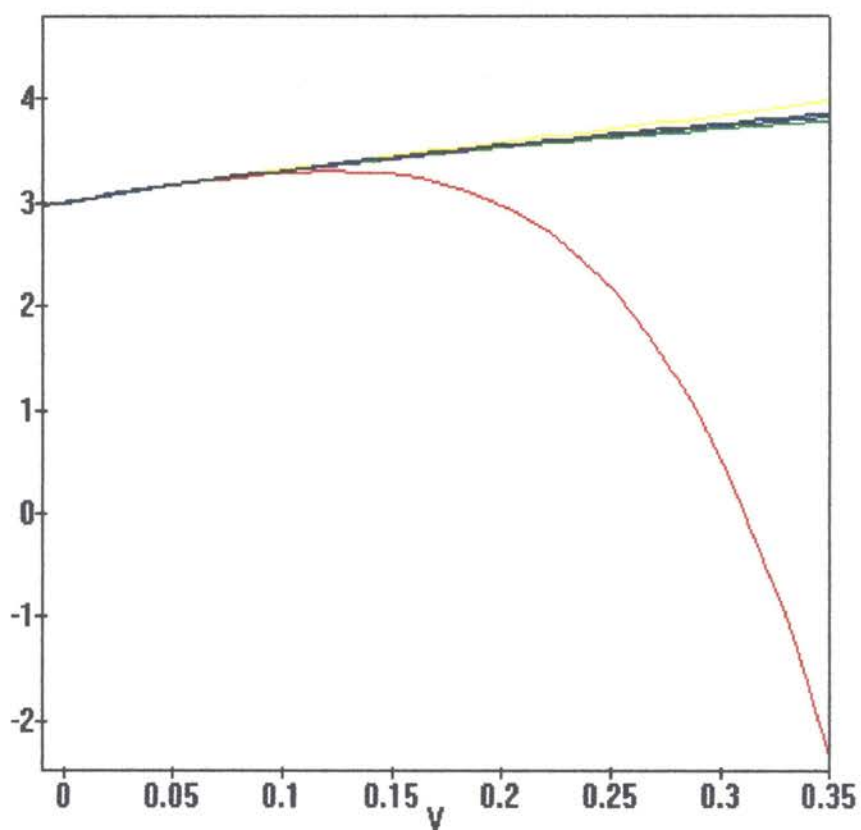


Figure 6.13 Energy Curve for the lowest possible level when  $l = 0$ , showing  $P_{ade}[2,3]$ ,  $Q_{op}P_{ade}[2,3]$ ,  $P_{ade}[2,3]$  and the correct Energy.

The lowest possible energy curve when  $l=0$  shall be referred as the 'ground orbit 0 energy' curve.



**Figure 6.14**

Padé Spectrum for the Ground Orbit 0 Energy ( Padé[2,2] —, OpOptPade[2,3] —, Padé[2,3] —, and Exact — ) and also the corresponding fourth order Perturbation Theory Result —.



The lowest possible energy curve when  $l=0$  shall be referred as the ground orbit 0 energy

curve.

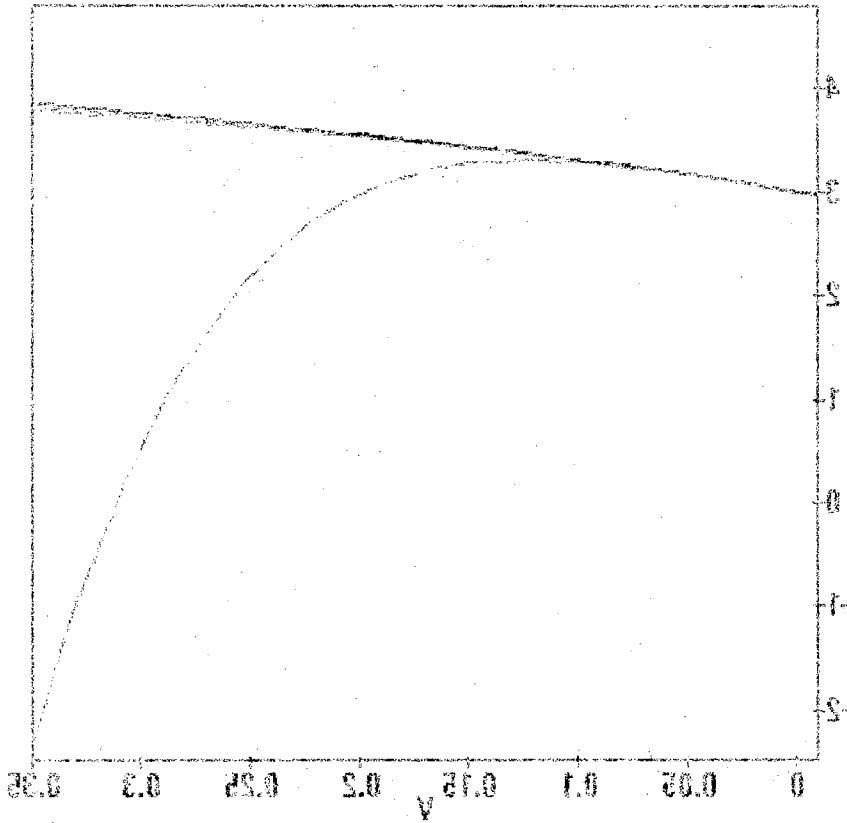
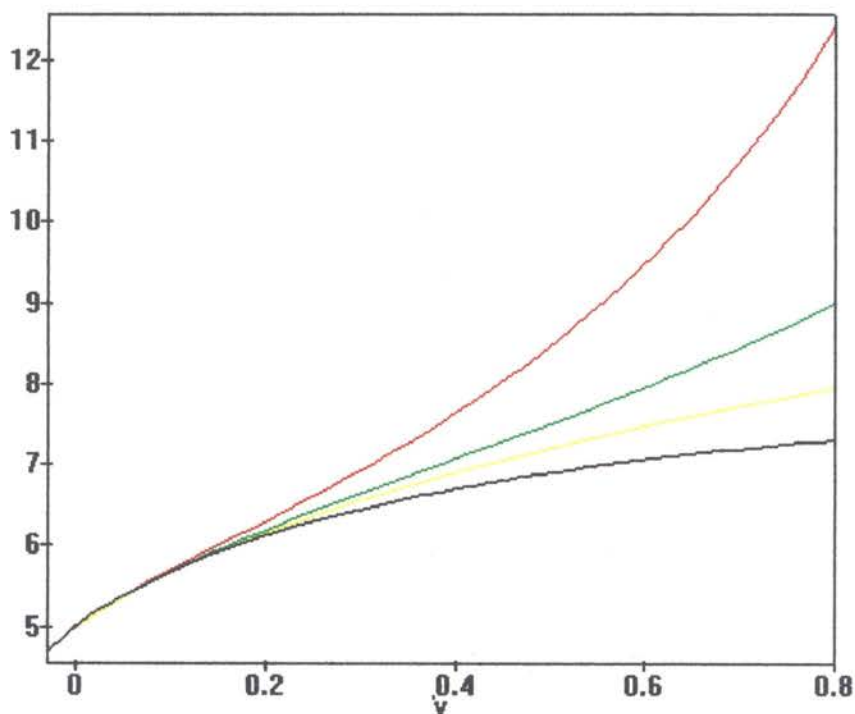


Figure 6.14

Padé spectrum for the Ground Orbit 0 Energy (Padé[2,2]) ---  
 OqOrPadé[2,3] --- Padé[2,3] and Exact --- and also the  
 corresponding fourth order Perturbation Theory Result ---

The Spherical harmonic oscillator spectrum is shown next for the lowest energy level in the case where orbital angular momentum quantum number  $l$  equals 1. In the next two pages we examine the example of the quartic harmonic oscillator in the second rotational case, where orbital angular momentum  $l$  equals one. Figures 6.15) and 6.16) are all of the results for the condition  $l = 1$ .



**Figure 6.15**

Padé Spectrum for the lowest Energy level when  $l=1$ , showing Padé[2,2] —, OpOptPadé[2,3] —, Padé[2,3] —, and the correct Energy —.

The spherical harmonic oscillator spectrum is shown next for the lowest energy level in the case where orbital angular momentum quantum number  $l$  is the next two pages we examine the example of the quartic harmonic oscillator in the second rotational case, where orbital angular momentum  $l$  equals one. Figures 6.15 and 6.16 are all of the results for the condition  $l = 1$ .

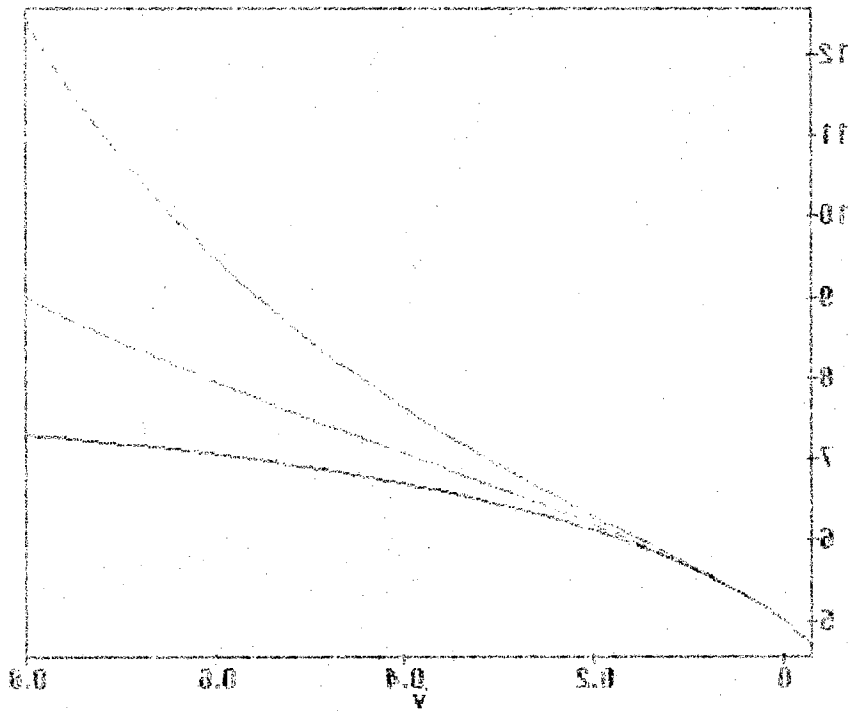
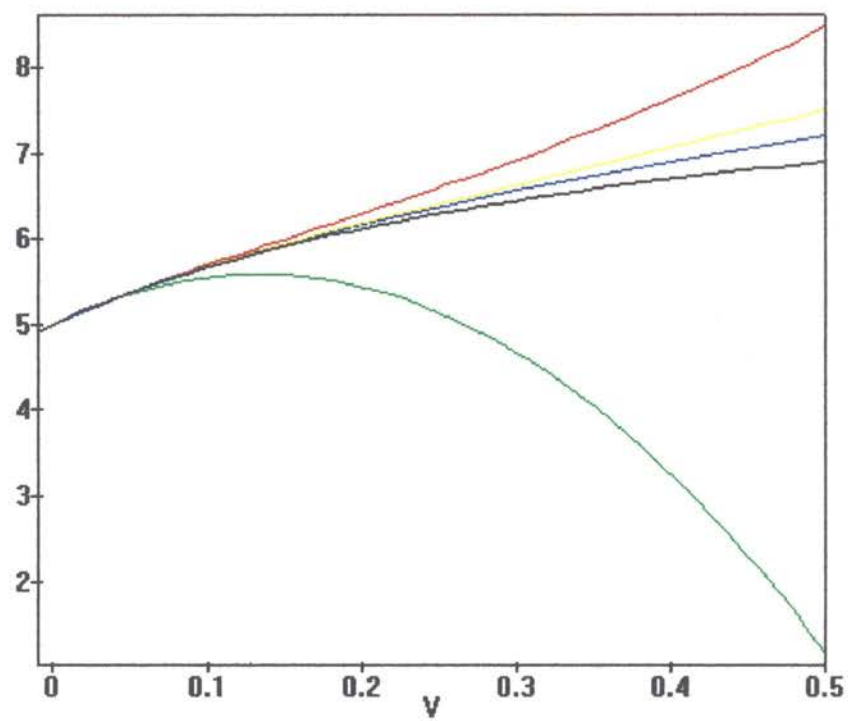


Figure 6.15

Padé spectrum for the lowest Energy level when  $l = 1$ , showing Padé[2,2] —, Padé[2,3] - - -, and the correct Energy



**Figure 6.16**

Padé Spectrum for the lowest Energy level when  $l=1$ , showing Padé[2,2] —, OpOptPadé[2,3] —, Padé[2,3] —, 2nd order NPT series —, and the correct Energy —.

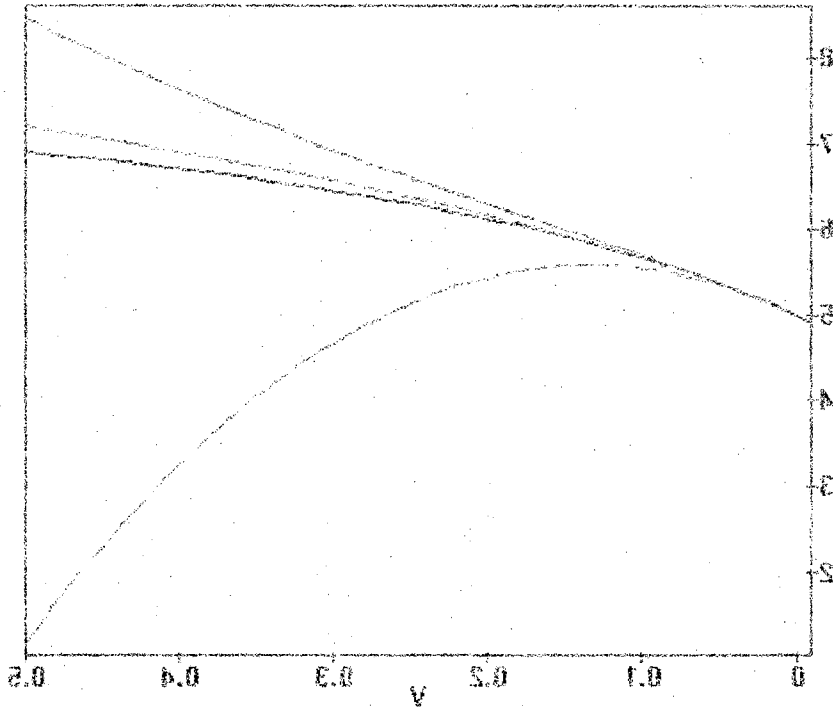


Figure 6.16

Padé spectrum for the lowest Energy level when  $l=1$ , showing  
 Padé[3,3] (---), OptPadé[3,3] (---), Padé[2,3] (---), 2nd order  
 MBT series (---), and the correct Energy (---)

## 6. Comparison of the Bender Perturbation Series to the Series extracted from Optimized Padé Approximants.

This section is dedicated strictly to making numerical comparisons with the older work of Bender and Wu. All of the results in this section involve perturbation series and the Padé approximant related expressions of these series for the ground state quartic harmonic oscillator. The Optimized Padé approximants are quoted from the equations written out in section # 5. From equation (6.30) we remember that

$$\text{OpOptPade}[2,3] := \frac{(1 + 11.0622987683344406 V + 22.2851225117544846 V^2)}{(1 + 10.3122987683344406 V + 15.86339884355036541 V^2 - 3.5657816931887873 V^3)}. \quad (6.36)$$

We remember that in section “5.” the series expansion of  $\text{OpOptPade}[2,3]$  was found.

The perturbative series calculated by Bender and Wu takes on the following appearance:

$$\text{BenderSum}(U) = 1/2 + 3/4 \cdot U - 21/8 \cdot U^2 + 333/16 \cdot U^3 - 30885/128 \cdot U^4 + \dots \quad (6.37)$$

This represents the ground state energy curve. None of the exact perturbation series representations of any of the energy levels of excitation are given in reference [12.b]. The coefficients of Bender’s ground energy expression come from the list on page 1233 of reference [12.b]. In this chapter of the dissertation, the main 1-dimensional Hamiltonian is:  $(-d^2/dx^2 + x^2) + V \cdot x^4$ . Bender uses the Hamiltonian  $(-d^2/dz^2 + 1/4 \cdot z^2) + 1/4 \cdot U \cdot z^4$ , where  $1/4 \cdot U \cdot z^4$  is the perturbation.  $V$  matches  $2 \cdot U$ , and  $x$  matches  $1/\sqrt{2} \cdot z$ . Keeping this linear transformation of parameters in mind, it is correct to compare  $2 \cdot \text{BenderSum}(V/2)$  with the optimal Padé approximant of the ground state energy for the quartic harmonic oscillator as a function of  $V$ . In terms of  $V$  and  $x$  ( $x$  for the eigenstates), Bender’s perturbation series grows in the following manner:

$$\begin{aligned} \text{BenderSum}(V/2) \cdot 2 = & 2 \cdot (1/2 + 3/4 \cdot (V/2) - 21/8 \cdot (V/2)^2 + 333/16 \cdot (V/2)^3 + \\ & (-1) \cdot (-30885/128) \cdot (V/2)^4 + (916731/256) \cdot (V/2)^5 + \\ & (-1) \cdot (65518401/1024) \cdot (V/2)^6 + (2723294673/2048) \cdot (V/2)^7 \dots \end{aligned} \quad (6.38)$$

Also see page 1233 of reference [12.b]. Numerically to the seventh order,

$$\begin{aligned} \text{BenderSum}(V/2) \cdot 2 \approx & 1 + .75000000 \cdot V - 1.3125000 \cdot V^2 + 5.2031250 \cdot V^3 - \\ & 30.161133 \cdot V^4 + 223.81128 \cdot V^5 - 1999.4629 \cdot V^6 + 20777.089 \cdot V^7 + \dots \end{aligned} \quad (6.39)$$

We remember that in section # 5 the series expansion of  $\text{OpOptPade}[2,3]$  was shown to equal:

$$\begin{aligned} \text{Taylor Series of OpOptPade}[2,3] \approx & 1 + .75000000 \cdot V - 1.3125000 \cdot V^2 + \\ & 5.2031250 \cdot V^3 + (-1) \cdot 30.16113 \cdot V^4 + 223.8113 \cdot V^5 + O \cdot V^6. \end{aligned} \quad (6.40)$$

Clearly, there is close agreement between the serial representation of the optimal Padé approximant and Bender's series out to fifth order.  $\text{OpOptPade}[2,3]$  underwent two successive iterations.

We should consider the results of the optimized Padé approximants  $\text{OpOptPade}[3,3]$ ,  $\text{OptPade}[3,4]$ ,  $\text{OpOptPade}[3,4]$ , and the Taylor series of these rational fractions. There is good agreement with the seventh order partial sum of the series  $\text{BenderSum}(V/2) \cdot 2$ . One can review from equations (6.31) and (6.32) of section "5." the semi-analytical expressions for  $\text{OpOptPade}[3,3]$  and  $\text{OptPade}[3,4]$  for the ground state energy.

$$\begin{aligned} \text{OpOptPade}[3,3] := & \frac{(1 + 16.4215261870 \cdot V + 65.1319296262 \cdot V^2 + 52.85484017 \cdot V^3)}{(1 + 15.671526187012 \cdot V + 54.6907849859 \cdot V^2 + 27.202504553 \cdot V^3)}. \end{aligned} \quad (6.41)$$

$$\begin{aligned} \text{OptPade}[3,4] := & \frac{(1 + 20.985617764121528 \cdot V + 115.5690757218338 \cdot V^2 + \\ & 154.34607522835382 \cdot V^3)}{(1 + 20.2356177641215284 \cdot V + 101.70486239874675 \cdot V^2 + \\ & 99.42355174470327 \cdot V^3 + (-1) \cdot 16.2186123918274 \cdot V^4)}. \end{aligned} \quad (6.42)$$

$$\text{OpOptPade}[3,4] := \frac{(1 + 20.99762723050 \cdot V + 115.7541242119793 \cdot V^2 + 154.83380302920 \cdot V^3)}{(1 + 20.247627230500 \cdot V + 101.88090378910 \cdot V^2 + 99.795010927405 \cdot V^3 + (-1) \cdot 16.317374593559 \cdot V^4)}. \quad (6.43)$$

In addition to inspecting the successful numerical results of the optimized Padé approximants in table 6.4) of section # 5, it is instructive and encouraging to see that the Taylor series of the second iterated optimized Pade[3,3] (OpOptPade[3,3]) matches term by term to the perturbative series of Bender and Wu at more than six significant figures. Bender's series is shown to seventh order. (Also see equation (6.39).)

$$\text{BenderSum7}(V/2) \cdot 2 = 1 + .75000000 \cdot V - 1.3125000 \cdot V^2 + 5.2031250 \cdot V^3 - 30.161133 \cdot V^4 + 223.81128 \cdot V^5 - 1999.4629 \cdot V^6 + 20777.089 \cdot V^7. \quad (6.44)$$

$$\text{Taylor Series of OpOptPade}[3,3] \approx 1 + .75000000 \cdot V - 1.31250000 \cdot V^2 + 5.20312500 \cdot V^3 - 30.161132748522 \cdot V^4 + 223.8112786 \cdot V^5 - 1999.4641 \cdot V^6 \quad (6.45)$$

$$\text{Taylor Series of OpOptPade}[3,4] \approx 1 + .750000000 \cdot V - 1.31250000 \cdot V^2 + 5.20312500 \cdot V^3 - 30.1611328 \cdot V^4 + 223.8112796 \cdot V^5 - 1999.4664 \cdot V^6 + 20777.186 \cdot V^7 \quad (6.46)$$

Table 6.6) will show in explicit numerical form the first ten coefficients of the series  $\text{BenderSum}(V/2) \cdot 2$ . The first eight coefficients of the Taylor series of  $\text{OpOptoPade}[3,3]$  and/or those of  $\text{OpOptPade}[3,4]$  for the ground state energy as well as the first ten coefficients  $\text{BenderSum}(V/2) \cdot 2$  from (6.39) are included in Table 6.6).



**Table 6.6)**

Table which lists coefficients of the Bender series for Ground State Energy

Order #	0	1	2	3	4
Bender's	1	.75000000	-1.3125000	5.2031250	-30.161133
Optimized Padé	1	.750000000	-1.31250000	5.2031250	-30.16113275

Order #	5	6	7	8	9
Bender's	223.81128	-1999.4629	20777.089	-245689.177	3256021.9
Optimized Padé	223.81128	-1999.4641	20777.186**	unknown	unknown

\*\* 20777.186 comes from OpOptPade[3,4], which is more accurate than OptPade[3,4].

It is worth noting that for orders 1 through 5 there is agreement at least to eight significant figures between the coefficients by Bender and the coefficients from the optimized Padé approximants. For order 6, there is agreement to six significant figures between the coefficient by Bender and the coefficients from the optimized Padé approximant. For order 7, there is agreement to five significant figures. If the partial fraction OpOptPade[3,4] were iteratively constructed, it is plausible to believe that there would be agreement to six significant figures for the seventh order. However, it becomes very difficult to do more than one iteration of the optimized Padé approximant [3,4] due to limitations of available RAM on the particular PC used for research. Overall, it is good to see that there is agreement to at least five significant figures for the first eight terms of the NPT series.

## 7. Comment on $V' \cdot x^6$ contributions and Closing Statement

All of the results presented in this chapter have been for the quartic harmonic oscillator. However, it is only moderately more difficult to calculate to good approximation of the lowest several energy curves of the harmonic oscillator with a 'hexic' perturbation of the form  $V' \cdot x^6$  by using optimized Padé approximants.

Appendix C presents the results of the optimized perturbative calculation of the ground state energy of the hexic (sixth order) harmonic oscillator. The  $V'$  dependent perturbative series of the optimized perturbative calculation is equivalent to the series that can be generated by the recursive method described by Bender and Wu in [12.b]. While this perturbative series of the 'hexic' energy curve quickly diverges, the optimized Padé approximants OpOptoPade23 and OpOptoPade33 for the 'hexic' harmonic oscillator provide reasonable predictions for the energy spectrum. See appendix C for results. This discussion does conclude chapter 6.

## Chapter 7

### Estimating Perturbative Coefficients in Quantum Field Theory by using Padé Approximants

#### Padé Approximant Predictions

The calculations of quantities and observables requiring Quantum Electrodynamics and Quantum Chromodynamics theory shall be discussed in the entirety of this chapter. Padé Approximant Predictions shall be used for most of the informative calculations. However, in the middle of this chapter, Padé Approximant results shall be shown for the anomalous magnetic moment calculation of the muon.

The method for generating Padé Approximant Predictions should be remembered from equation (1.13) of chapter 1. Given a series  $r_0 + r_1 \cdot x + r_2 \cdot x^2 + \dots$ ,  $r_{(n+m+1)}$  can be predicted usually to high level of accuracy by taking the Padé Approximant prediction $[n,m]$  (PAP $[n,m]$ ) from the partial sum going all the way up to  $r_{(n+m)} \cdot x^{(n+m)}$ .

We remember (1.13) as:

$$r_{(n+m+1)} \approx - ( b_1 \cdot r_{(n+m)} + b_2 \cdot r_{(n+m-1)} + b_3 \cdot r_{(n+m-2)} + \dots + b_m \cdot r_{(n+1)} ) \quad (7.1)$$

$b_1, b_2, b_3, \dots, b_m$  are calculated by using the method demonstrated in equations (1.6), (1.7), and (1.8). In a manner consistent with equations (5.4) and (5.5), the standard results for PAP $[1,1]$ , PAP $[2,1]$ , PAP $[0,2]$ , and PAP $[1,2]$  are listed:

$$\text{I} \quad r_3 \{\text{estimated}\} = (r_2)^2 / r_1 \quad , \quad (7.2a)$$

$$r_4 \{\text{estimated}\} = (r_3)^2 / r_2 \quad , \quad (7.2b)$$

$$\text{II} \quad r_3 \{\text{estimated}\} = 2 \cdot r_1 \cdot r_2 / r_0 - (r_1)^3 / (r_0)^2 \quad , \quad (7.2c)$$

$$\text{III} \quad r_4\{\text{estimated}\} = \frac{2r_1 \cdot r_2 \cdot r_3 - r_0 \cdot r_3^2 - r_2^3}{(r_1^2 - r_0 \cdot r_2^2)} \quad (7.2d)$$

Results I, II, and III, which are PAPs for  $r_3$  and  $r_4$ , will be used frequently in the applications of this chapter.

In chapter 7, the partial sum  $r_0 + r_1 \cdot x + r_2 \cdot x^2 + \dots + r_{(n+m-1)} \cdot x^{(n+m-1)} + r_{(n+m)} \cdot x^{(n+m)}$  shall always end up representing one of the perturbative quantum field theory expressions mentioned in the first paragraph. From all of the diverse examples of chapters 2 through 6 and all of the insights and near-theorems, it should be clear that Padé approximants and PAPs are more **reliable and** successful when a large number of terms are supplied from a series than when only a small number of terms is supplied from a series representing a perturbative function. In QED and in QCD to a lesser extent, it is with higher order partial sums of series that Padé approximants and PAPs are the most useful, since analytically one has hundreds of Feynman diagrams and then thousands of Feynman diagrams with complicated calculations. The material in the next several paragraphs is based on results in a Physical Review D publication. [18]

### **Predicting higher order Terms in QED.**

We begin with the difference between the muon and the electron anomalous magnetic moments (QED contributions)[19]:

$$a_u - a_e = 1.09 \cdot x^2 + 22.87 \cdot x^3 + 127 \cdot x^4 + 570(140) \cdot x^5, \quad (7.3)$$

where  $x = (\alpha/\pi)$  and  $570(140)$  means  $570 \pm 140$ , and the coefficient of  $x^5$  is a conservative estimate. The results are given in Table 7.1). It can be seen that there is a

beautiful agreement with the known results. Moreover the next term is predicted to be about 2500, and this agrees well with an estimate performed by Kinoshita

$$a(12)_u = 10 \cdot K^3 \cdot a(6) \cdot u(\text{gg}) = 2500(900), \quad (7.4)$$

where we take  $2 \leq K \leq 2.5$ . (See Kinoshita, Nizic, and Okamoto [20] for a discussion of this method.) For the next-next term, we estimate, using  $K=2.5$ ,

$$a(14)_u = 15 \cdot K^4 \cdot a(6) \cdot u(\text{gg}) = 12,500(4000). \quad (7.5)$$

NT means the next (unknown) term. NNT means the next-next term, or the second unknown term.

**Table 7.1)**

Comparison of the PAP for  $a_u - a_e$  with the Known Results

$a_u - a_e$	Equation	Estimate	Known result
I		705	570(140)
I		2558	1600-3400 NT
I		11480	8500-16500 NNT
II		2415	1600-3400 NT
II		11480	8500-16500 NT
III		2362	1600-3400 NT
III		11480	8500-16500 NNT

Next, we consider the anomalous magnetic moment of the electron [21]:

$$a_e = x/2 - 0.3285 \cdot x^2 + 1.176 \cdot x^3 - 1.434 \cdot x^4. \quad (7.6)$$

The results are given in Table 7.2).

Table 7.2)

Padé Estimates for  $a_e$ , which are compared to known Results

$a_e$ Equation	Estimate	Known result
I	-4.21	-4.23
I	1.74	NT
I	-2.12	NNT
II	-1.40	-1.43
III	3.22	NT
III	-2.13	NNT

Again there is good agreement with the known results, especially for the eighth-order coefficient from result II, where the prediction is -1.40 and the known result is -1.43. Moreover, the next term may be about 2.5. It is interesting to note that, if this is correct, the perturbation series for  $a_e$  continues to be an oscillating series. The next term, predicted to be -2.12, continues this pattern. We now consider the perturbation expansion for

$$a_u = x/2 + 0.7655 \cdot x^2 + 24.05 \cdot x^3 + 125.6 \cdot x^4 + 573(140) \cdot x^5, \quad (7.7)$$

where the  $x^5$  coefficient is a conservative estimate. The results are shown in Table 5.3). It can be seen that the agreement with the known values is quite good and the prediction for the next term and the second unknown term agree very well with the very well with the estimates using Kinoshita's method. (See equations (7.4) and (7.5).)

**Table 7.3)**

PAPs for  $a_u(\text{QED})$ , which are compared to known Results

$a_u$ Equation	Estimate	Known result
I	656	573(140)
	2614	1600-3400 NT
	11925	8500-16500 NNT
II	71.8	125.6
	2559	1600-3400 NT
	11925	8500-16500 NNT
III	2548	1600-3400 NT
	11929	8500-16500 NNT

### Padé Approximants applied to QED.

The first the terms of Equation (7.3) for  $a_u - a_e$  can be calculated out to higher precision. This has been done carefully in a fourth order (w.r.t  $x$ ) calculation [19],[21]:

$$a_u - a_e = 1.09433583(7) \cdot x^2 + 22.869265(4) \cdot x^3 + 127.00(41) \cdot x^4. \quad (7.8)$$

$$\text{diffaOverx2} = (\text{Partial Sum of (7.8)})/(x^2). \quad (\text{Local definition}). \quad (7.9)$$

As in (7.4),  $x$  equals  $(\alpha/\pi)$ . In some cases in which enough initial information is given, Padé approximants reveal more fully the functional dependence of a perturbative QED expression on  $\alpha$  than the NPT series of the same QED expression. In a SLAC Publication[22], the Padé approximant  $\text{Pade}[1,1]$  is taken of  $\text{diffaOverx2}$  of (7.9). By plugging in the precise value of  $\alpha$ , one obtains the value

$$x^2 \cdot (\text{Pade}[1,1]) = 6194839(12) \cdot 10^{(-12)} \quad (7.10)$$

The value from the partial sum in (7.8) is:

$$\text{Sum of (7.8)} = 6194791(12) \cdot 10^{(-12)}. \quad (7.11)$$

$a_e$  has been carefully evaluated as:

$$\text{Value of } a_e = 1159652173.5(24.0) \cdot 10^{(-12)}. [22] \quad (7.12)$$

Electro-weak corrections and quantum chromodynamic hadronic corrections [23],[24] to the QED perturbation series (7.8) also need to be considered. These corrections are shown and explained in references [23] and [24]. In these references, there are two independent phenomenological results given for the hadronic correction of  $a_u$ . The most recent known results are given in (7.13) a, b, and c.

$$\text{First recorded: } \Delta a_u\{\text{hadronic}\} = 69500(1500) \cdot 10^{(-12)} [24]; \quad (7.13a)$$

$$\text{Separately recorded: } \Delta a_u\{\text{hadronic}\} = 70110(940) \cdot 10^{(-12)} [24]; \quad (7.13b)$$

$$\text{For the weak correction: } \Delta a_u\{\text{E.W.}\} = 1510(40) \cdot 10^{(-12)} [23]. \quad (7.13c)$$

After adding (7.12) to (7.10) and after adding the small hadronic contribution of (7.13a) and the weak contribution (7.13c), one obtains first the phenomenological theoretical value

$$a_u = 1165918022.5(1576.0) \cdot 10^{(-12)} \quad (7.14)$$

for the anomalous magnetic moment of the muon. On the other hand after adding the small hadronic contributions of (7.13b) and the same weak contribution (7.13c), one obtains the other phenomenological theoretical value of

$$a_u = 1165918632.5(1016.0) \cdot 10^{(-12)} \quad (7.15)$$

for the anomalous magnetic moment of the muon. The two resulting theoretical values of  $a_u$  which are based on the partial sum (7.8) and the contributions of (7.13)(a,bc) are: first

$$\text{with the addition of (7.13a) plus (7.13c): } 1165917975(1576) \cdot 10^{(-12)} \quad (7.16a)$$

$$\text{and secondly with the addition of (7.13b) plus (7.13c): } 1165918585(1016) \cdot 10^{(-12)}. \quad (7.16b)$$

The experimental value [25][26] of  $a_u$  was found to be:



$$a_u^{\{\text{experimnt}\}} = 1165923000(9000) \cdot 10^{(-12)} \quad (7.17)$$

Comparison should be made of (7.14) (which is from  $x^2 \cdot (\text{Pade}[1,1])$ ) with the NPT value effected by (7.16a) and of (7.15) with the NPT value effected by (7.16b). Equations (7.17b), (7.17c), (7.17d), and (7.17e) show such comparisons:

The closeness of results with the assistance of the Pade approximant:

$$\text{percent difference between } a_u^{\{\text{experimnt}\}} \text{ and (7.14)} := -4.269158962 \cdot 10^{(-8)} \% \quad (7.17b)$$

$$\text{percent difference between } a_u^{\{\text{experimnt}\}} \text{ and (7.15)} := -3.745966226 \cdot 10^{(-8)} \% \quad (7.17c)$$

The closeness of results with the use of just NPT:

$$\text{percent difference between } a_u^{\{\text{experimnt}\}} \text{ and (7.16a)} := -4.309899392 \cdot 10^{(-8)} \% \quad (7.17d)$$

$$\text{percent difference between } a_u^{\{\text{experimnt}\}} \text{ and (7.16b)} := -3.786706634 \cdot 10^{(-8)} \% \quad (7.17e)$$

From these comparisons, it becomes apparent that  $a_u$  of (7.14) and (7.15) is slightly more accurate (closer to the known experimental value) than the value of  $a_u$  obtained solely from taking the partial sum of the QED series added to the hadronic and weak contributions. In summary, it can be said that the  $\text{Pade}[1,1]/(x^2)$  applied to the QED series (7.8) leads to slightly closer agreement to the experimental  $a_u$  than the plain QED partial sum which (7.8) displays.

In order to ever improve the ability to test and understand QED, it is quantitatively desirable to calculate exactly the fifth order term and to then use the fifth order partial sum version of (7.8). Then in great likelihood the partial sum for  $a_u$  plus the hadronic and weak contributions, and to even closer proximity the calculation  $x^2 \cdot (\text{Pade}[1,2])$  of  $a_u$  plus the hadronic and weak contributions, will lead to a more precise theoretical value of  $a_u$  which disagrees with the experimental value by only one decimal

place with respect to the experimental value of  $1165923(9) \cdot 10^{(-9)}$ . Note that this experimental value holds today in 1997, just as it did in 1977. [25] [26]

### Applications of PAPs to perturbative QCD

As our first example relevant to strong force phenomena, we turn to the beta function of QCD. A paper which treated the PAPs applied to  $\beta_{\text{QCD}}$  was submitted in 1993 [18]. The QCD beta function has recently been calculated to the fourth order.[27] [28]. It is given by the serial expression

$$\begin{aligned} \beta_{\text{QCD}}/(g^2) = & (-11 + 2/3 \cdot N_f) \cdot (z) + (-102 + 38/3 \cdot N_f) \cdot (z)^2 \\ & + (-2857/2 + 5033/18 \cdot N_f - 325/54 \cdot (N_f)^2) \cdot (z)^3 + \\ & (-29243.0 + 6946.30 \cdot N_f - 405.089 \cdot N_f^2 - 1.49931 \cdot N_f^3) \cdot (z)^4 \dots, \end{aligned} \quad (7.18)$$

where  $z = g^2/(4\pi)$  and  $N_f$  is the number of fermions (quarks). For the sake facilitating the clarity of results of the data table of this section, we conveniently use the symbol  $b(n)$  for the beta function over  $(g^2)$  of (7.15):

$$\beta_{\text{QCD}}/(g^2) = b_{(0)} \cdot z + b_{(1)} \cdot (z)^2 + b_{(2)} \cdot (z)^3 + b_{(3)} \cdot (z)^4 \dots \quad (7.18b)$$

Before the end of 1996, only  $b_{(0)}$ ,  $b_{(1)}$ , and  $b_{(2)}$  of (7.18b) were known.  $b_{(0)}$  shall be treated as 'r0'.  $b_{(1)}$  shall be treated as 'r1', and so forth.

Brief numerical results of PAPs are presented in Table 7.4) to predict the fourth coefficient for the cases when  $N_f = 5, 3,$  and  $1$ . The results for  $N_f=5$  are very good. The results for  $N_f=3,$  and  $1,$  although not as good, are still reasonable. For the case  $N_f=6,$  no prediction of sign nor order of magnitude was given due to the ominous failure to predict the correct sign of  $b_{(2)}$  from  $b_{(1)}$  and  $b_{(0)}$  with the Padé Approximant Prediction (I). (See

equations (7.2a) for (I).) In the cases of  $N_f=1$ ,  $N_f=2$ , through  $N_f=5$ , it was the fairly accurate results of the PAP (I) of  $b_{(2)}$  and the numerical consistency of the PAP (I) and PAP (II) of  $b_{(3)}$  that gave the author confidence in making a rough estimate of  $b_{(3)}$ . Before 1996, it was helpful and conducive for discussion to use these PAPs for predicting the sign of  $b_{(3)}$  and the order of magnitude of  $b_{(3)}$  (that is the predicted  $b_{(3)}$  +/- 70% of the correct  $b_{(3)}$ ).

Next, Table 7.4) is presented.

**Table 7.4)**

PAPs for the QCD beta Function

PAP formula for $\beta_{(n)}$ of $\beta_{\text{QCD}}/(g^2)$	$N_f$	PAP	Known results	Exact $b_{(3)}$ results which exclude the Casimir terms ***
I *	5	-195.0	-189.9 for $b_{(2)}$	--not applicable--
	5	-846.3	-4826.14 for $b_{(3)}$ **	-2909.40
II*	5	-841.2	-4826.14 for $b_{(3)}$ **	-2909.40
I	3	-455.1	-643.9	-----
	3	-6480	-12090.4 **	-9135.95
II	3	-5921	-12090.4 **	-9135.95
I	1	-772.3	-1155	-----
	1	-14931	-22703.3 **	-18658.3
II	1	-13292	-22703.3 **	-18658.3

\* The PAP formulas I and II are written out in (7.2a) and (7.2b).

\*\* The fourth order results,  $b_{(3)}$  (for  $z^4$ ) were not available at the time of publication in which the estimates in Table 7.4) were first presented. The two references [27] and [28]

contain the formula for calculating  $b_{(3)}$  as a function of  $N_f$  analytically and approximately, respectively.

\*\*\* The Casimir terms consists of the following single expression:

$$N^2 \cdot (N^2 + 36) / 24 \cdot (-80/9 + 704/3 \cdot \zeta(3)) + nf \cdot N \cdot (N^2 + 6) / 48 \cdot (512/9 - 1664/3 \cdot \zeta(3)) + nf^2 \cdot (N^4 - 6 \cdot N^2 + 18) / (96 \cdot N^2) \cdot (-704/9 + 512/3 \cdot \zeta(3)), \text{ where } N=3.$$

The exact expression of  $b_{(3)}$ , which is explained on pages 381 and 382 of [27], includes this single expression.

### PAPs applied to the Quantum Chromodynamic R ratio

The material in this section is based on results in Physical Review E publication [17]. We will consider the R ratio in perturbative QCD [29 to 32]. The R ratio is defined as follows:

$$R = \frac{\sigma(e^+e^- \rightarrow \text{hadrons})}{\sigma(e^+e^- \rightarrow \mu^+\mu^-)} \quad (7.19)$$

We first consider R in the general MS-type renormalization scheme given by the

$$\text{parameter } t, \quad \Lambda_t = \exp(-t/2) \cdot \Lambda_{\text{MS-bar}}. \quad (7.20)$$

Obviously  $t=0$  corresponds to the MS-bar scheme.  $t = \ln(4\pi) - \gamma = 1.95$  represents the MS scheme.  $t$  equals  $-2.0$  for the G scheme.  $t = 4 \cdot \zeta(3) - 11/2 = -0.692$  yields the special MS scheme selected for reference [29]. The scale-dependent R (in the general MS-type scheme) is given by

$$R = 3 \cdot \left( \sum_N (Q[N_f])^2 \cdot R(t) \right) - 1.24 \cdot \left( \sum_N Q[N_f] \right)^2 \cdot x^3, \quad (7.21)$$

where  $x = \alpha_s/\pi$  and  $N_f$  is the number of fermions (quarks). We neglect the second term in equation (7.21) as it is small in all cases of interest.  $R(t)$  is given by

$$R(t) = 1 + x + x^2 \cdot [(1.9857 + 2.75 \cdot t) - N_f \cdot (0.1153 + 0.1667 \cdot t)] + x^3 \cdot [ \\ (N_f^2 \cdot ((-1) \cdot 0.0052 + 0.0384 \cdot t + 0.0278 \cdot t^2)) + (-6.6369 + 17.2964 \cdot t + 7.5625 \cdot t^2) + \\ (-1) \cdot N_f \cdot (1.2001 + 2.0877 \cdot t + 0.9167 \cdot t^2) ] . \quad (7.22)$$

For the sake of back referencing, (7.22) shall also be expressed as:

$$R(t) = 1 + x \cdot r_1 + x^2 \cdot r_2 + x^3 \cdot r_3 . \quad (7.22b)$$

Padé Approximant Predictions have been calculated for the coefficients of the series  $R(t)$  with respect to  $x$ . Exact calculations and PAPs of these coefficients are displayed in Figures 7.1), 7.2), 7.3), and 7.4).

It can be seen that the method works very well, and we can predict with confidence the unknown next term (NT),  $r_4 \cdot x^4$ . Figures 7.1), 7.2), 7.3), 7.4) are presented on the next three pages. It is clear that there is almost complete agreement between the predictions of  $r_4$  of the  $R(t)$  perturbative series from PAP[1,2] and PAP[2,1] in Figures 7.3) and 7.4), especially when  $t$  is large.

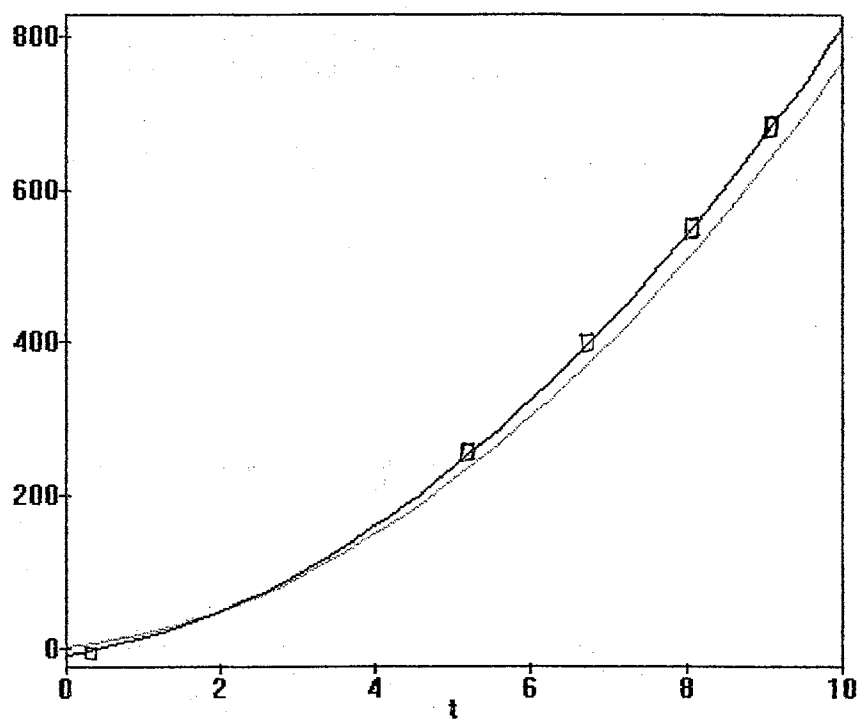


**Figure 7.1)**  
Comparison of PAP derived  $r_3$  — and the analytically  
known  $r_3$  -□-□- When  $N_f=1$ .

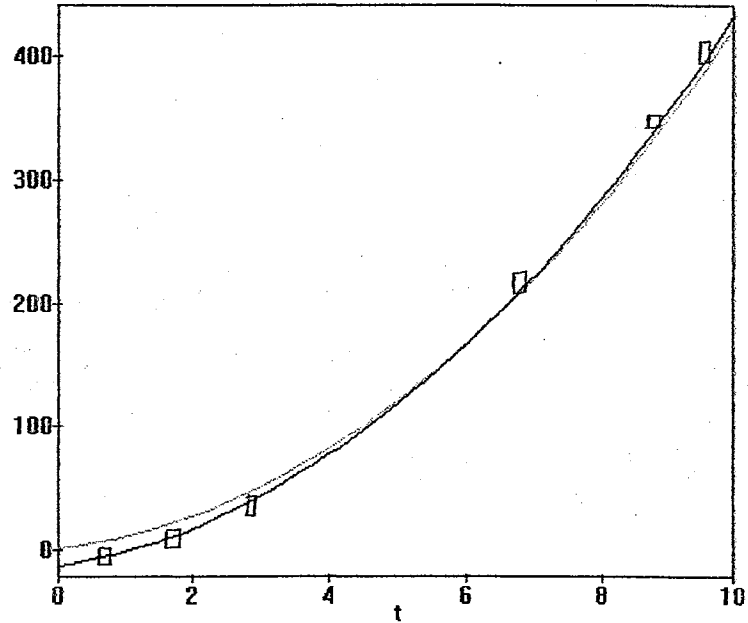


**Figure 7.2)**  
Comparison of PAP derived  $r_3$  — with the analytically known  $r_3$  □□□ When  $N_f=5$ .

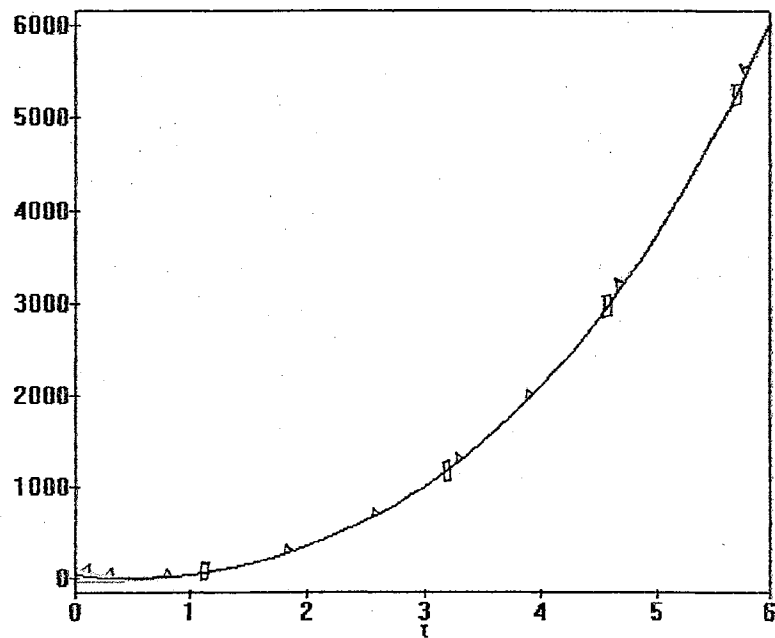


**Figure 7.3)**  
Comparison of the PAP[1,2] Estimate of  $r_4$  ▲▲▲ with the PAP[2,1] Estimate of  $r_4$  □□□ and with the Estimate using PAP[0,2]  $r_4$  — When  $N_f=1$ .

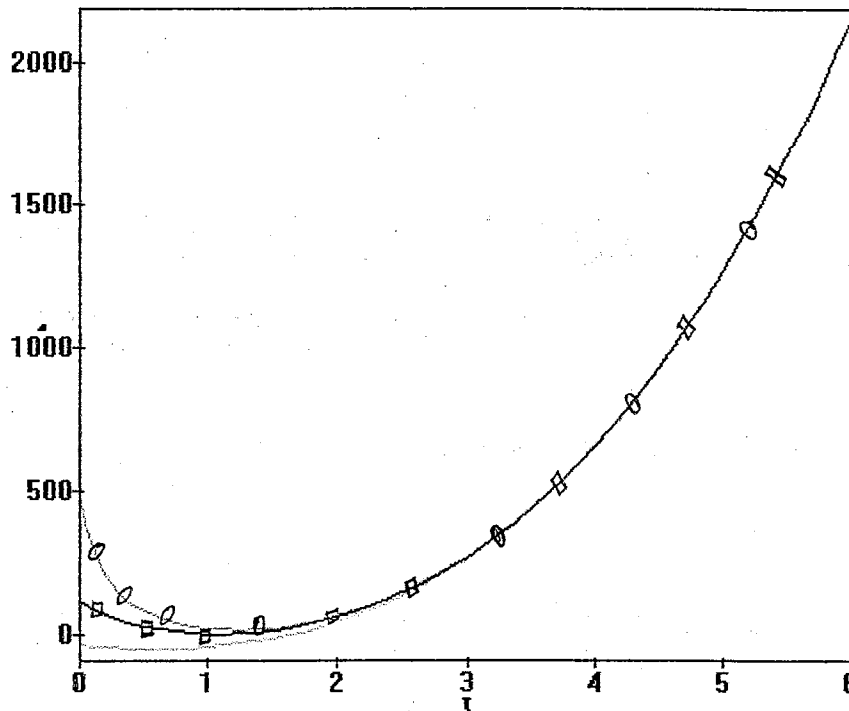


**Figure 7.4)**

Comparison of the PAP[1,2] Estimate of  $r_4$   $\diamond$  with the PAP[2,1] Estimate of  $r_4$   $\square$  and with the Estimate using PAP[0,2]  $\text{---}$  When  $N_f=5$ .

In Figures 7.1) and 7.2), we plotted the estimated and exact values of  $r_3$  as a function of  $t$  for the two representative values of  $N_f$  ( $N_f=1$  and  $N_f=5$ , respectively). It can be seen that the agreement is excellent for  $t > 1$  and improves as  $t$  increases. The reason for this behavior can be seen as follows.

By taking the Padé Approximant Prediction [1,1] of the RHS of (7.22), we obtain

$$r_3 = r_2^2/r_1 = 3.943 + 10.92 \cdot t + 7.5625 \cdot t^2 - N_f \cdot (.458 + 1.2962 \cdot t + 0.9167 \cdot t^2) + N_f^2 \cdot (0.0133 + .0384 \cdot t + 0.0278 \cdot t^2) . \quad (7.23)$$



The exact result is given by the  $x^3$  term in equation (7.22). It can be seen by comparing this term with equation (7.23) that the  $t^2$ ,  $t^2 \cdot N_f$ ,  $t^2 \cdot N_f^2$ , and  $t \cdot N_f^2$  coefficients agree. In fact, this agreement is exact. Now we understand why the estimate and the exact result agree so well for large  $t$ .

The reason for the agreement of the coefficients can be seen as follows [29].

Consider the function given by 
$$D(q^2/u^2, a_s) = \sum_i R_i(a_s/\pi)^i = R(t) \quad (7.24)$$

The perturbation series for  $D$  is

$$D = 1 + D_0 \cdot (\alpha_s/4\pi) + (D_1 - \beta_0 \cdot D_0 \cdot \ln(q^2/u^2)) \cdot (\alpha_s/4\pi)^2 + (D_2 - (\beta_1 \cdot D_0 + 2 \cdot \beta_0 \cdot D_1) \cdot \ln(q^2/u^2) + (\beta_0^2 \cdot D_0 \cdot (\ln(q^2/u^2))^2)) \cdot (\alpha_s/4\pi)^3 \quad (7.25)$$

where  $\beta_0$  and  $\beta_1$  are the first two coefficients of the beta function. Since  $t = \ln(q^2/u^2)$ ,

one can see that 
$$(r_2)^2/r_1 = (D_1 - \beta_0 \cdot D_0 \cdot t)^2/D_0 \quad (7.26)$$

The  $t^2$  coefficient is  $\beta_0^2 \cdot D_0$  which agrees with the coefficient of the  $t^2 \cdot \alpha_s^2$  term even if  $D_0$  does not equal 1. The cross term in equation (7.25) is  $-2 \cdot \beta_0 \cdot D_1 \cdot t$ . This agrees with one of the  $t \cdot (\alpha_s)^3$  terms. However, the other one does not have an  $N_f^2$  contribution. Thus the  $t \cdot N_f^2$  coefficients also agree. Thus, part of the  $r_3$  coefficient was predicted exactly by the Padé Approximant Prediction [1,1].

### Concluding Statement of Chapter 7

In conclusion, it has been shown how one can estimate coefficients of a perturbation series in perturbative quantum field theory. The results in the two QED sections agree well with known results for  $a_u - a_e$ ,  $a_e$ , and  $a_u$ .

Padé Approximant Predictions were less effective in providing accurate estimates for the QCD beta function. Nevertheless, we (the authors of Journal publication [18]) obtained somewhat reasonable results which are of the correct sign and the correct order of magnitude for the prediction of  $b_{(3)}$  of (7.18b) before  $b_{(3)}$  was known analytically.

The use of PAPs for estimating the next term in the QCD series for the  $R(t)$  of the  $R$  ratio of (7.21) does show more promise than the estimates attempted on the Quantum Chromodynamic Beta function. The very close agreement of PAP [1,1] to the exact  $r_3$  in Figures 7.1) and 7.2) is impressive. The close agreement of PAP [1,2] and PAP [2,1] in Figures 7.3) and 7.4) is quite reassuring for the estimate of the apparently unknown value of  $r_4$ , which is the next coefficient beyond  $r_3$  to be included in the perturbative series of  $R(t)$ .

In the not too far future, the value of  $r_4$  ought to be calculated analytically with the assistance of human mathematical prowess and a good symbolic software package such as Mathematica 3.0 on Linux or Unix. Soon after this accomplishment with modest additional effort, the author proposes that the Padé approximants  $\text{Pade}[2,2]$ , and  $\text{Pade}[3,1]$  be taken of the perturbative Quantum Chromodynamic expression for  $R(t)$  with respect to  $z$ , that is  $\alpha_s/4\pi$ . Perhaps there will be close agreement between  $\text{Pade}[2,2]$  and  $\text{Pade}[3,1]$  as two estimates of the entire function of  $R(t)$  when  $\alpha_s/\pi$  is sufficiently small at reasonably high energies.

## BIBLIOGRAPHY

- [1] John D. Walecka; *Theoretical Nuclear and Subnuclear Physics*; Chapter 6 and Chapter 7; Oxford University Press (1995).
- [2] A. I. Vainshtein, V. Zakharov; *Ultraviolet-Renormalon Calculus*; Physical Review Letters; Volume 73, #9; pages 1207-1210; August (1993).
- [3] Carl Bender, Steven Orszag; *Advanced Mathematical Methods for Scientists and Engineers*; McGraw-Hill Book Company (1978).
- [4] S. Chandrasekhar; *Radiative Transfer*; Oxford at the Clarendon Press (1950).
- [5.a] Richard Liboff; *Introductory Quantum Mechanics*; Holden-Day, Inc. (1980).
- [5.b] Jon Mathews and R.L. Walker; *Mathematical Methods of Physics*, Second Edition; Chapter 10; Addison -Wesley Publishing Company, Inc. (1970).
- [6.a] Jon Mathews and R.L. Walker; *Mathematical Methods of Physics*, Second Edition; Addison -Wesley Publishing Company, Inc. (1970).
- [6.b] Jon Mathews and R.L. Walker; *Mathematical Methods of Physics*, Second Edition; page 303; Addison -Wesley Publishing Company, Inc. (1970).
- [7] M. A. Samuel, G. Li, and E. Steinfelds; *Estimating Perturbative Coefficients in Quantum Field Theory and Statistical Physics*; Physical Review E; Volume 51, #5; pages 3911-3933, (See page 3912); (1995).
- [7.b] P.P. Zabreyko et al.; *Integral Equations - a reference text*; page 273; Noordhoff International Publishing, Leyden (1975).
- [8] Eric Steinfelds, M. A. Samuel, N.J. McCormick, and J. H. Reid; *Radiative Transfer Single Scattering Albedo Estimation with a SuperPade' Approximation of Chandrasekhar's H-Function*; pages 997-1007; International Journal of Theoretical Physics, Vol. 36, #4 (April, 1997).
- [9.a] S. Chandrasekhar; *Radiative Transfer*; Oxford at the Clarendon Press; (1950).
- [9.b] S. Chandrasekhar; *Radiative Transfer*; page 124; Oxford at the Clarendon Press; (1950).
- [10] Walter Rudin; *Principles of Mathematical Analysis*; page 159; McGraw-Hill Book Company; (1976).

- [11] S. Chandrasekhar; *Radiative Transfer*; Oxford at the Clarendon Press; (1950).
- [12] Alexander L. Fetter and John D. Walecka; *Quantum Theory of Many Particle Systems*; Chapter 15; McGraw-Hill Book Company; (1971).
- [12.b] Carl Bender and Tai Tsun Wu; *Anharmonic Oscillator*; Physical Review; Vol. **184**, No. **5**; page 1231; August (1969).
- [12.c] Carl Bender and Tai Tsun Wu; Physical Review D; Vol. **7**, No. **6**; page 1620; (1973).
- [13.a] Carl Bender, Steven Orszag; *Advanced Mathematical Methods for Scientists and Engineers*; Chapter 8; McGraw-Hill Book Company; (1978).
- [13.b] George Baker and Peter Graves-Morris; *Padé Approximants, 2nd Edition*; Chapter 5; Cambridge University Press; (1996).
- [14] Jon Mathews and R.L. Walker; *Mathematical Methods of Physics*, Second Edition; Chapter 10; Addison -Wesley Publishing Company, Inc.; (1970).
- [15.a] Eugen Merzbacher; *Quantum Mechanics*, Second Edition; Chapter 17; John Wiley and Sons, Inc.; (1970).
- [15.b] Richard Liboff; *Introductory Quantum Mechanics*; page 555; Holden-Day, Inc.; (1980).
- [16] Mark A. Samuel, J. Ellis, and M. Karliner; Physical Review Letters; Volume 51; pages 4380 to 4383; (1995).
- [17] M. A. Samuel, G. Li, and E. Steinfelds; *Estimating Perturbative Coefficients in Quantum Field Theory and Statistical Physics*; Physical Review E; Volume 51, #5; pages 3911-3933; (1995).
- [18] M. A. Samuel, G. Li, and Eric Steinfelds; *Estimating Perturbative Coefficients in Quantum Field Theory Using Pade Approximants*; Physical Review D; Volume 48, #2; pages 869-871 (1993).
- [19] T. Kinoshita and W.J. Marciano, in *Quantum Electrodynamics*, edited by T. Kinoshita (World Scientific, Singapore, 1990), p. 419; M.A. Samuel and G. Li, Phys Rev. D **44**, 3935 (1991).
- [20] T. Kinoshita, B. Nizic, and Y. Okamoto, Physical Review D **41**, 593 (1990).
- [21] T. Kinoshita, in *Quantum Electrodynamics* [19], page 28.

- [22] John Ellis, Marek Karliner, and M. A. Samuel, Eric Steinfelds; *The Anomalous Magnetic Moments of the Electron and Muon - Improved QED Predictions using Padé Approximants*; SLAC Publication, SLAC-PUB-6670 or hep-ph/9409376; Sept. (1994).
- [23] Maria Krawczyk and Jan Zhochowski; Physical Review D, Vol. 55, #11; page 6970; June (1997). Earlier: A. Czarnecki et al.; Physical Review Letters; Vol. 76; page 3267; (1996); Physical Review D, Vol. 52, R2619; (1995).
- [24] Richard Alemany, Michael Davier, and Andreas Höcker; *Improved Determination of the Hadronic Contribution to the Muon ( $g - 2$ ) and to  $\alpha(Mz^2)$  Using new Data from Hadronic  $\tau$  Decays*; listed on Los Alamos bulletin board; hep-hp/9703220. Earlier: U. Chattopadhyay and P. Nath, Physical Review D, Vol. 53; page 1648; (1996).
- [25] J. Bailey et al., Physics Letters 68B, 191 (1977).
- [26] Maria Krawczyk and Jan Zhochowski; Physical Review D, Vol. 55, #11; page 6969; June (1997).
- [27] T. van Ritbergen, J. Vermaseren, and S.A. Larin; *The four-loop  $\beta$ -function in Quantum Chromodynamics*; Physics Letters B; Vol. 400; page 379; May (1997).
- [28] John Ellis, Marek Karliner, Mark A. Samuel; A prediction for the 4-loop  $\beta$  function in QCD; Physics Letters B; Vol. 400; page 176; May (1997).
- [29] L. R. Surguladze and M. A. Samuel; Physics Letters B 309, page 157; (1993).
- [30] L. R. Surguladze and M. A. Samuel; Physical Review Letters; Vol. 66, page 560; (1991); **separately**: S.G. Gorishny, A. L. Kateav, and S.A. Larin, Physical Letters B 259; page 144; (1991).
- [31] M. A. Samuel and L. R. Surguladze; Physical Review D 44; page 1602; (1991).
- [32] L. R. Surguladze and M.A. Samuel; *Perturbative QCD calculations of total cross sections and decay widths in hard inclusive processes*; Review of Modern Physics; Vol. 68, page 259; (1996);

## APPENDIX A

The general formulas of Padé approximants Pade[2,3], Pade[3,2], and Pade[3,3] are listed among equations (8.1), (8.2), and (8.3) below. These Padé approximants shall be taken of the series  $r_0 + r_1 \cdot x + r_2 \cdot x^2 + r_3 \cdot x^3 + r_4 \cdot x^4 + r_5 \cdot x^5 + r_6 \cdot x^6 + \dots$  with respect to  $x$ . In this appendix,  $r_0$  equals  $r_0$  of chapter 1.  $r_1$  equals  $r_1$  of chapter 1.  $r_2 \equiv r_2$ ,  $r_3 \equiv r_3$ ,  $r_4 \equiv r_4$ , and so forth.

Pade[2,3] equals:

$$\begin{aligned} & (r_4 r_0^2 r_2 - r_0 r_4 r_1^2 - r_0 r_2^3 + 2 r_0 r_2 r_3 r_1 - r_3^2 r_0^2 + (-r_4 r_1^3 - r_1 r_2^3 \\ & + 2 r_2 r_3 r_1^2 - 2 r_1 r_3^2 r_0 - r_5 r_0^2 r_2 + r_0 r_5 r_1^2 + r_0 r_3 r_2^2 + r_4 r_3 r_0^2) x + ( \\ & 2 r_4 r_0 r_2^2 - 2 r_2 r_4 r_1^2 - r_2^4 + 3 r_2^2 r_3 r_1 - 2 r_2 r_3^2 r_0 - 2 r_1 r_5 r_0 r_2 + r_5 r_1^3 \\ & - r_3^2 r_1^2 + 2 r_1 r_4 r_3 r_0 - r_0^2 r_4^2 + r_0^2 r_3 r_5) x^2) / ( \\ & (-2 r_3 r_4 r_2 + r_3^3 + r_1 r_4^2 - r_1 r_3 r_5 + r_5 r_2^2) x^3 \\ & + (-r_0 r_4^2 + r_0 r_3 r_5 + r_4 r_2^2 - r_2 r_3^2 - r_2 r_1 r_5 + r_4 r_3 r_1) x^2 \\ & + (-r_5 r_0 r_2 + r_5 r_1^2 + r_3 r_2^2 - r_3^2 r_1 + r_4 r_3 r_0 - r_4 r_2 r_1) x + r_4 r_0 r_2 - r_4 r_1^2 \\ & - r_2^3 + 2 r_2 r_3 r_1 - r_3^2 r_0) \end{aligned} \quad (8.1)$$

Pade[3,2] equals:

$$\begin{aligned} & (r_0 r_2 r_4 - r_0 r_3^2 + (r_1 r_2 r_4 - r_1 r_3^2 - r_0 r_2 r_5 + r_0 r_3 r_4) x \\ & + (r_2^2 r_4 - r_2 r_3^2 - r_1 r_2 r_5 + r_1 r_3 r_4 - r_0 r_4^2 + r_0 r_3 r_5) x^2 \\ & + (2 r_3 r_2 r_4 - r_3^3 - r_2^2 r_5 - r_1 r_4^2 + r_1 r_3 r_5) x^3) / ( \\ & (-r_4^2 + r_3 r_5) x^2 + (-r_2 r_5 + r_3 r_4) x + r_2 r_4 - r_3^2) \end{aligned} \quad (8.2)$$

Pade[3,3] equals:

$$\begin{aligned}
 & \left( 2 r_3 r_4 r_0 r_2 - r_3^3 r_0 - r_1 r_0 r_4^2 + r_1 r_0 r_3 r_5 - r_5 r_0 r_2^2 + (2 r_4 r_2 r_3 r_1 - r_1 r_3^3 \right. \\
 & \quad - r_4^2 r_1^2 + r_3 r_5 r_1^2 - r_2^2 r_1 r_5 - r_0 r_6 r_3 r_1 + r_0 r_6 r_2^2 + r_0 r_4 r_3^2 - r_0 r_4^2 r_2 \\
 & \quad \left. + r_0 r_5 r_4 r_1 - r_0 r_3 r_5 r_2) x + (2 r_3 r_4 r_2^2 - r_2 r_3^3 - 2 r_2 r_1 r_4^2 - r_5 r_2^3 \right. \\
 & \quad - r_6 r_3 r_1^2 + r_1 r_6 r_2^2 + r_1 r_4 r_3^2 + r_5 r_4 r_1^2 + r_0 r_1 r_4 r_6 - r_0 r_1 r_5^2 + r_0 r_5 r_3^2 \\
 & \quad - r_0 r_3 r_4^2 - r_0 r_3 r_2 r_6 + r_0 r_4 r_2 r_5) x^2 + (3 r_3^2 r_4 r_2 - r_3^4 - 2 r_3 r_1 r_4^2 \\
 & \quad + 2 r_1 r_3^2 r_5 - 2 r_3 r_5 r_2^2 - 2 r_2 r_6 r_3 r_1 + r_6 r_2^3 - r_4^2 r_2^2 + 2 r_2 r_5 r_4 r_1 \\
 & \quad + r_1^2 r_4 r_6 - r_1^2 r_5^2 + r_0 r_4^3 - 2 r_0 r_4 r_3 r_5 - r_0 r_2 r_4 r_6 + r_0 r_2 r_5^2 + r_0 r_6 r_3^2) \\
 & \quad \left. x^3 \right) / \left( (r_4^3 - 2 r_4 r_3 r_5 - r_2 r_4 r_6 + r_2 r_5^2 + r_6 r_3^2) x^3 \right. \\
 & \quad + (r_1 r_4 r_6 - r_1 r_5^2 + r_5 r_3^2 - r_3 r_4^2 - r_3 r_2 r_6 + r_4 r_2 r_5) x^2 \\
 & \quad \left. + (-r_6 r_3 r_1 + r_6 r_2^2 + r_4 r_3^2 - r_4^2 r_2 + r_5 r_4 r_1 - r_3 r_5 r_2) x + 2 r_3 r_4 r_2 - r_3^3 \right. \\
 & \quad \left. - r_1 r_4^2 + r_1 r_3 r_5 - r_5 r_2^2 \right)
 \end{aligned} \tag{8.3}$$

It ought to be remembered that equations (1.9) of chapter 1 give the full formula

for Pade[2,2] of the series  $\sum_{i=0}^{infini} r_j * x^i$ .

$$\text{Pade}[2,2] \text{ equals: } \frac{\text{numerat}}{\text{denom}} \tag{8.4}$$

$$\begin{aligned}
 \text{numerat} = & r_0 r_3 r_1 - r_0 r_2^2 + x r_3 r_1^2 - x r_1 r_2^2 - x r_0 r_1 r_4 + \\
 & x r_0 r_2 r_3 + x^2 r_4 r_0 r_2 - x^2 r_4 r_1^2 + 2 x^2 r_2 r_3 r_1 - x^2 r_3^2 r_0 + x^2 r_2^3 .
 \end{aligned}$$

$$\text{denom} = x^2 r_4 r_2 - x^2 r_3^2 - x r_1 r_4 + x r_2 r_3 + r_3 r_1 - r_2^2 . \tag{8.5}$$

Next, a sequence of Padé Approximant Predictions is given for: Pade[1,2],

Pade[2,1], Pade[2,2], Pade[3,2], Pade[2,3], and Pade[3,3], and Pade[3,4]. The Padé

Approximant Prediction [n,m] shall be written as PAP[n,m].

$$\text{PAP}[1,1] = (r_2)^2 / (r_1) . \tag{8.6}$$

$$\text{PAP}[1,2] = \frac{-r2 \cdot (-r2^2 + r1 \cdot r3) - r3 \cdot (-r0 \cdot r3 + r1 \cdot r2)}{r0 \cdot r2 - r1^2} \quad (8.7)$$

$$\text{PAP}[2,1] = (r3)^2 / (r2) \quad (8.8)$$

$$\text{PAP}[2,2] = \frac{-r3 \cdot (-r3^2 + r2 \cdot r4) - r4 \cdot (-r1 \cdot r4 + r2 \cdot r3)}{r1 \cdot r3 - r2^2} \quad (8.9)$$

$$\text{PAP}[2,3] =$$

$$\begin{aligned} & \left( -r3 \left( r3^3 - 2r3r2r4 + r1r4^2 - r1r3r5 + r5r2^2 \right) \right. \\ & \quad - r4 \left( -r0r4^2 + r0r3r5 + r2^2r4 - r2r1r5 - r2r3^2 + r3r1r4 \right) \\ & \quad \left. - r5 \left( -r5r0r2 + r5r1^2 + r3r2^2 - r1r3^2 + r4r0r3 - r2r1r4 \right) \right) / \left( \right. \\ & \quad \left. -r2^3 + 2r2r1r3 - r1^2r4 - r0r3^2 + r0r2r4 \right) \end{aligned} \quad (8.10)$$

$$\text{PAP}[3,2] = \frac{-r4 \cdot (-r4^2 + r3 \cdot r5) - r5 \cdot (-r2 \cdot r5 + r3 \cdot r4)}{r2 \cdot r4 - r3^2} \quad (8.11)$$

$$\text{PAP}[3,3] =$$

$$\begin{aligned} & \left( -r4 \left( -2r4r5r3 + r4^3 + r2r5^2 - r2r4r6 + r6r3^2 \right) \right. \\ & \quad - r5 \left( -r1r5^2 + r1r4r6 + r5r3^2 - r3r2r6 - r3r4^2 + r5r4r2 \right) \\ & \quad \left. - r6 \left( r6r2^2 - r6r1r3 + r4r3^2 - r4^2r2 + r5r4r1 - r5r3r2 \right) \right) / \left( \right. \\ & \quad \left. -r5r2^2 + r5r1r3 - r3^3 + 2r3r4r2 - r4^2r1 \right) \end{aligned} \quad (8.12)$$



PAP[3,4]=

$$\begin{aligned}
& (-r_4 (-r_1 r_5^3 + r_2^2 r_6^2 + r_5^2 r_3^2 - r_3^3 r_7 + r_4^4 - 2r_2 r_4^2 r_6 - 3r_5 r_4^2 r_3 + 2r_4 r_2 r_5^2 + 2r_3^2 r_4 r_6 \\
& + 2r_4 r_6 r_5 r_1 + r_1 r_3 r_5 r_7 - r_1 r_3 r_6^2 - r_4^2 r_1 r_7 - r_2^2 r_5 r_7 + 2r_2 r_4 r_3 r_7 - 2r_2 r_6 r_5 r_3) - r_5 ( \\
& -2r_0 r_4 r_6 r_5 + r_0 r_5^3 - r_0 r_3 r_5 r_7 + r_0 r_3 r_6^2 + r_0 r_4^2 r_7 - r_4 r_2^2 r_7 + r_5 r_2^2 r_6 + r_3^2 r_7 r_2 \\
& - r_2 r_1 r_6^2 - 2r_5^2 r_2 r_3 + r_4^2 r_2 r_5 + r_2 r_1 r_5 r_7 + r_4^2 r_6 r_1 + r_3 r_1 r_6 r_5 + 2r_4 r_3^2 r_5 - r_5^2 r_4 r_1 \\
& - r_3^3 r_6 - r_3 r_4^3 - r_3 r_1 r_7 r_4) - r_6 (r_0 r_2 r_5 r_7 - r_0 r_2 r_6^2 + r_0 r_6 r_4^2 - r_0 r_4 r_5^2 - r_0 r_4 r_3 r_7 \\
& + r_0 r_6 r_5 r_3 + r_4 r_2^2 r_6 - r_2^2 r_3 r_7 - r_4^3 r_2 + r_2 r_1 r_7 r_4 - r_2 r_6 r_5 r_1 + r_3^2 r_6 r_2 + r_4^2 r_3^2 \\
& + r_4^2 r_1 r_5 - 3r_3 r_1 r_6 r_4 - r_5 r_7 r_1^2 + r_5^2 r_3 r_1 + r_6^2 r_1^2 + r_3^2 r_1 r_7 - r_3^3 r_5) - r_7 (-r_0 r_2 r_4 r_7 \\
& + r_0 r_2 r_5 r_6 - r_0 r_5^2 r_3 + r_0 r_3^2 r_7 - r_0 r_4 r_3 r_6 + r_0 r_4^2 r_5 + r_7 r_2^3 - r_2^2 r_3 r_6 - 2r_2^2 r_5 r_4 \\
& + r_2 r_3^2 r_5 + 2r_2 r_4^2 r_3 + r_2 r_5^2 r_1 - 2r_2 r_3 r_1 r_7 + r_2 r_4 r_1 r_6 - r_4^3 r_1 - r_3^3 r_4 - r_5 r_6 r_1^2 \\
& + r_3^2 r_1 r_6 + r_4 r_7 r_1^2) \Big) \Big/ (r_0 r_2 r_4 r_6 - r_0 r_2 r_5^2 - r_0 r_3^2 r_6 - r_0 r_4^3 + 2r_0 r_5 r_4 r_3 - r_6 r_2^3 \\
& + 2r_2^2 r_5 r_3 + r_2^2 r_4^2 - 3r_2 r_4 r_3^2 - 2r_2 r_5 r_4 r_1 + 2r_2 r_3 r_1 r_6 + r_5^2 r_1^2 + r_3^4 + 2r_4^2 r_3 r_1 \\
& - 2r_5 r_3^2 r_1 - r_4 r_6 r_1^2)
\end{aligned}$$

(8.13)

## APPENDIX B

'Sca' equals approximately 1.182. V equals 1/5 in this example. In all of this text, a one dimensional quartic harmonic oscillator is defined as a harmonic oscillator whose potential energy is modified by the additional term  $V' \cdot x^4$ . The estimated ground state of a quartic harmonic oscillator is:

$$\begin{aligned}
 &.751125444649425 \%1 - .03045053710822796 (4. x^2 - 2.) \%1 \\
 &- .002272479705501470 (16. x^4 - 48. x^2 + 12.) \%1 \\
 &- .0001373877831248834 (64. x^6 - 480. x^4 + 720. x^2 - 120.) \%1 \\
 &- .5961771313873175 10^{-5} (256. x^8 - 3584. x^6 + 13440. x^4 - 13440. x^2 + 1680.) \%1 - \\
 &.9638767990754212 10^{-7} (1024. x^{10} - 23040. x^8 + 161280. x^6 - 403200. x^4 + 302400. x^2 - 30240.) \%1 \\
 &- .4812018743154766 10^{-9} (4096. x^{12} - 135168. x^{10} + 1520640 10^7 x^8 - 7096320 10^7 x^6 \\
 &+ .13305600 10^8 x^4 - .7983360 10^7 x^2 + 665280.) \%1 \\
 &\%1 = e^{-.5000000000000000 x^2}
 \end{aligned}
 \tag{9.1}$$

Note that the symbol '%1' signifies  $\exp(-1/2 \cdot x^2)$ .

Mathematical expression (9.1) comes from the following representation of a perturbative series:

$$\begin{aligned}
 \Psi(m, V) = & \Psi^0(m) + V \cdot \sum_{n \neq m} \frac{G(m, n) \cdot \Psi^0(n)}{Lam(m, V) - L^0(n)} + \\
 & V^2 \cdot \sum_{n \neq m} \sum_{p \neq n} \frac{G(m, n) \cdot G(n, p) \cdot \Psi^0(p)}{(Lam(m, V) - L^0(n)) \cdot (Lam(m, V) - L^0(p))} + \\
 & V^3 \cdot \sum_{n \neq m} \sum_{p \neq m} \sum_{q \neq n} \frac{G(m, n) \cdot G(n, p) \cdot G(p, q) \cdot \Psi^0(q)}{(Lam(m, V) - L^0(n)) \cdot (Lam(m, V) - L^0(p)) \cdot (Lam(m, V) - L^0(q))} ,
 \end{aligned}$$

$$\text{where } Lam(m, V) = Sca \cdot L^0(m) .
 \tag{9.2}$$

$V$  is the adjustable strength of the perturbation. It should be clear that this perturbative series has been written out to the third order of  $V$ .  $S_{ca}$  can be considered a rather insensitive function of  $V$ . In this appendix,  $S_{ca}$  has been set equal to the constant value of 1.182. If  $V$  equal 25/100 rather than 1/5 with  $S_{ca}$  still set equal to 1.182, the  $x$  dependent results from expression (9.1) are still very good. Taking Pade approximants of the series in equation middlem results in even more precise expressions for the corrected ground level eigenstate  $\Psi(m,V)$ .

It will be explained in chapter 6 that the Hamiltonian for  $\Psi(m,V)$  is:

$\hat{H} = (-d^2/dx^2 + x^2) + V \cdot x^4$ . The ground state is  $\Psi^0 = 1/((\pi)^{1/4}) \cdot \exp(-1/2 \cdot x^2)$ , and the corresponding Hamiltonian part is:  $(-d^2/dx^2 + x^2)$ .

## APPENDIX C

The 1-dimensional hexic (sixth order) anharmonic oscillator example has a non-relativistic Hamiltonian of the following form:

$$H = (-d^2/dx^2 + x^2) + V' \cdot x^6, \quad (10.1)$$

where  $V' \cdot x^6$  is the perturbation. Optimal Padé approximants  $\text{OpOptoPade}[2,3]$  and  $\text{OpOptoPade}[3,3]$  (See chapter 6) have been calculated by the author. 'Partial Sum-5' is defined as the Taylor series of  $\text{OpOptoPade}[2,3]$  calculated all the way out to the fifth order with respect to  $V'$ .  $\text{OpOptoPade}[3,3]$ , which was generated by using  $(-d^2/dx^2 + x^2)$  as the source Hamiltonian and  $V' \cdot x^6$  as the perturbation, was found to equal the following approximation:

$$\frac{1. + 330.70629531100 V + 19530.460544024 V^2 + 145663.31125222 V^3}{1. + 328.83129531100 V + 18941.206552816 V^2 + 117916.56460719 V^3} \quad (10.2)$$

Table 10.1) presents the numerical results for the ground state energy curve of the hexic (sixth order) anharmonic oscillator as a function of  $V'$ .  $V'$  ranges from 0.010 to 0.400.  $\text{OpOptPade}[3,3]$ ,  $\text{OpOptPade}[2,3]$ , the accurate numerical spectral solution (Matrix perturbation theory), and 'Partial Sum-5' are included.

**Table 10.1)**

The Ground State Energy Curve of the Hexic Harmonic Oscillator as a Function of the  $V'$  of the Perturbation Term  $V' \cdot x^6$

$V'$	OpOptpad[2,2]	OpOptpad[3,3]	Correct Numerical Value	OpOptpad[2,3]	Partial Sum -5
.0100	1.0167006723	1.0167327438	1.01674	1.0167618210	1.01762054
.0200	1.0305136592	1.0307630468	1.03090	1.0311365003	1.06740993
.0250	1.0366161960	1.0370588083	1.03734	1.0378343516	1.15449503
.0500	1.0612898525	1.0633090088	1.06538	1.0690724201	5.24199021
.1000	1.0928577335	1.0991372237	1.10924	1.1293709422	143.142854
.1500	1.1122290121	1.1225710481	1.14437	1.1929614129	1103.44810
.2000	1.1253321830	1.1391144363	1.17447	1.2625602570	4698.69986
.3000	1.1419304475	1.1609343594	1.22553	1.4269013644	36084.6504
.4000	1.1520090416	1.1746834602	1.26879	1.6386073341	152946.484

It was explained chapter 6 that Carl Bender's publication [12.b] includes a list of many of the perturbative coefficients generated for the quartic harmonic oscillator.

However, Carl Bender's publications [12.b] and [12.c] do not include any specific list of an exact perturbative series generated for the hexic anharmonic oscillator. The author was not able to find any publications by Bender from the 1970's or later which is dedicated specifically to the hexic anharmonic oscillator.

## APPENDIX D

The number of terms in the coefficient  $g\{n\}[u]$  from the serial expression for the H-function of chapter 3 has been partially discussed in chapter 3.  $H_{\{n\}}(u, W_2)$  equals  $g_0[u] + W_2 \cdot g_1[u] + (W_2)^2 \cdot g_2[u] + \dots + (W_2)^n \cdot g\{n\}[u]$ , where  $W_2 = \omega/2$ . Asymptotically, the number of terms in each  $g\{n\}[u]$  as an integer numerical function of  $n$  grows as  $\text{Constant} \cdot 4^n$ . The one table in this appendix gives list of this number of terms, as found by use of the recursive counting algorithm (see relationship (3.6) in chapter 3). This one particular table also gives the successful estimates for the number of term by a method very similar to but more specialized than the method of Padé Approximant Predictions. This method involves Asymptotic Padé Approximant Predictions (APAP's). Asymptotic Padé Approximant Predictions are introduced and explained chapter 5.

Now let us examine the results of the predictions for the number of terms in a given  $g\{n\}[u]$ . It was only for values of  $n$  larger than 16 where disagreement for the number of terms occurred between the APAP results and the Analytical predictions.

Compilation of the Number of terms for the first ten  
Perturbative Coefficients of the H-function

Value of Order $n$	Analytical Recursive Results	APAP Results
1	1	N.A.
2	2	N.A.
3	5	N.A.
4	14	14
5	42	42
6	132	132
7	429	429
8	1430	1430
9	4862	4862
10	16796	16796

N.A.  $\equiv$  Not Available.

2

## VITA

Eric V. Steinfelds

Candidate for the Degree of

Doctor of Philosophy

Thesis: PERTURBATIVE QUANTUM FIELD THEORY AND OTHER PHYSICAL  
PERTURBATIONS - GOING TO HIGHER ORDER WITH ANALYTICAL  
AND APPROXIMATIVE SCHEMES

Major Field: Physics

Biographical:

Education: Graduated from Driscoll High School, Addison, Illinois in May 1982; received Bachelor of Arts in Physics and Mathematics in May 1986 from Luther College, Decorah, Iowa; received Masters of Arts in Physics in May 1990 from Kent State University, Kent, Ohio; completed the requirements for Doctor of Philosophy in Physics from Oklahoma State University, Stillwater, Oklahoma in December 1997.

Experience: Substitute Lecturer, Oklahoma State University, Stillwater, Oklahoma; employed by Oklahoma State University as a Teaching Assistant and Research Assistant, 1990 to present.

Professional Accomplishments: Theoretical creativity; discovered an integral solution to an entire small family of difficult nonlinear differential equations. Extensive computer programming skills. Participated as a speaker at the Student Research Symposium sponsored by Oklahoma State University Graduate College in March 1997 and in the APS Computational Physics Conference (PC 97) in August 1997.